SYNTHESIS, CHARACTERIZATION AND CATALYTIC APPLICATIONS OF MCM-41 TYPE MESOPOROUS MATERIALS

A THESIS
SUBMITTED TO THE
UNIVERSITY OF PUNE
FOR
THE DEGREE OF
M.Sc. CHEMISTRY

BY
TEJAS R GAYDHANKAR

UNDER THE GUIDANCE OF
Dr. RAJIV KUMAR

CATALYSIS DIVISION
NATIONAL CHEMICAL LABORATORY
PUNE – 411008, INDIA

(NOVEMBER - 2006)

…..DEDICATED

TO

MY BELOVED PARENTS

ACKNOWLEDGEMENTS

First of all, let me express my sincere thanks to my research guide, Dr. Rajiv Kumar, Head of Catalysis Division, National Chemical Laboratory, Pune, for his constant support, sincere guidance and constructive suggestions through out the course of this investigation. I am grateful to him for giving me liberty in the work undertaken and for continuous encouragement during the course of the present study. I preserve an everlasting gratitude for him.

I am also thankful and have deep sense of gratitude to my supervisor, Dr. P. N. Joshi, Scientist, National Chemical Laboratory, Pune, for his constant support and invaluable discussions during my day-to-day research work. It gives me a great pleasure to express my deep sense of gratitude and indebtedness to Dr. P. N. Joshi for his expert and inspiring guidance and suggestions in carrying out the research work. He has taught me scientific and non-scientific lessons better and how to remain optimistic.

I am grateful to Mr. G. M. Chaphekar and Dr. M. W. Kasture for providing me various facilities required for carrying out my research work.

It gives me great pleasure to thank my labmates, Mr. Prashant Niphadkar, Amit Deshmukh, Mr. Pranjal Kalita and Mr. Mahesh

Kadgaokar for their constant scientific and non-scientific help, encouragement and had a nice time with them.

I owe my special thanks to Dr K.J. Waghmare, Dr. Shaikh, Dr. Agashe, Mr. Shelar, Mr. Jadhav, Mr. Gaikwad, Dr. S. Awate, Mr. Sonawane, Mr. Kalal, Dr. A.A. Belhekar, Dr. Mirajkar, Dr. B.S. Rao, Dr. V. Ramaswamy, Dr.N. Jacob, Dr. A.V. Ramaswamy, Dr. S.A. Pardhy, Miss S. Violet, Dr. Deshpande and all other scientific and nonscientific staff in the Catalysis Division

I am also grateful to Dr. Rojatkar (Organic Chemistry Division) and Dr G. Suryavanshi (CEPD Division) NCL, Dr. I.S. Mulla (Physical Chemistry Division) NCL, for their help and constant support given to me during my research work.

I am highly obliged to my parents, brother Ashish R Gaydhankar and his wife Himani, sister Dr. Varsha R Ohatker (IICT, Hyderabad), and all other family members for their love, unfailing support, tremendous patience, sacrifice and encouragement they have shown in their own way during my long period of studies. They have been a constant source of strength and inspiration for me.

I also give my special thanks to my friends, S. P. Mahajan, R. Ingle, S. Jain, M. Sankar, P. Karndikar, H. Jagtap, M. Akbar, D. Bhange, G. Kokate, S.R. Kadam, N. Jagtap, P Shah, P Awati, V. Paike, P. Desai, P. Lihitkar, U. Taralkar many others, from whom I have received invaluable help and support.

Finally, I am thankfull to Dr. Sivaram, Director and Dr. B. D. Kulkarni, Deputy Director, NCL, for permitting to register for M.Sc. Chemistry (PPPR) degree course of Pune University and allowing me to carry out the research at NCL and to submit the work in the form of thesis for the award of the M. Sc. degree.

Once again, I am grateful to Dr. Rajiv Kumar for providing the financial support to carry out the research work under Task Force Project (P-23 CMM-0005A) funded by CSIR.

Tejas R Gaydhankar

CERTIFICATE

Certified that the work incorporated in the thesis entitled "**Synthesis, characterization and catalytic applications of MCM-41 type mesoporous materials**" submitted by Mr. TEJAS R GAYDHANKAR, for the degree of M.Sc. Chemistry (P.P.P.R), was carried out by the candidate under my supervision in the Catalysis Division, National Chemical Laboratory, Pune, India.

Dr. Rajiv Kumar
(Research Guide)
Head of Catalysis Division
National Chemical Laboratory
Pune-411008, India

CONTENTS

ABBREVIATIONS

CTMABr - Cetyltrimethylammonium bromide

CTMAOH - Cetyltrimethylammonium hydroxide

CTMACl - Cetyltrimethylammonium chloride

GC - Gas chromatography

FID - Flame ionization detector

IPA - Isopropyl alcohol

MCM-41 - Mobil Composition of Matter No. 41

MCM-48 - Mobil Composition of Matter No. 48

TBHP - *tert*-Butyl hydroperoxide

TEOS - Tetraethyl orthosilicate

TMAOH - Tetramethylammonium hydroxide

TS-1 - Titano-silicalite-1

H_2O_2 – Hydrogen peroxide

MSU - Michigan state university material

HMS - Hexagonal mesoporous silica

NMR - Nuclear magnetic resonance

FSM-16 - Folded Sheet mesoporous Materials-16

AMS-n - Anionic surfactant templated Mesoporous Silica-n

SBA – Santa Barbara

HCl - Hydrochloric Acid

HF - Hydrofluoric Acid

H_2SO_4 - Sulfuric Acid

TLCT - True liquid crystal templating

NaOH – Sodium hydroxide

NH_4OH - Ammonium hydroxide

FWHM – Full Width at Half Maximum

CHAPTER – 1

INTRODUCTION

This chapter presents the general background and available literature on mesoporous molecular sieve materials. Different synthesis strategies, the role of templating surfactants, various proposed mechanisms for synthesis, characterization techniques and catalytic applications of ordered mesoporous materials in particular MCM-41 are discussed in brief. The objectives of the present investigation are outlined at the end of this chapter.

1.1. GENERAL BACKGROUND

According to the IUPAC definition, porous materials are divided into three classes; micro porous (pore size < 2 nm), mesoporous (2–50 nm), and macro porous (>50 nm) materials [1]. Among the family of microporous materials, the best known members are zeolites which have a narrow and uniform pores of molecular dimensions [2]. Zeolite was discovered in 1756 and named by the Swedish mineralogist Baron Cronstedt. The name Zeolite is derived from Greek words meaning “boiling stone. In 1931, McBain proposed the term ‘molecular sieve’ to describe a class of materials containing pores of a precise and uniform size that can be used as an absorbent for gases and liquids. A material to be called as molecular sieve, it must separate components of a mixture on the basis of molecular size and shape differences. Thus zeolites are classified as crystalline microporous molecular sieve in which Si and Al are tetrahedrally coordinated by oxygen atoms in a three-dimensional network. However, a variety of trivalent (B, Ga, Fe, etc.) and tetravalent (Ti, V, Sn, etc.) transition and non-transition metal ions have been incorporated in a variety of different zeolite structures. Till 1990 heterogeneous catalysis available with zeolites was restricted to the use of materials with pore sizes less than 2 nm and consequently the reactant molecules trapped and transformed inside them were also small. Thus the usefulness of the microporous molecular sieves in processing high molecular

weight reactants of increasing importance was limited by their smaller pore size. Hence there has been an ever-growing interest in expanding the pore sizes of the microporous molecular sieves from the micropore region to mesopores region. Attempts to improve the diffusion of reactants to the catalytic sites have so far focused on increasing the zeolite pore sizes [3], on decreasing zeolite crystal size [4], or on providing an additional mesopore system within the microporous crystals [5,6]. The first synthesis of an ordered mesoporous material was described in the patent literature in 1969. However, due to a lack of analysis, the remarkable features of this product were not recognized [7,8]. In 1992, a similar material was obtained by scientist in Mobil Oil Corporation who discovered the remarkable features of this novel type of ordered mesoporous silica [9]. A new family of mesoporous molecular sieves designated as M41S was thus introduced by Mobil scientists. The most popular members of this family are MCM-41 and MCM-48. MCM-41, which stands for Mobil Composition of Matter No. 41, shows a highly ordered hexagonal array of unidimensional pores with a very narrow pore size distribution [10,11]. The walls, however, resemble amorphous silica. Other related phases such as MCM-48 and MCM-50 have a cubic and lamellar mesostructure, respectively. At the same time, an alternative, but less versatile approach to mesoporous materials was described by Yanagisawa et al. [12]. Kanemite, a layered silicate, serves as a silica source, the pathway leading to the ordered mesoporous material is thought to proceed via surfactant intercalation into the silicate sheets, warping of the sheets and transformation to the hexagonally packed material. Modifying and optimizing the reaction conditions yielded highly ordered mesoporous silicates and aluminosilicates as well [13,14]. The obtained materials are designated as FSM-n, Folded Sheet mesoporous Materials-n, here n is the number of carbon atoms

in the surfactant alkyl-chain used to synthesize the material. Many reviews have been published covering various aspects of ordered mesoporous materials, such as their synthesis, characterization, surface modification, application as host materials, and in catalysis [15-31]. After the discovery of MCM-41 type and related materials in the early 1990s there has been impressive progress in the development of many new mesoporous solids based on surfactant co-operative assembly mechanisms related to the one used for the original MCM-41 synthesis. Depending on the synthesis conditions, the silica source or the type of surfactant used many other mesoporous materials can be synthesized following the co-operative assembly pathway [32-34]. From the viewpoint of the surfactant used for synthesis and the interaction of inorganic species and organic template molecule, some of the possible pathways for the synthesis of mesoporous materials are listed in Table 1.1.1.

Table 1.1.1: Some of the possible pathways for the synthesis of mesoporous materials

Template	Interaction		Synthesis conditions	Examples
Ionic surfactant	Direct interaction	$I^- S^+$ ^^^^^^^	Basic	MCM-41,MCM-48, MCM-50[9–11], FSM-16 [13,14]
	Ionic	$I^+ S^-$ ^^^^^^^	Neutral basic	Aluminum, iron, lead oxides, etc. [33,34]) AMS [45,46]
	Intermediated interaction	$I^+X^-S^+$ ^^^^^^^	Acidic	SBA-1, SBA-2, SBA-3 [37], HMS [54], TLCT [35]
	Ionic	$I^-X^+S^-$ ^^^^^^^	Basic	(Aluminum, zinc oxides etc. [33,34])
Non-ionic surfactant	Non-ionic	$I^0 S^0$ ^^^^^^^	Neutral basic	HMS [54,55]
Co-polymer	Neutral	I^0N^0 ^^^^^^^	Acidic	MSU [56,58], SBA-15 [62,63], TLCT [35]

(S = Surfactant, I = inorganic species and X = counter - ion mediated, eg Cl, Br, OH etc)

The first ordered mesoporous materials were prepared from ionic surfactants, such as quaternary ammonium ions. The formation of the inorganic–organic composites is based on electrostatic interactions between the positively charged surfactants and the negatively charged silicate species in solution. The packing parameter g may be used to rationalize and also in some cases predict the product structure and the conditions for possible phase transitions. Such prediction of the structure of surfactant aggregates and the corresponding mesophases in surfactant-water systems was made possible by Israelachivili et. al. [38, 39], who developed a microscopic model according to which the dimensionless packing parameter g plays a key role. This number, g, is defined as $g = V/a_0l_c$, where V is the effective volume of the hydrophobic chain of the surfactant, a_0 is the effective aggregate surface area of the hydrophilic head group, and l_c is the effective hydrophobic chain length. One should note that the variables in the definition of the packing parameters are not constants for a given surfactant, but are influenced by the solution conditions, such as for instance ionic strength, pH, co-surfactant concentration and temperature [39]. It was observed that the surfactant to silica ratio has a substantial impact on the composite structure obtained [40-42]. The co-operative assembly pathway was extended by Stucky and co-workers [37,41,44] to a series of other electrostatic assembly pathways, such as a reversed S^-I^+ (S = surfactant, I = inorganic species) pathway and counter- ion mediated $S^+X^-I^+$ and $S^-M^+I^-$ pathways. The use of anionic surfactant via S^-I^+ or $S^-M^+S^-$ interaction has resulted mainly in lamellar and disordered mesostructures. Recently, a novel synthetic route for mesoporous silica by the use of anionic surfactants has been reported by Che et al. (named AMS-n, Anionic surfactant templated Mesoporous Silica) [45,46]. Pinnavaia et al. have developed

two additional approaches for the synthesis of mesoporous materials, based on non-ionic organic–inorganic interactions. They used neutral surfactants such as primary amines and poly(ethylene oxides) to prepare HMS (hexagonal mesoporous silica) [54,55] and MSU (Michigan State University material) [56], respectively. The pore systems of the latter silicas have been shown to have rather worm-like structures than long-range ordered hexagonal arrays which are characteristic for MCM-41 [57, 58]. Compared to MCM-41, HMS and MSU have very similar surface areas and pore volumes, but the pore size distributions are somewhat broader.

1.2. MECHANISMS FOR THE FORMATION OF MESOPOROUS MATERIALS

A number of models have been proposed in order to explain the mechanism of formation of mesoporous materials by various synthesis routes. All these models are based on the presence of surfactants in solution to guide the formation of inorganic mesostructure. Knowledge of the chemistry of surfactant/silicate solution is a prerequisite for understanding the synthesis and mechanisms responsible for the formation of MCM-41 type mesoporous materials from its precursors. The lowest concentration at which surfactant molecules present in the solution aggregate to form spherical isotropic micelles is called critical micelle concentration (CMC_1). Further increase in the surfactant concentration initiates aggregation of spherical into cylindrical or rod-like micelles known as (CMC_2). As the concentration increases, hexagonal close packed arrays appear, producing the hexagonal phases [43]. According to [51], the particular phase present in a surfactant aqueous solution at a given concentration depends not only on the concentrations but also on the nature of (the length of the hydrophobic carbon chain, hydrophilic head group, and counter-ion) and other environmental parameters (pH,

temperature, the ionic strength, and other additives). Generally, the CMC decreases with the increase of the chain length of a surfactant, the valency of the counterions, and the ion strength in a solution, respectively. On the other hand, it increases with increasing counterion radius, pH, and temperature.

In order to explain the synthesis mechanism, Mobil Researchers proposed a liquid crystal templating (LCT) mechanism, based on the similarity between liquid crystalline surfactant assemblies and M41S [10,11]. Two mechanistic pathways were postulated for the formation of M41S type materials for the LCT mechanism. Fig. 1.2.1 depicts the two different pathways for formation of mesoporous molecular sieves by LCT mechanism

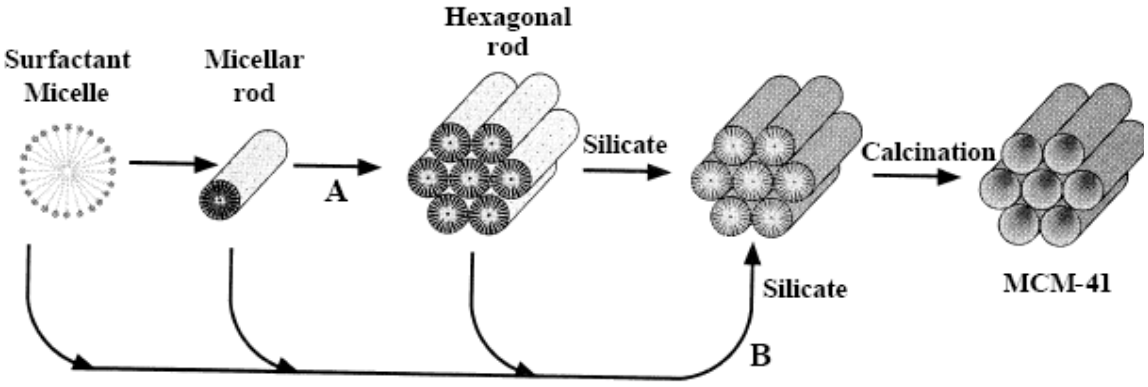

Fig 1.2.1: Liquid crystal templating mechanism proposed for the formation of MCM-41: (A) Liquid crystal phase initiated and (B) Silicate anion initiated.

In the first pathway, it is considered that first there is a formation of the surfactant hexagonal liquid-crystal phase around which the growth of the inorganic materials is directed. The surfactant micelles aggregate to form hexagonal arrays of rods. Silicate anions present in the reaction mixture interact with the surfactant cationic head groups. Condensation of the silicate species leads to the formation of an inorganic polymer. However, this pathway did not get much support in the literature. It has been observed that

at lower concentrations only micelles exist in solution [42]. Moreover, in situ ^{14}N-NMR spectra revealed that the hexagonal liquid-crystalline phase of CTMA ions was not present at any time during MCM-41 formation [52]. Thus the first synthesis pathway shown in Fig 1.2.1 (A) was abandoned. In the second pathway, it has been proposed that the randomly ordered rod like micelles interact with silicate species by coulombic interactions in the reaction mixture to produce approximately two or three monolayers of silicate around the external surfaces of the micelles. These randomly ordered composite species spontaneously pack into a highly ordered mesoporous phase with an energetically favorable hexagonal arrangement, accompanied by silicate condensation. With the increase in heating time, the inorganic wall continues to condense. The investigation on the formation mechanism [52, 53] using XRD, ^{29}Si NMR, in situ ^{14}N NMR, and thermo-gravimetric analysis (TGA) techniques proves the absence of hexagonal liquid crystalline mesophases, either in the synthesis gel or in the surfactant solution used as template. It was therefore, concluded that formation of MCM-41 phase is possibly via pathway 2 (Fig. 1.2.1B) rather than pathway 1.

Davis and co-workers [52] by carrying out in situ ^{14}N NMR spectroscopy concluded that the liquid crystalline phase is not present in the synthesis medium during the formation of MCM-41, and consequently, this phase cannot be the structure-directing agent for the synthesis of the mesoporous materials (Fig 1.2.2).

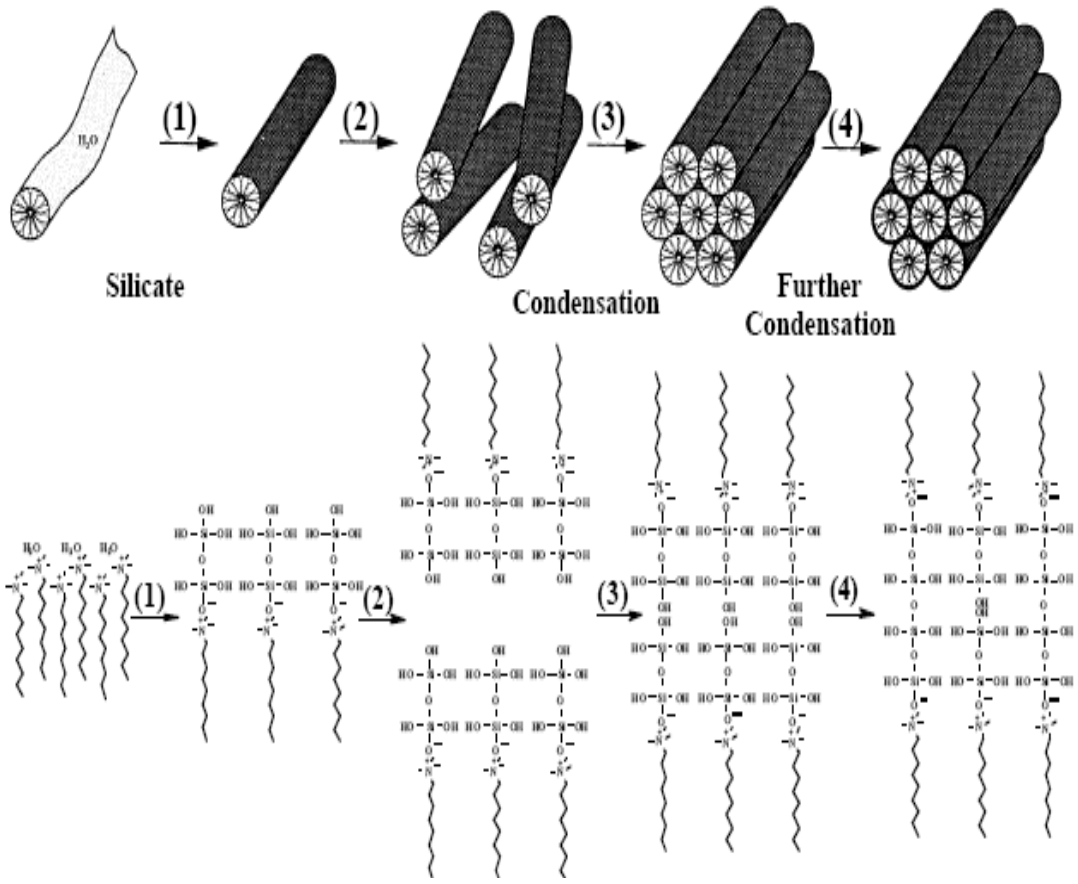

Fig. 1.2.2: Silicate rod assembly proposed for the formation of MCM-41: (1) and (2) involve the random ordering of rod-like micelles and interaction with silicate species; (3) represents the spontaneous packing of the rods and (4) is the remaining condensation of silicate species upon final heating of the organic/inorganic composites.

A generalized LCT mechanism includes different routes such as 1) Ionic Route (electrostatic interaction), 2) Templating Route (hydrogen bonding interaction) and 3) Ligand-Assisted Templating Route (covalent interaction) for the formation of mesostructures.

Ionic route was proposed Huo and co-workers.[33,34] for the formation of mesostructured materials was based on the specific type of electrostatic interaction between a given inorganic precursor I and surfactant head group S. In this concept,

cationic quaternary ammonium surfactants (S^+) are used for the structuring of anionic inorganic silicate species (I^-), which could be categorized as the S^+I^- pathway. On the other hand, anionic surfactants (S^-) are employed for structuring cationic inorganic species (I^+) (S^-I^+ mesostructures). Organic-inorganic combinations with identically charged partners are also possible, but then the formation of the mesostructure is mediated by the counter-charged ions, which must be present in stoichiometric amounts $S^+X^-I^+$ (X^- is a counter anion) and $S^-M^+I^-$ (M^+ is a metal cation). Another generalized LCT mechanism with templating route proposed Tanev and Pinnavaia [54,59,60] have neutral amine template surfactants (S^0) and hydroxylated TEOS (I^0) which have been used to prepare hexagonal mesoporous silica's (HMS) that have thicker pore walls, high thermal stability and smaller crystallite size but, have higher amounts of interparticle mesoporosity and lower degree of long-range ordering of pores than MCM-41 materials. In ligand-assisted templating route, Ying and co-workers have successfully synthesized hexagonally packed mesoporous metal oxide materials completely stable to surfactant removal through a ligand-assisted templating (LAT) mechanism [66]. The surfactants were pre- treated with the metal alkoxides precursor in the absence of water to form metal-ligated surfactants by nitrogen-metal bond formation between the surfactant head group and the metal alkoxide precursor. The control of mesostructure phases was found possible by adjustment of the metal/surfactant ratio.

1.3. SYNTHESIS OF MESOPOROUS MATERIALS

Most of the research has been concentrated on mesoporous molecular sieves and especially on MCM-41 type mesoporous materials because of its hexagonal arrangement of uni-dimensional mesopores with uniform but controllable diameter in the range of 2 - 10

nm [2,15,19,44]. Some of the various mesoporous molecular sieves reported till dates are given in Table 1.3.1.

Table 1.3.1: Some of the mesoporous molecular sieves reported till date.

Mesophase Terminology	Reference	Resulting Mesophase
MCM-41	Beck et al.[11]	2D hexagonal
MCM-48	Beck et al.[11]	Cubic
FSM-16	Inagaki et al.[67]	2D hexagonal
SBA-1	Huo et al.[33]	Cubic
SBA-2	Huo et al.[37]	3D hexagonal
SBA-3	Huo et al.[33]	2D hexagonal
SBA-8	Zhao et al.[70]	2D Rectangular
SBA-11	Zhao et al.[62]	Cubic
SBA-12	Zhao et al.[62]	3D hexagonal
SBA-14	Zhao et al.[62]	Cubic
SBA-15	Lukens et al.[71]	2D hexagonal
SBA-16	Zhao et al.[62]	Cubic
HMM	Inagaki et al.[83]	2D hexagonal
HMM	Inagaki et al.[83]	3D hexagonal
MSU-1	Bagshaw et al.[56]	Hexagonal (disordered)
MSU-2	Bagshaw et al.[56]	Hexagonal (disordered)
MSU-3	Bagshaw et al.[56]	Hexagonal (disordered)
MSU-4	Prouzet et al.[72]	Hexagonal (disordered)
MSU-V	Tanev et al.[73]	Lamellar
MSU-G	Kim et al.[74]	Lamellar
HMS	Zhang et al.[61]	Hexagonal (disordered)
KIT-1	Ryoo et al.[75]	Hexagonal (disordered)
CMK-1	Ryoo et al.[76]	Cubic
APO	Kimura et al.[77,82]	2D hexagonal

The main purpose and advantage of synthesizing mesoporous materials is to overcome the diffusional constraints with zeolites, along with this advantage these materials posses additional benefits like very high surface area (>1000 m^2/g), adjustable pore size (2-10 nm), high specific pore volumes, narrow pore size distribution, high degree of flexibility in adjusting their catalytic properties by incorporating desired metals into the framework making them a fascinating class of porous solids. Mesoporous molecular sieves are hydrothermally synthesized by mixing organic molecules (surfactants), silica, and/or

silica-metal source to form a gel which is then heated in the temperature range 343 - 423 K for a selected period of time. The structure of mesoporous materials can be altered by varying the surfactant/SiO_2 ratio [11]. It has been found that [42] as the surfactant/silica molar ratio is varied different siliceous products are obtained which could be classified into four groups as presented in Table 1.3.2 and Fig. 1.3.1. It had been demonstrated that the preparation of MCM-41 materials can be achieved by wide range of synthesis conditions (e.g. type and concentration of surfactants, temperature, pH, reaction time, silica source, etc) [15, 84, 85, 89].

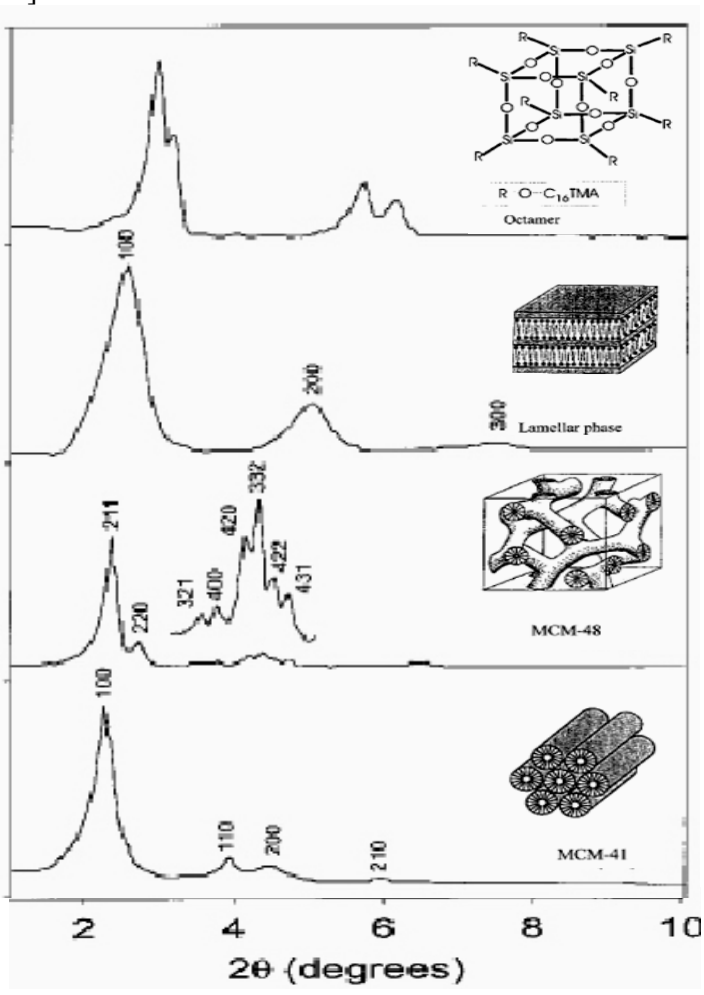

Fig. 1.3.1: Powder XRD patterns of different phases obtained with varying surfactant/silica ratio of the M41S family.

Table 1.3.2: Classification of M41S mesoporous molecular sieves.

Surfactant/silica	Phase
< 1.0	Hexagonal (MCM-41)
1.0 - 1.5	Cubic (MCM-48)
1.2 - 2.0	Lamellar Phase (MCM-50)
2.0	Octamer [(CTMA)$SiO_{2.5}$] [19]

MCM-41 can also be obtained at room temperature [32, 116-120]. For many applications it is desirable to have a simplistic and reproducible method which allows the preparation of large amounts of high quality MCM-41 in a short period which can achieved using room temperature synthesis. The benefits of using room-temperature route are 1) short reaction times, 2) cost and power savings, 3) excellent reproducibility and 4) no need to use expensive autoclaves. In most of the room-temperature synthesis procedures, tetra-n-alkoxysilanes such as tetraethylorthosiliate (TEOS), or tetrapropylorthosiliate (TPOS) were employed as a silica source which is added to an aqueous solution of a cationic surfactant. In view of making MCM-41 in more cost effective way, the synthesis of Si-MCM-41 at room temperature has also been thoroughly investigated [16] using sodium silicate, a cheaper silica source. However, the requirements such as high surfactant concentration, prolonged calcination time and pH adjustment using some dilute acids or with some other chemicals such as ethyl acetate make the method inconvenient when MCM-41 is to be used for industrial applications.

The use of simple and elegant microwave heating methods in the synthesis of MCM-41 is currently gaining much importance. The novelty of the microwave assisted preparation of MCM-41 over the conventional hydrothermal method is remarkable decrease in reaction times, as well as homogeneous heating [123-125]. It is also possible to quickly synthesize MCM-41 with small particle size and enhanced pore wall thickness by ultrasound [126,127].

The hydrothermal and room temperature synthesis of mesoporous materials has also been done in acidic medium. Huo et al.[33,53] reported the synthesis of mesoporous silica under acidic conditions. In the acid route, the silica source is silicon alkoxides. The acid catalysis speeds up the hydrolysis versus the condensation rate and promotes mostly condensation at the ends of silica polymers to form linear silicate ions [95]. On the other hand, the alkaline catalysis favors both hydrolysis and condensation. Thus, the alkaline route leads to a highly condensed and compact structure, and the acid route leads to a more fuzzy and soft network [95]. The acid route is popular for studying its rich morphology, whereas the alkaline route usually provides more stable and ordered materials because silica are highly condensed. The products obtained are filtered, washed several times with water and dried at ambient temperature. Surfactant molecules are removed by calcination leaving porous silicate/aluminosilicate network. The conventional method of surfactant removal by calcination ($\geq$773 K under a flow of Ar, N_2, O_2, or air) of the as-synthesized MCM-41 affects the surface area, pore size, and pore volume of the material. Several other methods such as acid treatment [128], liquid extraction [52,54,125], and supercritical fluid extraction [151,152] have been employed to extract the occluded surfactant molecules.

1.4. MODIFICATION OF MOLECULAR SIEVES

Pure siliceous mesoporous molecular sieves possess a neutral framework, which limits their applications. In order to provide molecular sieves with potential catalytic applications, it is possible to modify the nature of the framework by introduction of heteroatoms. Attempts were made to modify the nature of framework by isomorphous substitution of desired heteroatoms during their hydrothermal synthesis. Another route

followed to modify the property of silica based mesoporous molecular sieves is to incorporate the heteroatoms on the surface of the materials by grafting or impregnation.

When hydrothermal method is used to substitute silicon by trivalent cations like Al^{3+}, B^{3+}, Ga^{3+} and Fe^{3+} etc [96-100, 102, 146] in the walls of the mesoporous silica, the framework possesses negative charges that can be compensated by protons providing acid sites. The number of acid sites and strength depend on the amount and nature of the incorporated metal. Such materials are used in acid catalyzed reactions and have potential applications in various petroleum refining processes [103,104]. When other tetravalent cations like Ti^{4+}, Sn^{4+}, V^{4+} etc [105-108] are incorporated, the corresponding mesoporous materials are used in oxidation reactions of bulky molecules using either H_2O_2 or TBHP as oxidant [33,104-106,109-111]. The synthesis and characterization of mesoporous silica modified by metals like Cr [112-114], Mn [94] or Mo [113] has been found to be catalytically active in the hydroxylation of phenol, 1-naphthol and oxidation of aniline with aqueous H_2O_2.

In addition to variable pore diameters and large surface area, mesoporous molecular sieves have a number of surface silanol groups, which can be functionalized by introducing functional organic groups. This is normally achieved through attachment of silane-coupling agents to the mesoporous walls of previously synthesized materials [115].Ti grafted MCM-41 sample showed higher catalytic activity for the epoxidation of alkenes than other supports containing Ti in their framework [121].

Certain reactions such as hydroisomerization and aromatization are carried out on bifunctional catalysts possessing acid functionality of the molecular sieves and the hydrogenation-dehydrogenation property of the metal impregnated on the surface

of the molecular sieves. Such catalysts are usually prepared by loading the metals (Cu, Co, Cs, Ni, Pt, etc.) by impregnation methods [47-49].

1.5. PORE SIZE AND STRUCTURAL STABILITY

One of the most unique and useful features of M41S family materials is the ability to tailor the pore diameter (2–10 nm). This can be achieved in three different ways; (i) by varying the chain length of alkyl groups (from 10 to 18 atoms) in surfactant molecules [11,86] , (ii) by adding auxiliary chemicals such as aromatic hydrocarbons, alkanes of different chain length, trialkylamines, alkyldimethylamines, [11,34,86,87] (iii) by adjusting the composition of the gel and the crystallization variables[129,132]. Other methods used in altering pore diameter of mesoporous molecular sieves are reaction temperature, time and pH [88,89,90]. Water concentration, surfactant concentration, calcination conditions, silicon source and adding sequence of reactant were also found to influence the pore size distribution of MCM-41[85,129,132]. For many applications in catalysis, chemical sensoring or as optical devices etc require well-defined morphologies. The morphology of originally obtained MCM-41 type mesoporous materials [130,131] consists of aggregates and loose agglomerates of small particles. Mono-meric silica source enhance the nucleation rate and give smaller crystals or their aggregates, whereas larger crystals or their agglomerates can be obtained from a solid polymeric silica source [133, 134]. Different synthetic parameters such as gel composition, temperature, pH etc usually yield materials with different particle sizes and shapes [19,119]. MCM-41 can be prepared in the form of spherical and rod like powders, discoids and gyroids, millimeter to micrometer sized particles and hollow spheres, monolithic gels and thin films. Some of the fundamental reasons for such rich morphological behaviors for mesoporous materials are:

the silicate ions act as counterions to the cylindrical micelles to organize into soft hexagonal liquid crystalline phase, the organization of surfactant system can be exploited to form many mesostructures, control of higher hierarchical order of size above the nanometer scale can be achieved by fine-tuning the interface curvature either by changing composition or reaction condition and finally silica condensation reaction can be controlled as in the late stage of the reaction. The self-organization and siloxane bond formation processes can be separately controlled.

For practical applications, the materials under consideration should have good thermal and hydrothermal stabilities. MCM-41 exhibits high thermal stability (1173 K) in dry air [52]. In addition to this, it is relatively stable under acidic conditions, whereas it degrades readily in basic environments [50]. The latter is, however, expected as it is known that (amorphous) silica dissolves partially in water, especially at high pH. On the other hand MCM-41 has a low hydrothermal stability in water, in aqueous solutions, and even in air saturated with water vapor [50, 63]. Furthermore, the structure collapses by mechanical compression through the hydrolysis of siloxane bonds in the presence of adsorbed water [69]. However, the structural stability can be improved by increasing the pore wall thickness and hydrophobicity, i.e., by decreasing the number of silanol groups in the framework structure by varying different synthesis parameters and also by post synthesis treatments [2, 19].

1.6. PHYSICO-CHEMICAL CHARACTERIZATION

Characterization of the mesoporous materials by means of analytical techniques is far most important to know its properties. A number of techniques have been used to characterize different types of mesoporous materials and related molecular sieve

materials. Each technique is unique by itself and provides important information for the understanding of different structural/compositional features of a particular mesoporous material. Among all, the most commonly used characterization techniques to determine the structure and composition of mesoporous materials are given in Table. 1.6.1.

Table 1.6.1: Physico-chemical characterization techniques, basis and information.

Analysis method	Physical basis	Information
X-ray diffraction (XRD)	Monochromatic beam of X-rays of wavelength λ, incident on a sample made of small crystallites, will be diffracted by sets of planes of high atomic concentrations.	Crystallinity of the samples, unit cell parameter, particle size, composition, etc.,
N_2 adsorption-desorption of gases at low temperature (N_2 Sorption)	Adsorptions of gaseous molecules or liquids at lower temperature and high pressure and desorption of the same at decreased pressure.	Surface area, pore size distribution and pore volume of solid materials.
Electron microscope (TEM, SEM)	Interaction of electron with matter	Morphology, particle size and compositions.
Ultra violet-visible adsorption spectroscopy (DRUV-Vis)	Electronic excitation of atoms or molecules by adsorption of radiation in the ultra violet-visible region.	Identification of the metal ion co-ordination and its existence in the framework or extra-framework position
Thermogravimetric analysis (TG/DTG)	Change in weight of a system under examination as the temperature is increased at a predetermined and preferably at a linear rate/Measuring of thermal effects associated with physical and chemical changes by a differential method.	Determination of compositions of complex mixture, purity and thermal stability associated with physical/ chemical changes with respect to temperature.
Chemical Analysis and Spectroscopic (Atomic absorption spectrometer (AAS),	The basis of quantitative analysis depends on measurement of radiation intensity given out by atoms when excited to higher energy levels when some sort of energy is provided to them in ground state by a source such as a flame.	Determination of concentration of various elements in liquids and solids.

1.6.1. Powder X-ray Diffraction (XRD)

Powder X-ray diffraction is the most important tool used to identify and measure the orderness of structure, phase purity, degree of crystallinity and unit cell parameters of mesoporous and microporous materials. It also helps in the study of the kinetics of formation of molecular sieves. As the powder pattern is the finger print of the molecular sieve structure, phase purity and percent crystallinity of the synthesized molecular sieve can be ascertained by comparing with the standard pattern for the molecular sieve under investigation. Microporous solids show characteristic peaks in the 2θ range of 5-50º whereas the mesoporous materials exhibit characteristic peaks in the low angle region between 1.5-10º (2θ). X-ray diffraction pattern of MCM-41 structures shows a typical four-peak pattern with (100) diffraction peak at lower angle and three (110), (200) and (210) diffraction peaks at higher angle [10,11]. In the case of MCM-41 the wall thickness of hexagonal channels is usually calculated by subtraction of the inner pore diameters obtained by gas adsorption from the unit cell dimensions determined by XRD. Isomorphous substitution of a heteroatom in the framework of the molecular sieves can be predicted by calculating the changes in the unit cell parameters and unit cell volume. This is one of the indirect ways to confirm isomorphous heteroatom substitution.

1.6.2. N_2 Adsorption-Desorption Measurements (N_2 Sorption)

Adsorptions of gaseous molecules or liquids at lower temperature and high pressure yield information about the hydrophilicity/hydrophobicity, surface area, pore dimensions and pore volume while desorption of the same gives information about pore size distribution of the mesoporous molecular sieves. The most common method for

measuring surface area, pore volume and pore size distribution of mesoporous materials was developed by Brunauer, Emmett and Teller (BET) using nitrogen as adsorbent. Measurement of the amount of nitrogen gas adsorbed or desorbed is the most commonly used procedure for determining the pore size distribution of mesopores. The BET volumetric gas adsorption technique using nitrogen, argon, etc. is a standard method for the determination of the surface areas, pore volumes and pore size distribution of molecular sieves [135]. Relation between the amount adsorbed and the equilibrium pressure of the gas at constant temperature is defined by the adsorption isotherm. N_2-adsorption-desorption isotherms of MCM-41 and MCM-48 are of the type IV isotherm [2,10,19]. The steep increase in N_2 adsorption (within the P/P_0 range between 0.2 to 0.4) corresponds to capillary condensation within uniform pores. The sharpness and the height of this step reflects the uniformity of the pore size and the pore volume respectively. The wall thickness of hexagonally packed silicates (MCM-41) was determined as the difference between the repeat distance $a_0 = 2d_{100}/\sqrt{3}$ (from XRD) and the BJH (Barret-Joyner-Halenda) pore diameter using N_2 adsorption. Although NLDFT (Non local density functional theory) can be used for pore size estimation [64, 65], simpler BJH method is useful for comparison purpose even though is known to underestimate the pore sizes.

1.6.3. Transmission Electron Microscopy (TEM)

The topographic information obtained by TEM at near atomic resolution has been a key method for the structural characterization and identification of the various phases of mesoporous materials, i.e. hexagonal (MCM-41), cubic (MCM-48) and lamellar (MCM-50) phases [11,33,52,136,137,138]. More than one model with a hexagonal array of large cylindrical pores with thin walls gives a similar XRD pattern, but

TEM gives a direct, precise and simultaneous measurement of the pore diameter and pore thickness. HRTEM (High Resolution Transmission Electron Microscopy) can be successfully used to examine the microstructural feature of mesoporous molecular sieves [137,138]. In addition to structural characterization, it can also be used to detect the location of metal clusters and heavy cations in the framework [138].

1.6.4. Scanning Electron Microscopy (SEM)

Electron microscopes are instruments, which uses beam of highly energetic electrons to create magnified images of tiny crystals or particles. An electron gun emits a beam of high energy electron that travels through a series of magnetic lenses, which focus the electrons to a very fine spot or sample. The main difference between SEM and TEM is that SEM sees contrast due to the topology of a surface, whereas TEM projects all information in a two dimensional image, which is of nanometer resolution.

Scanning Electron microscope (SEM) is also an important tool that has been used particularly to examine the topology and morphology of microporous and mesoporous molecular sieve materials. Different types of morphology of the synthesized materials as well as the presence of any amorphous phase in the samples can be characterized using this technique.

1.6.5. Diffuse Reflectance UV-Vis Spectroscopy (DRUV-Vis)

This technique measures the scattered light reflected from the surface of samples in the UV-visible range (200-800 nm). The diffuse reflectance UV-Vis spectroscopy is known to be a very sensitive and useful technique for the identification and characterization of the metal ion coordination and its existence in the framework or extra-framework position of metal containing molecular sieves. The position of "ligand-

to-metal charge transfer" (L→M) band depends on the ligand field symmetry surrounding the metal center and the electronic transitions from ligand-to-metal require higher energy for a tetra-coordinated metal ion than for a hexa-coordinated one. For most of the isomorphously substituted microporous and mesoporous metallo–silicate (particularly Ti, Sn and V-containing) molecular sieves, transitions in the UV region (200-400 nm) are of prime interest [139-141].

1.6.6. Thermal Analysis (TG-DTG)

An important thermal analytical technique thermogravimetry (TG) and its derivative differential thermal gravimetry (DTG) have been widely used to get information on the thermal stability of as-synthesized microporous and mesoporous molecular sieves. Further, it provides information of temperature at physisorbed water is removed, oxidative decomposition of the occluded organic cations in the pores and channels of molecular sieves and dehydroxylation of Si-OH groups in the channels of molecular sieves takes place. The temperature at which an exotherm appears in the DTG after the loss of water molecules, gives helpful information about the temperature required to remove the template molecules from the pores of the molecular sieves during calcination [68].

1.6.7. Chemical Analysis (Chem. Anal.)

Chemical analysis by gravimetric and volumetric methods followed by atomic absorption spectrometer (AAS) analysis gives vital information about the chemical composition of the reagents/raw materials and various solid materials. The principle of atomic absorption is based on energy absorbed during transitions between electronic energy levels of an atom. When some sort of energy is provided to an atom in ground state by a source such as a flame (temperature ranging from 2373 - 3073 K), outer-shell

electrons are promoted to a higher energy excited state. The radiation absorbed as a result of this transition between electronic levels can be used for quantitative analysis of metals and metalloids present in solid matrices, which have to be dissolved by appropriate solvents before analysis. The basis of quantitative analysis depends on measurement of radiation intensity and the assumption that radiation absorbed is proportional to atomic concentration. Analogy of relative intensity values for reference standards is used to determine elemental concentrations [142].

1.7. CATALYTIC APPLICATIONS OF MESOPOROUS MATERIALS

Catalysts are substances that facilitate a chemical reaction by lowering the energy barrier of the reaction pathway and thus increasing the reaction rate [143]. Three groups of materials can be recognized as catalysts on the basis of nature of the substances: homogeneous catalysts, bio-catalysts (e.g. enzyme), and heterogeneous catalysts. It is evident from the literature survey on mesoporous molecular sieves, that these materials have opened new opportunities in the field of catalysis [144].

The unique physical properties (e.g. high specific surface area, large pore size etc.) of MCM-41 have made these materials highly desirable hosts for the fixation of large active complexes. The high surface area and large pore size of MCM-41 favour high dispersion of the active species and provide easy accessibility to large feed stock molecules making it an attractive catalyst. Due to large void space the diffusional restrictions of reactants/products are absent and therefore, these materials are quite suitable for catalytic applications involving bulky molecules. Other potential applications for these novel materials are in sorption, separations, polymer chemistry etc. To date several mesoporous metallosilicates with significant catalytic properties have been

synthesized. Some of the reactions studied on different metallosilicate with MCM-41 prepared with hydrothermal or impregnation methods are listed in Table 1.7.1. The advantages of mesoporous materials in the synthesis of fine chemicals have got paramount importance due to fast diffusion of large reactants as well as products through the pores, which substantially minimize the formation of unwanted secondary products. A good example for the shape selective alkylation of 2,4-di-tert-butylphenol with cinnamyl alcohol, carried out on Al-MCM-41, demonstrates that unlike large pore HY zeolite, benzopyran is the major product since there is no diffusional problems in MCM-41 [101].

Table 1.7.1: Reactions studied on mesoporous metallosilicate molecular sieves

Sr.No.	Catalysts	Reaction	Ref
1	Cr-MCM-41	Oxidation of 1-naphthol, phenol and aniline with H_2O_2	114
2	Mn-MCM-41	Oxidation of cyclohexane and propene to CO_2	139
3	Fe-MCM-41	Oxidation of cyclohexane	139
4	Co-MCM-41	Oxidation of cyclohexane	139
5	Sn-MCM-41	Hydroxylation of phenol and 1-naphthol with H_2O_2 and epoxidation of norbornene with TBHP	140
6	Mo-MCM-41	Oxidation of cyclohexanol and cyclohexane with H_2O_2	139
7	Zr-MCM-41	Oxidation of cholesterol and 1-naphthol with TBHP	141
8	Ti-MCM-41	Epoxidation of *cis*-cyclooctene with TBHP	145
9	Al-MCM-41	Conversion of plastic wastes into hydrocarbons with low aromatic content	150
10	V-MCM-41	Oxidation of cyclodecane and 1-naphthol using H_2O_2 as oxidant	107
11	Na-MCM-41/ Cs-MCM-41	Knoevenagel condensation of benzaldehyde with ethyl cyanoacetate	147
12	Cs-MCM-41	Addition of diethyl malonate to neopentyl glycol	122
13	Cu-MCM-41	Oxidation of n-hexane using TBHP as oxidant	148
14	Pt-MCM-41	Oxidation of carbon monoxide	149
15	Ni-MCM-41/ Mo-MCM-41	Hydrodenitrogenation, hydrodesulfurization and hydrocracking of gas oil	153

Mesoporous Ti-MCM-41 were used for the epoxidation of norbornene with tert-butyl hydroperoxide (TBHP) and oxidation of 2,6-di-tert-butylphenol (2,6-DTBP) with aqueous H_2O_2, respectively[106]. Although the intrinsic activity of Ti-MCM-41 is lower than that of TS-1 and Ti-beta particularly for the epoxidation of small molecules with aqueous H_2O_2, it showed higher catalytic activity in the epoxidation of bulkier norbornene with TBHP.

1.8. SCOPE AND OBJECTIVES OF THE THESIS

The present work deals with optimization of synthesis parameters for the preparation of Si-MCM-41 and Sn-MCM-41 mesoporous and its characterization. So far there are no reports on systematic study on the influence of nature of relatively cheaper silica source with high silica content on the kinetics of phase development and on the textural/structural, stability and morphological properties of MCM-41 materials. The influence of different silica sources, surfactant, surfactant concentration, temperature, time, pH, synthesis method on the progressive phase development, textural properties, structural stability and morphological properties of Si-MCM-41 were investigated. The results on the synthesis, characterization and catalytic application of Sn-MCM-41 materials are also described.

The objectives of the thesis:

1. To optimize the synthesis variables such as gel composition, temperature, time and pH for hydrothermal synthesis of Si-MCM-41.
2. To optimize the hydrothermal synthesis of Si-MCM-41 from SiO_2: xCTMABr: yCTMAOH: zTMAOH: $25H_2O$ system where x = 0.0 - 0.18, y = 0.0 - 0.32 and z = 0.0 - 0.25.

3. To optimize the hydrothermal synthesis and characterization of Si-MCM-41 using different silica sources such as ethyl silicate, fumed silica, silica sol, spray dried precipitated silica, flash dried precipitated silica.
4. To optimize the synthesis parameters for preparation of Si-MCM-41 at room temperature using ethyl silicate as a silica source and comparison with conventional TEOS.
5. To carry out synthesis, characterization and catalytic evaluation of various Sn-MCM-41 obtained by using different tin and silica sources. The results on the performance of selected Sn-MCM-41 materials in Mukaiyama aldol condensation reaction are discussed.
6. To characterize the synthesized samples in detail using various techniques and tools such as elemental analysis, XRD, TG/DTG, N_2 Sorption, TEM, SEM, DRUV-Vis, AAS, GC etc.

1.9. OUTLINE OF THE THESIS

The thesis has been divided into four chapters.

Chapter I: **Introduction**.

This chapter presents the general introduction and available literature on mesoporous molecular sieve materials. Different synthesis strategies, the role of templating surfactants, various proposed mechanisms of synthesis, characterization techniques and catalytic applications of ordered mesoporous materials in particular MCM-41 are discussed in brief. The objectives of the present investigation are outlined at the end of this chapter.

Chapter II: **Experimental.**

This chapter is divided into 3 sections viz. Synthesis, Characterization and Catalytic evaluation.

Synthesis: This section describes the hydrothermal and room temperature synthesis routes followed for the preparation of mesoporous Si-MCM-41 and Sn-MCM-41 molecular sieves. A list of reagents/raw materials used and its composition is included. Typical synthesis procedures including details of preparation of synthesis gel, synthesis conditions, product recovery, drying, calcinations are described. Schematic diagrams are also presented depicting the overall synthesis procedure.

Characterization: In this section**,** instrumental techniques and sampling methods for various techniques such as XRD, N_2 sorption, TEM, SEM, TG/DTG, UV-Vis were described. In order to assess the thermal stability, the procedure followed for conducting different tests such as rehydration followed by calcination, thermal and hydrothermal treatments are also described.

Catalytic Evaluation: This section provides the details regarding the experiments that were carried out for solvent free Mukaiyama-aldol reaction of 1-Methoxy-2-methyl-1-(trimethylsiloxy) propene and benzaldehyde. The experimental set up, reaction conditions, reagents used and product analysis techniques are described in detail.

Chapter III: **Results and Discussion**.

In this chapter, the results obtained from the numerous synthesis trials, characterization of selected silica based and modified materials and catalytic performance of Sn-MCM-41 materials are discussed. The discussion is focused on influence of various synthesis parameters on the textural properties, structural stability and morphological

properties for MCM-41 materials. The content of this chapter has been arranged to present and discuss the results dealing with following strategies.

6. Optimization of synthesis variable such as gel composition, temperature, time and pH for hydrothermal synthesis of Si-MCM-41.
7. Hydrothermal synthesis of Si-MCM-41 from SiO_2: xCTMABr: yCTMAOH: zTMAOH: wH_2O system where x = 0.0 - 0.18, y = 0.0 - 0.32, z = 0.0 - 0.25 and w = 25 - 33.
8. Hydrothermal synthesis and characterization of Si-MCM-41 using different silica sources such as TEOS, ethyl silicate, fumed silica, silica sol, spray dried precipitated silica, flash dried precipitated silica.
9. Optimization of synthesis parameters for preparation of Si-MCM-41 at room temperature using ethyl silicate as a silica source.
10. Synthesis, characterization and catalytic evaluation of various Sn-MCM-41 obtained by using different tin and silica sources. The results on the performance of selected Sn-MCM-41 materials in Mukaiyama aldol condensation reaction are discussed.

Chapter IV: **Summary and Conclusions**

The summary and findings of the present work are drawn in this chapter. Some of the findings are:

1. Nature of the silica source was found to influence the course of structural development, textural/structural and morphological properties of MCM-41. Depending upon the type of silica source used, the % contraction of unit cell parameter caused by calcination was found to vary from 2.17 to 10.8.

2. Amount of water and ammonia were found to play a crucial role in the formation and quality Si-MCM-41 materials at room temperature.
3. The quality of Sn-MCM-41 was found to depend not only on the silica source but also on tin source.
4. Sn-MCM-41 was found to be the potential catalyst for solvent free Mukaiyama-aldol reaction of 1-Methoxy-2-methyl-1-(trimethylsiloxy) propene and benzaldehyde.

A list of paper publications that are originated from the above work is enclosed at the end of this chapter.

1.10. REFERENCES

[1] K.S. Sing, D.H. Everett, R.A. Haul, L. Moscou, R.A. Pierotti, J. Rouquerol, T. Siemieniewska, Pure Appl. Chem. 57 (1985) 603.

[2] D.W. Breck, "Zeolites Molecular Sieves" Wiley, New York (1974).

[3] M.E. Davis, C. Saldarriaga, C. Montes, J. Garces, C. Crowder, Nature 331 (1988) 698.

[4] B.J. Schoeman, J. Sterte, J.E. Otterstedt, J. Chem. Soc. Chem. Commun. (1993) 994.

[5] A.H. Janssen, A.J. Koster, K.P. de Jong, Angew. Chem. Int. Ed 40 (2001) 1102.

[6] I. Schmidt, A. Boisen, E. Gustavsson, K. Stahl, S. Pehrson, S. Dahl, A. Carlsson, C.J.H. Jacobsen, Chem. Mater. 13 (2001) 4416.

[7] V. Chiola, J.E. Ritsko, C.D. Vanderpool, US Patent No. 3 556 25, 1971.

[8] F. Di-Renzo, H. Cambon, R. Dutartre, Micropor. Mater. 10 (1997) 283.

[9] J.S. Beck, C.T. Chu, I.D. Johnson, C.T. Kresge, M.E. Leonowicz, W.J. Roth, J.W. Vartuli, WO Patent 91/11390, 1991.

[10] C.T. Kresge, M.E. Leonowicz, W.J. Roth, J.C. Vartuli, J.S. Beck, Nature 359 (1992) 710.

[11] J.S. Beck, J.C. Vartuli, W.J. Roth, M.E. Leonowicz, C.T. Kresge, K.D. Schmitt, C.T.W. Chu, D.H. Olson, E.W. Shepp- ard, S.B. McCullen, J.B. Higgins, J.L. Schlenker, J. Am. Chem. Soc. 114 (1992) 10834.

[12] T. Yanagisawa, T. Shimizu, K. Kuroda, C. Kato, Bull. Chem. Soc. Jpn. 63 (1990) 988.

[13] S. Inagaki, Y. Fukushima, K. Kuroda, J. Chem. Soc. Chem. Commun. (1993) 680.

[14] S. Inagaki, A. Koiwai, N. Suzuki, Y. Fukushima, K. Kuroda, Bull. Chem. Soc. Jpn. 69 (1996) 1449.

[15] A. Corma, Chem. Rev. 97 (1997) 2373.

[16] U. Ciesla, F. Schuth, Micropor. Mesopor. Mater. 27 (1999) 131.

[17] M. Linden, S. Schacht, F. Schuth, A. Steel, K. Unger, J. Porous. Mater. 5 (1998) 177.

[18] A. Tuel, Micropor. Mesopor. Mater. 27 (1999) 151.

[19] P. Selvam, S.K. Bhatia, C.G. Sonwane, Ind. Eng. Chem. Res. 40 (2001) 3237.

[20] Y. Liu, T.J. Pinnavaia, J. Mater. Chem. 12 (2002) 3179.

[21] J.M. Thomas, Angew. Chem. Int. Ed. 38 (1999) 3588.

[22] R. Anwander, Chem. Mater. 13 (2001) 4419.

[23] J.Y. Ying, C.P. Mehnert, M.S. Wong, Angew. Chem. Int. Ed. 38 (1999) 56.

[24] X. He, D. Antonelli, Angew. Chem. Int. Ed. 41 (2002) 214.

[25] A.P. Wight, M.E. Davis, Chem. Rev. 102 (2002) 3589.

[26] D.E. De Vos, M. Dams, B.F. Sels, P.A. Jacobs, Chem. Rev. 102 (2002) 3615.

[27] G.J. De, A.A. Soler-Illia, C. Sanchez, B. Leveau, J. Patarin, Chem. Rev. 102 (2002) 4093.

[28] D. Trong On, D. Desplantier-Giscard, C. Danumah, S. Kaliaguine, Appl. Catal. A: Gen. 253 (2003) 545.

[29] A. Wingen, F. Kleitz, F. Schuth, Basic Principles in Applied Catalysis, Springer, Berlin, (2003) 281.

[30] S. Biz, M.L. Occelli, Cata.Rev. 40 (1998) 329.

[31] F. Di Renzo, A. Galarneau, P. Trens, F. Fajula, in: F. Schuth, K.S.W. Sing, J. Weitkamp, Handbook of Porous Solids, Wiley-VCH, Weinheim, (2002) 1311.

[32] A. Monnier, F. Schuth, Q. Huo, D. Kumar, D. Margolese, R.S. Maxwell, G. Stucky, M. Krishnamurty, P. Petroff, A. Firouzi, M. Janicke, B. Chmelka, Science 261 (1993) 1299.

[33] Q. Huo, D. Margolese, U. Ciesla, P. Feng, T. Gier, P. Sieger, R. Leon, P.M. Petroff, U. Ciesla, F. Schuth, G. Stucky, Nature 368 (1994) 317.

[34] Q. Huo, D. Margolese, U. Ciesla, D. Demuth, P. Feng, T. Gier, P. Sieger, A. Firouzi, B. Chmelka, F. Schu¨ th, G.D. Stucky, Chem. Mater. 6 (1994) 1176.

[35] G.S. Attard, J.C. Glyde, C.G. Goltner, Nature 378 (1995) 366.

[36] C.F. Cheng, H. He, W. Zhou, J. Klinowski, Chem. Phys. Lett., 244 (1995) 117.

[37] Q. Huo, R. Leon, P.M. Petroff, G.D. Stucky, Science 268 (1995) 1324.

[38] J.N. Israelachivili, D.J. Mitchell, B.W. Ninham, J. Chem. Soc. Faraday Trans. 72 (2) (1976) 1525.

[39] J.N. Israelachivili, Intermolecular and Surface Forces, Academic Press, London, 1991.

[40] G.D. Stucky, A. Monnier, F. Schuth, Q. Huo, D. Margolese, D. Kumar, M. Krishnamurty, P. Petroff, A. Firouzi, M. Janicke, B.F. Chmelka, Mol. Cryst. Liq. Cryst. 240 (1994) 187.

[41] A. Firouzi, D. Kumar, L.M. Bull, T. Besier, P. Sieger, Q. Huo, S.A. Walker, J.A. Zasadzinski, C. Glinka, J. Nicol, D.I. Margolese, G.D. Stucky, B.F. Chmelka, Science 267 (1995)1138.

[42] J.C. Vartuli, K.D. Schmitt, C.T. Kresge, W.J. Roth, M.E. Leonowicz, S.B. McCullen, S.D. Hellring, J.S. Beck, J.L. Schlenker, D.H. Olson, E.W. Sheppard, Chem. Mater. 6 (1994) 2317.

[43] M. Lawrence, J.Chem. Soc. Rev. (1994) 417.

[44] Q. Huo, D.I. Margolese, G.D. Stucky, Chem. Mater. 8 (1996) 1147.

[45] S. Che, A.E. Garcia-Bennett, T. Yokoi, K. Sakamoto, H. Kunieda, O. Terasaki, T. Tatsumi, Nature Mater. 2 (2003) n801.

[46] A.E. Garcia-Bennett, O. Terasaki, S. Che, T. Tatsumi, Chem. Mater. 16 (2004) 813.

[47] J. Okamura, S. Nishiyama, S. Tsuruya, M. Masai, J. Mol. Catal. A Chem., 135 (1998) 133.

[48] K.L. Kloestra, H. Bakkum, Stud. Surf. Sci. Catal., 105 A (1997) 431.

[49] K.L. Kloestra, H. Bakkum,, J. Chem. Soc., Faraday Trans., 93 (1997) 1211.

[50] L.Y. Chen, S. Jaenicke, G.K. Chuah, Micropor. Mater. 12 (1997) 323.

[51] D. Myers, Surfactant Science and Technology; VCH: New York, (1992).

[52] C.Y. Chen, S.L. Burkett, H.X-Li, M.E. Davis, Micro. Mater. 2 (1993) 27.

[53] A. Steel, S.W Carr, M.W. Anderson, J. Chem. Soc. Chem. Comm. (1994) 1571.

[54] P.T. Tanev, T.J. Pinnavaia, Science 267 (1995) 865.

[55] P.T. Tanev, M. Chibwe, T.J. Pinnavaia, Nature 368 (1994) 321.

[56] S.A. Bagshaw, E. Prouzet, T.J. Pinnavaia, Science 269 (1995) 1242.

[57] T.R. Pauly, Y. Liu, T.J. Pinnavaia, S.J.L. Billige, T.P. Rieker, J. Am. Chem. Soc. 121 (1997) 8835.

[58] E. Prouzet, T.J. Pinnavaia, Angew. Chem. Int. Ed. 36 (1997) 516.

[59] P.T Tanev, and T.J. Pinnavaia, Science 271 (1996) 1267.

[60] W. Zhang, M. Fröba, J. Wang., P.T. Tanev, J. Wong, T.J. Pinnavaia, J. Am.Chem. Soc. 118 (1996) 9164.

[61] W. Zhang, T.R. Pauly, T.J. Pinnavaia, Chem. Mater. 9 (1997) 2491.

[62] D. Zhao, Q. Huo, J. Feng, B.F. Chmelka, G.D. Stucky, J. Am. Chem. Soc. 120 (1998) 6024.

[63] D. Zhao, J. Feng, Q. Huo, N. Melosh, G.H. Fredrickson, B.F. Chmelka, G.D. Stucky, Science 279 (1998) 548.

[64] A.V. Neimark, P.I. Ravikovitch, M. Grun, F. Schuth and K.K.Unger, J. of Colloid and Interface Science 207 (1998) 159

[65] K.Schumacher, P.I.Ravikovitch, A.D.Chesne, A.V. Neimark, K.K.Unger, Langmuir 16 (2000) 4648.

[66] D.M. Antonelli, J.Y. Ying, Angew. Chem. Int. Ed. 35 (1996) 426.

[67] S. Inagaki, Y. Fukushima, K. Kuroda, J. Colloid Interface Sci. 180 (1996) 623.

[68] F. Klietz, W. Schmidt, F. Schuth, Micropor. Mesopor. Mater. 65 (2003) 1.

[69] Y.G. Vladimir, F. Xiaobing, B. Zimei, H.L. Gary, A.O. James, J. Phys. Chem. 100 (1996) 6.

[70] D. Zhao, Q. Huo, J. Feng, J. Kim, Y. Han, G. D. Stucky, Chem. Mater. 11 (1999) 2668.

[71] W.W. Lukens, P. Schmidt-Winkel, D. Zhao, J. Feng, G.D. Stucky, Langmuir 15 (1999) 5403.

[72] E. Prouzet, F. Cot, G. Nabias, A. Larbot, P. Kooyman, T. Pinnavaia, J. Chem. Mater. 11 (1999) 1498.

[73] P.T. Tanev, Y. Liang, T.J. Pinnavaia, J. Am. Chem. Soc. 119 (1997) 8616.

[74] S.S. Kim, W. Zhang, T.J. Pinnavaia, Science 282 (1998) 1302.

[75] R. Ryoo, J.M. Kim, C.H. Ko, C.H. Shin, J. Phys. Chem. 100 (1996) 17718.

[76] R. Ryoo, C.H. Ko, I.S. Park, Chem. Commun. (1999) 1413.

[77] T. Kimura, Y. Sugahara, K. Kuroda, Chem. Commun. (1998) 559.

[78] G.S. Attard, C.G. Goltner, J.M. Corker, S. Henke, R.H. Templer, Angew. Chem. Int. Ed. 36 (1997) 1315.

[79] C.G. Goltner, M. Antonietti, Adv. Mater. 9 (1997) 431.

[80] G.S. Attard, P.N. Bartlett, N.R.B. Coleman, J.M. Elliott, J.R. Owen, J.H. Wang, Science 278 (1997) 838.

[81] J.C. Vartulli, C.T. Kresge, M.E. Leonowicz, A.S. Chu, S.B. McCullen, I.D. Johnson, E.W. Sheppard, Chem. Mater. 6 (1994) 2070.

[82] T. Kimura, Y. Sugahara, K. Kuroda, Micropor. Mesopor. Mater. 22 (1998) 115.

[83] S. Inagaki, S. Guan, Y. Fukushima, T. Ohsuna, O. Terasaki, J. Am. Chem. Soc. 121 (1999) 9611.

[84] A. Taguchi, F. Schuth, Micropor. Mesopor. Mater. 77 (2005) 1.

[85] T.R. Gaydhankar, U.S.Taralkar, R.K. Jha, P.N. Joshi, R. Kumar, Catalysis Commun. 6 (2005) 361.

[86] C.T. Kresge, M.E. Leonowicz, W.J. Roth, J.C. Vartuli, U.S. Patent, 5,098,684 (1992).

[87] J.S. Beck, U.S. Patent , 5. 057, 296 (1991).

[88] D. Khushalani, A. Kuperman, G.A. Ozin, K. Tanaka, J. Garcés, M.M. Olken, N. Coombs, Adv. Mater. 7 (1995) 842

[89] X.S. Zhao, G.Q. (Max) Lu, G.J. Miller, Ind. Eng. Chem. Res., **35** (1996) 2075.

[90] X. Chen, L. Huang, Q. Li, J. Phys. Chem. B, 101 (1997) 8460.

[91] R. Schimdt, D. Akporiaye, M. Stöcker, O.H. Ellestad, J. Chem. Soc., Chem. Commun., (1994) 1493

[92] K.A. Koyoano, and T. Tatsumi, Chem. Commun. (1996) 145.

[93] N. Ulagappan, Neeraj, V.N.R. Battaram, C.N.R. Rao, J. Chem. Soc., Chem. Commun. (1996) 2243.

[94] D. Zhao, and D.J Goldfarb, J. Chem. Soc., Chem. Commun. (1995) 875.

[95] C. Sanchez and F. Ribot. New J. Chem. 18, (1994) 1007.

[96] A. Tuel, and S. Gontier, Chem. Mater., 8 (1996), 114.

[97] A. Sayari, I. Moudrakovaski, C. Danumah, C.I. Ratcliffe, J.A. Ripmeester, K.F. Preston, J. Phys. Chem., 99 (1995) 16373.

[98] U. Oberhagemann, I. Topalovic, B. Marler, H. Gies, Stud. Surf. Sci. Catal., 98 (1995) 17.

[99] S. Liu, H. He, Z. Luan, Klinowski, J. Chem. Soc., Faraday Trans., 92 (1996) 2011.

[100] C.F. Cheng, and J.J. Klinowski, Chem. Soc., Faraday Trans., 92 (1996) 289.

[101] E. Armengol, M.L. Cano, A. Corma, H. García, M.T. Navarro, J. Chem. Soc., Chem. Commun. 519 (1995).

[102] Z.Y. Yuan, S.H. Liu, T.H. Chen, J.Z Wang, H.X. Li, J. Chem. Soc., Chem. Commun., (1995) 973.

[103] J.L Casci, Stud. Surf. Sci. Catal., 85 (1994) 329

[104] A. Sayari, Chem. Mater., 8 (1996) 1840.

[105] C.T. Kresge, M.E. Leonowicz, W.J. Roth, J.C. Vartuli, U.S. Patent , 5, 250, 282(1993).

[106] A. Corma, M.T. Navarro, J. Perez-Pariente, J.Chem.Soc.,Chem. Commun.,(1994) 147.

[107] K.M. Reddy, I.L. Moudrakovski, A. Sayari, J.Chem.Soc.Chem. Commun.,(1994) 1059

[108] Z. Luan J. Xu, H. He, J. Klinowski, L. Kevan, J.Phys. Chem., 100 (1996) 19595.

[109] A. Corma, M.T Navarro, Perez-Pariente, F. Sanchez, Stud. Surf. Sci. Catal., 84 (1994) 69.

[110] T.J. Pinnavaia, P.T. Tanev, J. Wang, W. Zhang, Mater. Res. Soc. Symp. Proc.,371 (1995) 53.

[111] J.S. Reddy, P. Liu, A. Sayari, Appl. Catal. A: General, 148 (1996) 7.

[112] W. Zhang, T.J. Pinnavaia, Catal. Lett., 38 (1996) 261.

[113] W. Zhang, J. Wang, P.T. Tanev, T.J. Pinnavaia, T.J., Chem. Commun., (1996) 979.

[114] N. Ulagappan, and C.N.R. Rao, J. Chem. Soc., Chem. Commun., (1996) 1047.

[115] D.H. Olson, G.D. Stucky, J.C. Vartuli, U.S. Patent, 5, 364, 797 (1994).

[116] N. Igarashi, K. Koyano, Y. Tanaka, S. Nakata, K. Hashimoto, T. Tatsumi, Micropor. Mesopor. Mater. 59 **(**2003) 43.

[117] I.S. Paulino and U. Schuchardt , Stud. Surf.Sci.Catal. 141 (2002) 93.

[118] Q.Cai, W.Y. Lin, F.S. Xiao, W.Q. Pang, X.H. Chen and B.S. Zou, Micropor. Mesopor. Mater. 32 (1999) 1.

[119] M. Grün, K.K. Unger, A. Matsumoto, K. Tatsumi, Micropor. Mesopor. Mater. 27 **(**1999) 207.

[120] A.C. Voegtlin, A. Matijasic, J. Patarin, C. Sauerland, Y. Grillet, L. Huve , Micropor. Mater. 10 (1997) 137.

[121] T. Maschmeyer, F. Rey, G. Sanker, J.M. Thomas, Nature, 378 (1995) 159.

[122] K.L Kloestra, and H, Bakkum, Stud. Surf. Sci. Catal., 105 A (1997) 431.

[123] S. Shangzhao and Y.H. Jiann Journal of Minerals & Materials Characterization & Engineering, 2 (2003) 101.

[124] D.S. Kim, J.S. Chang, J.O. Ryu, and S.E. Park, Zeolitic Materials, 1 (2000) 49.

[125] S.E. Park, D.S. Kim, J.S. Chang, and W.Y. Kim, Catal. Today, 44 (1998) 301.

[126] M. Run, S. Wu, G. Wu, Micropor. Mesopor. Mater. 74 (2004) 37.

[127] X. Tang, S. Liu, Y. Wang, W. Huang, E. Sominski, O. Palchik, Y. Koltypin and A. Gedanken, Chem. Commun., (2000) 2119.

[128] S. Kawi, M.W. Lai, Chem. Commun. (1998) 1407.

[129] C.C. Wu, T S. Tsai, C.N. Liao, K.J. Chao, Mesopor. Mater. 7 (1996) 173.

[130] B.L. Meyers, S.R. Ely, N.A Kutz, J.A Kudak, E.J. Van den Bossche, J. Catal. 91, 352 (1985).

[131] B.D. McNicol, and G.T Pott, J. Catal. **25**, 223 (1972).

[132] A. Corma, Q. Kan, M.T. Navarro, J.P. Pariente and F. Key, Chem. Mater. 9 (1997) 2123.

[133] E.G. Derouane, S. Detremmerie, Z. Gabelica and N. lom, Appl. Catal. 1 (1981) 201.

[134] K.J. Chao, T.C. Tsai and M.S. Chen, J. Chem. Soc. Faraday Trans. 77 (1981) 547.

[135] S. Brunauer, P.H. Emmett, and E. Teller, J.Am. Chem. Soc. 60 (1938) 309.

[136] J.S. Beck, J.C. Vartuli, G.J. Kennedy, W.J. Roth, and S.E. Schramm, Chem. Mater., 6 (1994) 1816.

[137] V. Alfredsson, M. Keung, A. Monnier, G.D. Stucky, K.K. Unger, and F. Schüth, J. Chem. Soc., Chem. Commun., (1994) 921.

[138] A. Chenite, Y.L. Page, A. Sayari, Chem. Mater., **7** (1995) 1015.

[139] W.A. Carvalho, P.B. Varaldo, M. Wallau, U. Schuchardt, Zeolites 18 (1997) 408

[140] K. Chaudhari, T.K. Das, P.R. Rajmohanan, K. Lazar, S. Sivasanker, A.J. Chandwadkar, J. Catal. 183, 281 (1999).

[141] K. Chaudhari, R. Bal, D. Srinivas, A.J. Chandwadkar, S. Sivasanker, Micropor. Mesopor. Mater. 50, 209 (2001).

[142] J.W. Robinson, Atomic Absorption Spectroscopy, Marcel Dekker, New York, 1975. Chapter 1 Introduction and Literature Survey.

[143] J.M. Thomas, Principles and Practice of Heterogeneous Catalysis, VCH, Weinheim, 1997.

[144] Anon, Fed. Reg. 13 (1992) 57.

[145] I. Vankelecom, K. Vercruysse, N. Moens, R. Parton, J.S. Reddy, P.A. Jacobs, Chem. Commun. 137 (1997).

[146] C.F Cheng, H. He, W. Zhou, J. Klinowski, L.F. Sousa Goncalves, L.F. Gladden, J. Phys. Chem., 100 (1996) 390.

[147] R.K. Kloetstra, and H. Bekkum, J. Chem. Soc., Chem. Commun. (1995) 1005.

[148] S. Ernst, R. Glaser, M. Selle, Stud. Surf. Sci. Catal., 105 A (1997) 69.

[149] U. Junges, W. Jacobs, I. Voigt-Martin, B. Krutzsch, F. Schüth, J. Chem. Soc., Chem. Commun. (1995) 2283.

[150] J. Aguado, D.P Serrano, M.D. Romero, J.M. Escola, J. Chem. Soc., Chem. Commun., (1996) 725.

[151] F. Schuth,. Ber. Bunsen-Ges. Phys. Chem. 99 (1995) 1306.

[152] S. Hitz, R.J. Prins, J. Catal. 168, (1997) 194.

[153] A. Corma, A. Martínez, V. Martínez-Soria, J.B. Monton, J. Catal., 153 (1995) 25.

CHAPTER – 2

EXPERIMENTAL

This chapter is divided into 3 sections viz. Synthesis, Characterization and Catalytic evaluation

2.1. SYNTHESIS

The present chapter deals with the detailed description for synthesis of mesoporous silicates, using different sources of silica, surfactant and its concentration at various synthesis times and temperatures. Synthesis of mesoporous materials was carried out by hydrothermal method and by room temperature method. Syntheses of mesoporous materials by hydrothermal method are carried in Teflon lined stainless steel autoclave (Fig 2.1.1).

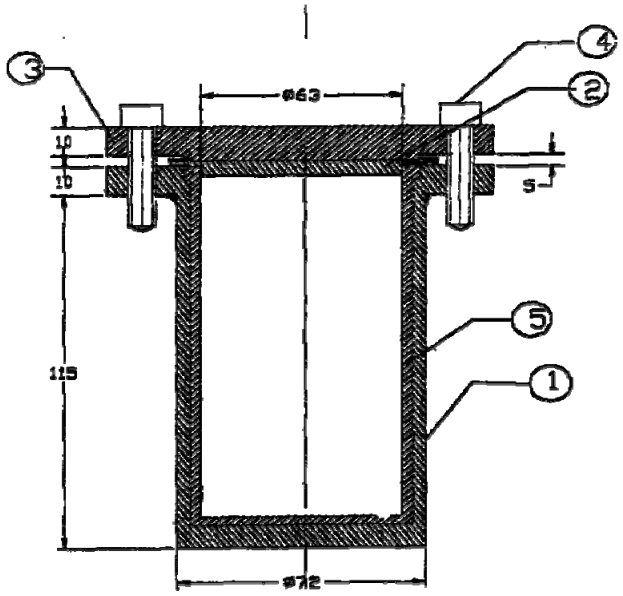

Fig. 2.1.1: Teflon lined Stainless steel autoclave [1-Housing, 2-Teflon Cover, 3-Flange, 4-Allen Bolt, 5-Teflon Liner]

Autoclaves were cleaned with aqueous hydrofluoric acid and flushed with distilled water several times, prior to the synthesis. Syntheses of mesoporous materials by room temperature method are carried out in polypropylene containers. As-synthesized samples are to be calcined to remove the surfactant and before they can be useful for further investigation. To study the effect of calcination on the as-synthesized sample two different

calcination programs were performed in presence of air. These experiments were performed using 2 gms of the as-synthesized sample. In program 1 gm the sample was heated to 813 K from room temperature at rate of 1 K/min. and then kept at this temperature for 6 hrs. Samples calcined using this program I gave only amorphous materials. In program II a stepwise heating was used for removal of the template by calcination in air at 813 K for 6 hrs (heating rate of 1 K/min, dwell time of 2 hrs at 373 K, 473 K and 623 K). Finally the sample was allowed to cool slowly to room temperature. Sample calcined with program II exhibited a typical four peak pattern with a very strong (100) reflection and three weaker (110), (200) and (210) reflections which indicate good quality MCM-41, hence all the samples were calcined using program two in the following chapters. An alternative method of solvent extraction was also used for surfactant extraction of as-synthesized sample. To study the effect of various extraction media on template extraction and the quality of the product formed, various trial runs where conducted using ethanol + hydrochloric acid, methanol + hydrochloric acid and ethanol + ammonium nitrate as extraction media, which was stirred at 323 K for a few hours followed by calcination at 813 K for a 4 hrs. Extracted samples were weighted before and after calcination in order to determine the amount of surfactant removed by the extraction mixture. It was found that only 70-80 % surfactant is removed in various extractions runs, hence all samples were calcined using program II of calcination.

A list of reagents/raw materials and its composition used in synthesis, characterization and catalytic evaluation are tabulated in Table 2.1.1. The chemicals were used as received without any further purification if not mentioned specifically.

Table 2.1.1: Specifications of chemical used in synthesis, characterization and catalytic evaluation.

Sr. No.	Reagents/Raw Materials	Chemical formula	Purity
1	Fumed silica (Aldrich)	SiO_2	99.9 wt % SiO_2 (Surface area 360-400 m^2/g)
2	Ethyl silicate (V.P. Chemicals, Pune, India)	SiO_2	99%, 40 wt % SiO_2
3	Silica sol (V.P. Chemicals, Pune, India)	SiO_2	99%, 40 wt % SiO_2
4	Spray dried precipitated silica (V.P. Chemicals, Pune, India)	SiO_2	99.2 wt % SiO_2 (Surface area 280-320 m^2/g)
5	Flash dried precipitated silica (V.P. Chemicals, Pune, India)	SiO_2	99.2 wt % SiO_2 (Surface area 170-210 m^2/g)
6	CTMABr (Dishman Pharmaceutical and Chem. Ltd, Mumbai, India)	$C_{16}H_{33}N(CH_3)_3Br$	99.0 %
7	Tin tert-butoxide (Lancaster)	$Sn(OC(CH_3)_3)_4$	99.5%
8	Aqueous CTMAOH (National Chemical Laboratory, Catalysis Division, Pune, India)	$C_{16}H_{33}N(CH3)_3OH$	14.0 wt % $[OH^-]$
9	Aqueous Ammonium hydroxide (V.P. Chemicals, Pune, India)	NH_4OH	28.0 wt % $[OH^-]$
10	Tin-Chloride (Loba Chemie, India)	$SnCl_4.5H_2O$	98.0 %
11	Sodium-Stannate (Robert Johnson)	Na_2SnO_3	98.0 %
12	Aqueous TMAOH (V.P. Chemicals, Pune, India)	$(CH_3)_4NOH$	25.0 wt % $[OH^-]$
13	Methyl trimethyl silyl ketene acetal (Merck India Ltd)	$C_8H_{18}O_2Si$	95.0 %
14	Benzaldehyde (Merck)	C_6H_5CHO	98.0 %
15	Hydrochloric Acid (Thomas Baker, Mumbai, India)	HCl	36.5 %
16	Hydrofluoric Acid (Thomas Baker, Mumbai, India)	HF	48 % (Electronic Grade)
17	Sulfuric Acid (Qualigens, Mumbai, India)	H_2SO_4	98%

2.1.1. Synthesis of Si-MCM-41 Type Mesoporous Materials

Silica source were added slowly to a mixture of surfactant solution and aqueous TMAOH/NH_4OH under constant stirring to obtain homogeneous gel. The schematic diagram given in Fig 2.1.1.1 shows typical procedure followed for the synthesis of Si-MCM-41 materials**.**

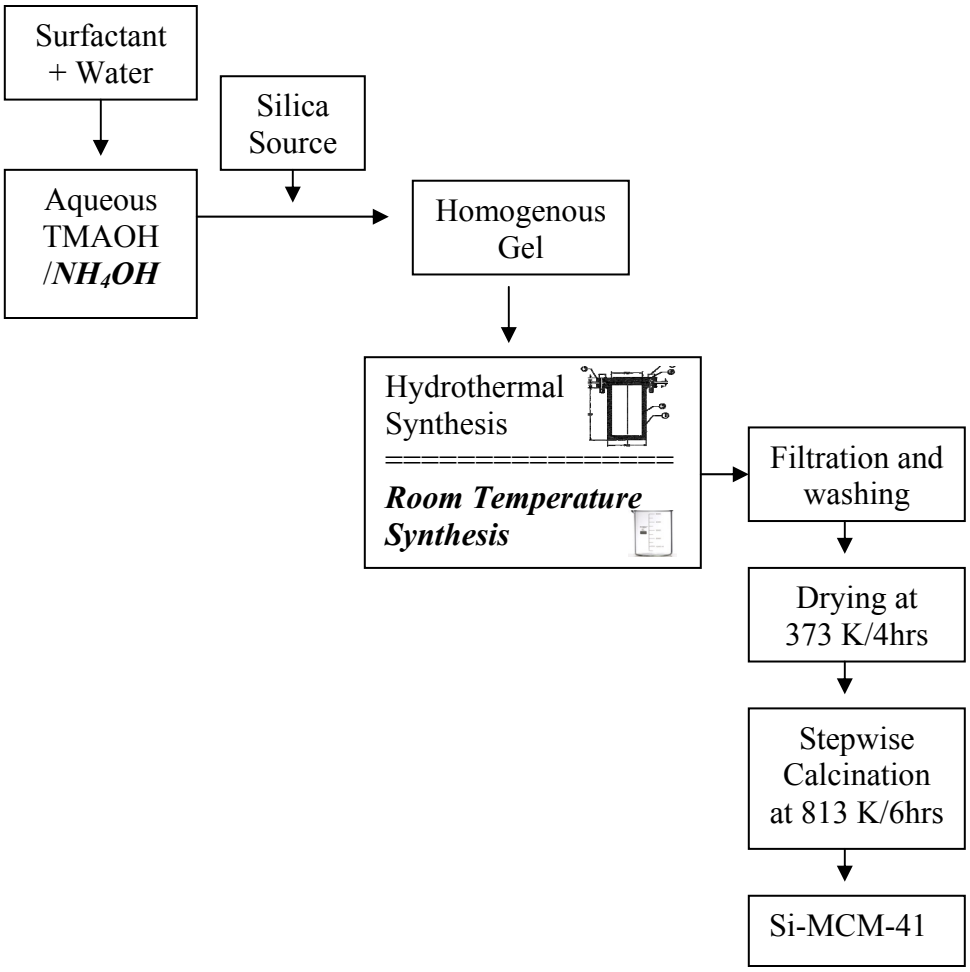

Fig. 2.1.1.1: Schematic diagram showing typical procedure for the synthesis of Si-MCM-41 materials

2.1.1.1. Hydrothermal synthesis of Si-MCM-41

In order to investigate the role of silica source materials, type and concentration of the different surfactants on the quality of Si-MCM-41, gels with different combinations of

silica sources, surfactants and concentrations were prepared and subjected to hydrothermal treatment. Synthesis of Si-MCM-41 by hydrothermal method was done with various molar gels compositions SiO_2 : x CTMABr : y CTMAOH : z TMAOH : w H_2O where x = 0 - 0.18, y = 0 - 0.32, z = 0 - 0.25 and w = 25 - 33. In typical synthesis procedure 3.5 gms of CTMABr was dissolved in 15.2 gms of water. This solution was added to an aqueous solution containing 4.9 gms TMAOH with constant stirring. Then 3.2 gms fumed silica was added to this mixture under stirring for 1 hrs. After further stirring for 2 hrs, the resulting gel having molar gel composition SiO_2 : 0.18 CTMABr : 0.25 TMAOH : 25 H_2O was heated in a sealed teflon lined stainless steel autoclave as shown in section 2.1 at 383 K for 48 hrs. The product was recovered by filtration, washed thoroughly with distilled water and then dried at 373 K for 4 hrs. In the synthesis of Si-MCM-41 wherein CTMAOH was used in place of CTMABr, the required quantity of CTMAOH was mixed with required amount of aqueous TMAOH solution. Then the desired silica source was added slowly to the above mixture and further stirred and then autoclaved at desired temperature and time. Pre-Optimized calcination procedure as mentioned in section 2.1 was used in order to drive-off the surfactant

Five different silica sources (Fumed silica, Silica sol, Ethyl silicate, Spray dried precipitated silica and Flash dried precipitated silica) were used in preparation Si-MCM-41 under the identical set of synthesis conditions. Except desired silica source, other synthesis parameters such as gel composition, addition sequence, synthesis temperature, ratio of charged reaction mass to autoclave volume and downstream process conditions were kept constant

2.1.1.2 Room temperature synthesis of Si-MCM-41

Optimization of synthesis parameters for preparation of Si-MCM-41 at room temperature using ethyl silicate as a silica source was carried out. Si-MCM-41 was prepared at room temperature using two different silica sources (ethyl silicate and TEOS) for comparison purpose. The typical procedures adopted for synthesizing Si-MCM-41 using TEOS and ethyl silicate are similar. Synthesis of Si-MCM-41 at room temperature with various molar gels compositions SiO_2 : x CTMABr : y NH_4OH : z H_2O where x, y and z was varied in the range of $0.06 < x < 0.24$, $2.5 < y < 32.5$, $25 < z < 800$ were prepared using ethyl silicate as a source of silica. In a typical room temperature synthesis of Si-MCM-41, 2.04 gms CTMABr was dissolved in 114 ml of distilled water under constant stirring. To this solution, 16.33 gms of aqueous ammonia solution was added and stirred for 10 min. Finally, the desired silica source (7.0 gms ES or 10 gms TEOS) was added drop wise with vigorous stirring to obtain final gel of composition SiO_2 : 0.12 CTMABr: 2.50 NH_4OH : 150 H_2O. The stirring was continued for a period of 4 hrs. The product was recovered by filtration, washed thoroughly with distilled water and then dried at 373 K for 4 hrs. The removal of the template was accomplished by pre-optimized calcination procedure as mentioned in section 2.1.

2.1.2. Synthesis of Sn-MCM-41 Type Mesoporous Materials

Silica source were added slowly to a mixture of surfactant solution and aqueous TMAOH under constant stirring. After stirring this gel for sufficient time Tin source was added and stirring was further continued to obtain homogeneous gel. The schematic diagram given below in Fig. 2.1.2.1 shows typical procedure followed for the synthesis of Sn-MCM-41 materials**.**

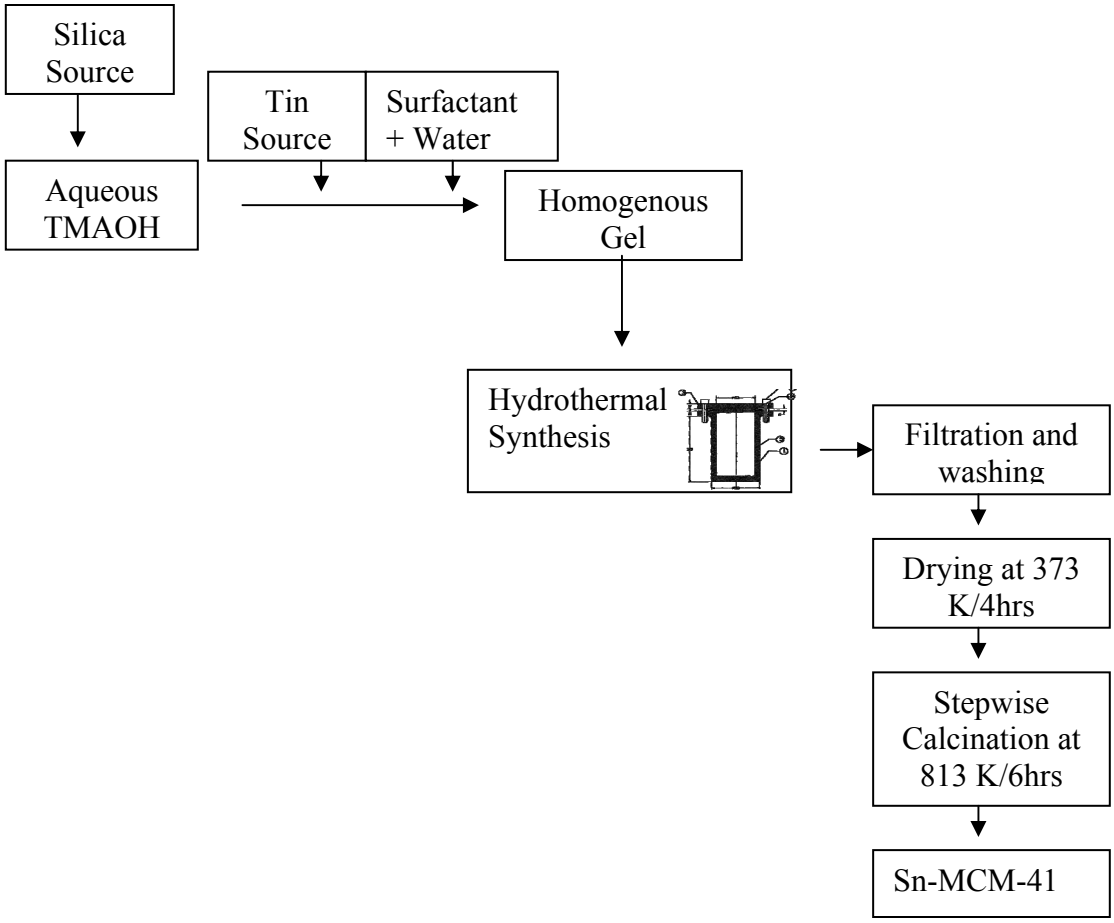

Fig. 2.1.2.1: Schematic diagram showing typical procedure for the synthesis of Sn-MCM-41 materials

2.1.2.1. Hydrothermal synthesis of Sn-MCM-41

Since Si-MCM-41 possesses a neutral framework, it has been used as a catalyst support rather than as a catalyst. In view of making them potential catalysts for suitable applications, incorporation of various Sn into the silicate framework was carried out. In order to investigate the influence of silica and/or tin source materials on the quality of Sn-MCM-41, gels with different combinations of silica and tin sources were prepared and subjected to hydrothermal treatment. The hydrothermal syntheses of Sn-MCM-41 were carried out using different gels with compositions SiO_2 : w SnO_2 : x CTMABr : y TMAOH : z H_2O where w, x, y and z were varied in the range of $0.004 < w < 0.01$, $0.18 < x < 0.32$,

$0.25 < y < 0.35$, $25 < z < 45$. Each system was subjected to identical set of synthesis conditions including down-stream processing to investigate influence of individual parameter on the quality of the phase formed. In a typical synthesis of Sn-MCM-41, 10 gms of fumed silica was added slowly to 18.22 gms of aqueous TMAOH solution with constant stirring. After homogenizing the mixture, 0.24 gms of tin tetrachloride dissolved in 20.33 gms of distilled water was added slowly with constant stirring. To this mixture, 14.66 gms of CTMABr dissolved in 40 gms of distilled water was added with constant stirring. The thick gel thus obtained was stirred for another 2 hrs. The molar composition of this starting synthesis gel was SiO_2 : 0.004 SnO_2 : 0.24 CTMABr : 0.30 TMAOH : 25 H_2O. This gel was then heated in a sealed teflon lined stainless steel autoclave at 383 K for 66 hrs. The product was recovered by filtration, washed thoroughly with distilled water and then with about 50 ml acetone. The material is then dried in air oven at 373 K for 4 hrs. The removal of the template was accomplished by pre-optimized calcination procedure as mentioned in section 2.1. Another Sn-MCM-41 sample with high tin content was prepared by following the identical procedure described above using 0.86 gms tin tetrachloride while preparation of the initial gel (molar SiO_2/SnO_2 ratio=100) and optimal synthesis period was found to be 72 hrs. Several synthesis parameters such as molar $TMAOH/SiO_2$, $CTMABr/SiO_2$, H_2O/SiO_2 and SiO_2/SnO_2 ratios in the starting gel, type of silica and/or tin sources and synthesis time whose cause and effect relationship on the properties of Sn-MCM-41 materials have been explored. Under identical and judiciously pre-optimized synthesis conditions, the influence of different combinations of silicon sources and tin sources on structural properties, tin configuration and morphology of Sn-MCM-41 has been investigated. Three silica sources (Fumed silica, Silica sol and Ethyl

silicate) and three tin sources (Tin tetrachloride, Tin tert-butoxide and Sodium stannate) were used in this study for the preparation Sn-MCM-41 under the identical set of synthesis conditions. Except desired silica and/or tin source, other synthesis parameters such as gel composition (same as stated above), addition sequence, synthesis temperature, ratio of charged reaction mass to autoclave volume and downstream process conditions were kept constant.

2.1.2.2. Synthesis of Sn-impregnated MCM-41

For comparison of catalytic properties Sn-impregnated MCM-41 was prepared and compared with hydrothermally prepared Sn-MCM-41. Calcined Si-MCM-41 prepared previously as per the procedure mentioned in section 2.1.1.1 was used for preparation of Sn-impregnated MCM-41. 2.55 gms of calcined pre-activated Si-MCM-41 sample was added to a solution of 0.06 gms $SnCl_4.5H_2O$ in 5 gms of ethanol. The mixture was then heated at 353 K with constant stirring till the sample became completely dry. The impregnated sample was then dried for 2 hrs at 373 K and calcined at 673 K for 6 hrs.

2.2. CHARACTERIZATION

The details of various spectroscopic, gravimetric, volumetric and thermo-gravimetric techniques used to characterize the mesoporous materials are described.

2.2.1 Powder X-ray Diffraction (XRD)

The powder X-ray diffractogram of as-synthesized and calcined sample were recorded on Rigaku Miniflex (Japan) diffractometer using Ni filtered monochromatic Cu Kα radiation (λ= 1.5406 A°, 40 kV, 25mA). The diffraction data were recorded in the 2θ range of 1.5^o to 10^o at an interval of 0.02^o with a scanning rate of 1^o min^{-1}.

2.2.2. N_2 Adsorption-Desorption Measurements (N_2 Sorption)

The specific surface area, pore size and pore volume of calcined samples were determined by BET method from nitrogen adsorption/desorption isotherm. Nitrogen adsorption and desorption isotherms were obtained at 77 K using Omnisorb, 100 CX, Corporation, USA. Approximately, 150-200 mg calcined sample was first degassed at 673 K for 5 hrs at 10^{-5} Torr and then slowly cooled to room temperature under vacuum and the anhydrous weight of the sample was taken. This sample was cooled to 77K using liquid nitrogen and adsorption of nitrogen was carried out different equilibrium pressures. The pore size distribution was calculated using desorption branches of nitrogen isotherms and BJH (Barret-Joyner-Halenda) method. Although NLDFT (Non local density functional theory) can be used for pore size estimation, simpler BJH method is useful for comparison purpose even though is known to underestimate the pore sizes.

2.2.3. Transmission Electron Microscopy (TEM)

The TEM images were scanned on a JEOL – 1200 EX Transmission Electron Microscope instrument with a tungsten electron source (100 kV of acceleration voltage). Small amount of calcined samples were suspended in 5 ml IPA (99%) and ultrasonicated for about 5 min. These samples were dispersed on Cu-grid coated with thin polymeric film, which was then coated with carbon to avoid vaporization of the samples under high vacuum and in the presence of high-energy electron beam.

2.2.4. Scanning Electron Microscopy (SEM)

The size and morphology was examined using scanning electron microscope (JEOL-JSM-5200) after coating with Au-Pd evaporated film. The samples were suspended in acetone and loaded on metallic stubs. After drying the metallic stubs were sputtered with

thin Au-Pd film to prevent surface charging and also to protect from thermal damage from electron beam, prior to scanning.

2.2.5. Diffuse Reflectance UV-Vis Spectroscopy (DRUV-Vis)

Fine powders of calcined samples were prepared as thin layer on solid sample holder, prior to scanning. The UV-vis diffuse reflectance spectra of the samples were obtained using a Shimadzu (Model UV-2101 PC) spectrometer. The base line correction was made using barium sulfate as the reference standard. The UV spectra were recorded in the 200-600 nm range.

2.2.6. Thermal Analysis (TG-DTG)

The thermo-gravimetry (TG) and differential thermal analyses (DTG) of the as-synthesized samples were carried out using thermo-gravimetric Mettler TA - 4000, under a flow of air (100 ml/min) with a linear heating rate of 10 K/min, between 298 and 1273 K. The base line correction was made using inert α-alumina as the reference sample. Approximately 15 mg of the sample was used in each experiment to find out the temperature of adsorbed water, decomposition of the organic surfactants and weight loss.

2.2.7. Chemical Analysis (Chem. Anal.)

The chemical compositions of the MCM-41 samples were determined by a combination of wet chemical methods and atomic absorption spectrometry (Varian SpectrAA 220 FS) to find out the weight percentage of silica, tin and loss on ignition in the calcined samples. An average of two analyses runs was done to calculate the concentrations of elements in the samples. 0.2 gms of the calcined sample is taken in a previously weighed platinum crucible, which is heated strongly on the non-luminous meker flame with the lid partially closed for about two hrs. Cool in desiccators over

anhydrous self indicating silica gel and weigh. Repeat heating, cooling and weighing tell constant weight is obtained. The difference in the weigh before and after heating gives the loss on ignition. Same sample is used to determine the weight percentage of silica. After determining loss on ignition 2 drops of distilled water (to make the sample wet), 2 to 3 drops of 1:1 H_2SO_4 and 5 ml HF are added slowly, which is heated carefully on an asbestos pad over a wire gauze till thick fumes of H_2SO_4 start to evolve. Cool and rinse the sides of the crucible with 5 ml HF. Then again, heat carefully till the residue becomes dry. Then the residue is ignited first with small non-luminous flame then volatize the H_2SO_4 with a mekker type burner to constant weigh. Allow to cool in a desiccator and weigh. Moistening the cooled residue with ammonia and again heating will help to complete the decomposition. The loss in weigh represents the weight of silica that is used to calculate the weight percentage of silica in the calcined sample.

While the above is being done, another 0.2 gms of same calcined sample is taken in a platinum crucible. 2 drops of distilled water(to make the sample wet), 5 to 6 drops of 1:1 H_2SO_4 and 5 ml HF are added slowly, which is heated carefully on an asbestos pad over a wire gauze till thick fumes of H_2SO_4 start to evolve. Cool and rinse the sides of the crucible with 5 ml HF. Add a drop of 1:1 H_2SO_4 and again heat till fumes of H_2SO_4 are almost all expelled. Care is taken not to over heat the crucible. Remove the flame, cool and dissolve the contents in approximately 5 % (v/v) HCl. Filter if necessary and make up to 100 ml. The above solution prepared is used to determine elements like Sn, Na, etc by Spectra AA220 FS Atomic Absorption Spectrometer.

To find out the percentage of OH^- (hydro-oxide ions) in TMAOH and CTMAOH volumetric chemical analysis method was used. About 2 gms of sample was mixed with 2-

4 ml amount of distilled water in a conical flask to which few drops of phenolphthalein was added. Addition of phenolphthalein changes the color of the solution to pink. This pink solution was titrated against 0.1 molar HCl taken in a 25 ml burette till pink color becomes colorless which is the end point. Percentage of OH^- (hydro-oxide ions) is calculated using the amount of HCl, weight of sample and molecular weight of TMAOH or CTMAOH.

2.2.8. Structural Stability

To assess the structural stability, calcined samples were subjected to different tests such as rehydration followed by calcinations, thermal and hydrothermal treatments. The difference between the intensity of the characteristic d_{100} XRD peak before and after the rehydration followed by calcinations, thermal and hydrothermal treatments was taken as a measure for evaluating the various stability tests.

Following the reported procedure [1], rehydration was conducted by exposing 1gm of calcined sample to water vapours in a desiccator containing supersaturated aqueous NH_4Cl solution for 48 hrs. After rehydration, the sample was calcined under the same controlled conditions used for converting as-synthesized form into calcined one.

Thermal stability was assessed by heating the calcined samples at different temperatures viz. 923 K, 1023 K and 1123 K. The heating rate of 2 K/min was employed and sample was kept at end temperature for 6 hrs.

The hydrothermal stability was checked by mixing 1 gm of calcined sample in 10 ml of water and heating it in closed vessel for 4 hrs at 373 K. The mixture was then filtered and dried immediately at 363 K for 2 hrs.

2.3. CATALYTIC EVALUATION

Sn-containing analogs of MCM-41 (Sn-MCM-41) were found to be a good catalyst for oxidation/epoxidation reactions. The applications of these mesoporous stannosilicate molecular sieves in areas other than the oxidation/epoxidation catalysis have not been explored yet, hence Mukaiyama-type aldol reaction was carried out over Sn-MCM-41. Mukaiyama-type aldol reaction [2-4] of silyl enol ethers and aldehydes is a facile method for C-C bond formation. Condensation reactions are important as condensed bigger molecule serve as the intermediates for many kinds of substances, include, dyes, flavors, fragrances, polymers and drug intermediates. Aldol condensation reaction between aldehydes and ketone is one such important condensation in which an intermediate having alcohol and ketone functional groups formed during reaction eliminates a water molecule to give α-β-unsaturated ketone. Efficiency of Sn-MCM-41 for carbon-carbon bond formation in heterogeneously catalyzed Mukaiyama aldol condensation reaction has been investigated here. Detail experimental setup, reaction conditions and product analysis techniques are described.

2.3.1 Experimental Setup

A typical schematic diagram of the experimental setup is show in Fig.2.3.1.1 The liquid phase reaction was carried out in a 50 ml two necked round bottom flask attached to a condenser and a septum. The reaction mixture was flushed with nitrogen before heating to required temperature. The temperature of the reaction vessel was maintained using an oil bath. The reaction mixture was magnetically stirred and heated to the required temperature at atmospheric pressure.

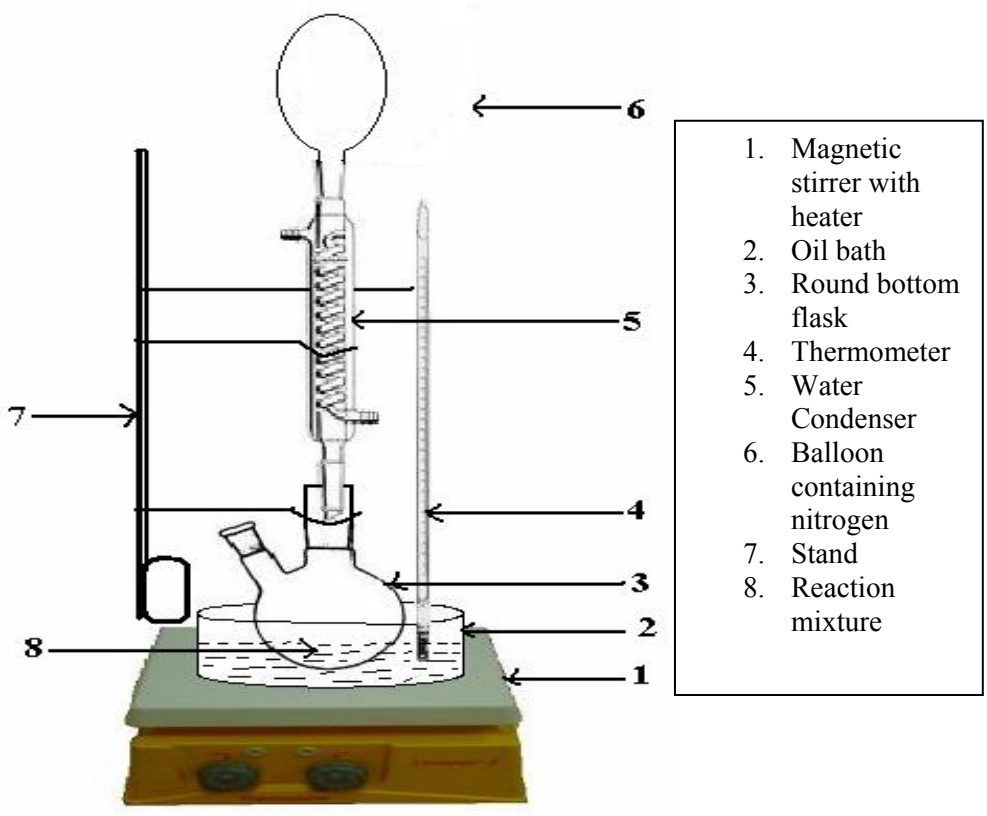

Fig. 2.3.1.1: A typical schematic diagram of the experimental setup.

2.3.2 Reaction Conditions

Anhydrous A.R. grade chemicals were used without further purification. Catalytic liquid-phase Mukaiyama-aldol condensation reaction of methyltrimethyl silyl ketene acetal and benzaldehyde was performed at 373 K to produce β-hydroxy ester under solvent free system. This catalytic reaction was carried out using a batch reactor at atmospheric pressure under nitrogen atmosphere. Before the reaction, each catalyst was activated at 393 K in a vacuum oven and immediately used for the reaction under extremely dry condition. The progress of the reaction was monitored by analyzing the aldol products removed at different intervals (upto 24 hrs). In this reaction, to get the aldol (final product) product, the reaction was quenched by the 1N HCl solution. In a typical reaction, the mixture consisted of 10 mmol of 1-Methoxy-2-methyl-1- (trimethylsiloxy) propene, 10 mmol of

benzaldehyde and 0.35 gms of catalyst were stirred in a 25 ml round bottom glass flask for 24 hrs at 373 K. The progress of the reaction was monitored by analyzing the products at end of 3, 6, 12 and 24 hrs.

2.3.3 Product Analysis

The products withdrawn at regular intervals of time were analyzed periodically on a gas-chromatograph (Varian CP 3800) equipped with a flame ionization detector and a capillary column (20 meters in length). The products were also identified by injecting authentic samples.

2.4 REFERENCES

[1] X.S. Zhao, F. Audsley, and G.Q. Lu, J.Phys.Chem B 102 (1998) 4143.

[2] K. Narasaka, K. Soai, T. Mukaiyama, Chem. Lett. (1974) 1223.

[3] T. Mukaiyama, K. Banno, K. Narasaka, J. Am. Chem. Soc. 96 (1974) 7503.

[4] Y. Yamamtoo, K. Maruyama, K. Matsumoto, J. Am. Chem. Soc. 105 (1983) 6963.

CHAPTER – 3

RESULTS AND DISCUSSION

In this chapter the results obtained from the numerous synthesis trials and characterization of Si-MCM-41, Sn-MCM-41 and catalytic performances of Sn-MCM-41 materials are discussed in detail. The discussion is focused on optimization of synthesis parameters and its influence on the textural properties, structural stability and morphological properties.

3.1. SYNTHESIS AND CHARACTERIZATION OF Si-MCM-41 TYPE MESOPOROUS MATERIALS

Most of the research has been concentrated on MCM-41 because of its unique textural/structural properties. Three variables have a major influence on the formation and properties of mesostructured phases: gel parameters, temperature and time. Even though each variable contributes to a specific aspect of the formation, there is substantial interplay between these elements during the course of synthesis. Several parameters such as silica source, type and concentration of surfactant, synthesis method, calcination, pH etc. whose cause and effect relationship on the properties of MCM-41 materials have been explored [1-13]. Although, hydrothermal and room temperature synthesis methods are well known for the preparation of MCM-41, the pursuit of new objectives is originating the emergence of new pathways for identifying the procedure which is cost-effective, facile, scalable, reproducible and environmentally friendly producing high yield.

3.1.1. Hydrothermal Synthesis of Si-MCM-41

In view of making cost-effective, simple and reproducible methods for the high yield synthesis of MCM-41 using cheaper, readily available and high silica containing silicon source materials various optimization studies for the preparation of Si-MCM-41 have been done using various silica sources and varying the type and concentration of the surfactant. A systematic and comparative study of textural/structural, stability and

morphological properties of MCM-41 materials prepared using with different synthesis parameters such as time, pH, temperature, surfactant to silica ratio, nature of the surfactant and silica sources has been done.

3.1.1.1. Effect of Time

Synthesis time is a critical variable in the formation of M41S materials. Initially synthesis of Si-MCM-41 was done as described in chapter 2 section 2.1.1.1 with the molar composition: SiO_2 : 0.18 CTMABr : 0.25 TMAOH : 25 H_2O with fumed silica as a silica source at 383 K. It is well known [1-4] that lower temperatures (353 K - 383 K) favors formation of MCM-41 phase during hydrothermal synthesis. Hence 383 K has been chosen as a suitable temperature for studying the time effect initially. The gel obtained was divided into six equal portions, transferred into six autoclaves and was heated at different times. After the heating process, the product was filtered, washed with distilled water and dried at 373 K for 4 hrs. Fig 3.1.1.1.1 shows the XRD patterns of the as-synthesized samples for 0 hrs, 6 hrs, 12 hrs, 24 hrs, 48 hrs and 66 hrs synthesis times using fumed silica as a silica source.

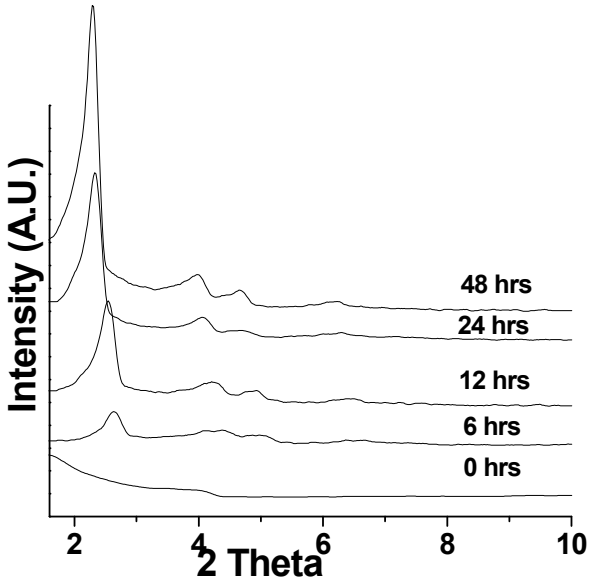

Fig 3.1.1.1.1: XRD patterns of as-synthesized samples showing progressive development of Si-MCM-41 as a function of time using fumed silica as a silica source.

It is interesting to note that as time progresses, not only intensity of characteristic peaks increases but also peak shifts towards lower 2θ values. The XRD patter of as-synthesized sample obtained after 48 hrs exhibited a typical four-peak pattern with a very strong (100) diffraction peak and three (110), (200) and (210) diffraction peaks, which matches well with the hexagonal mesoporous MCM-41 phase as reported earlier [14, 15]. Shifting of the peak to lower 2θ values suggest growth of the unit cell occurs with time. In order to verify such improvement in the degree of ordering, the unit cell parameter 'a_o' was calculated using the relation $2d_{100}/\sqrt{3}$. The a_o values calculated using X-ray diffraction data of the profiles shown in Fig 3.1.1.1.1 are summarized in Table 3.1.1.1.1.

Table 3.1.1.1.1: Variation in unit cell parameter of as-synthesized materials obtained at different synthesis times using fumed silica as a silica source.

Synthesis times (hrs)	d_{100}	Unit cell parameter a_o (nm)
0	-	-
6	3.55	4.09
12	3.58	4.13
24	3.69	4.27
48	3.89	4.50
66	3.84	4.42

It is evident from Table 3.1.1.1.1 that, the progressive increase in unit cell parameter occurs with the increase in synthesis time, reaches to maximum and then decreases slightly on further heating. The intensity of d_{100} diffraction peak and a_o value was found to be maximum at 48 hrs. For still longer synthesis times (66 hrs), the a_o values were found to decrease slightly with no considerable increase in the peak intensity. However, if

the heating time is increased up to 120 hrs, the hexagonal phase transforms into the lamellar form, which on calcination collapses resulting in amorphous materials.

3.1.1.2. Effect of Temperature

Synthesis temperature plays an important role in the formation of MCM-41 phase. As seen from time dependent study given in section 3.1.1.1 it was observed that good quality MCM-41 is obtained after 48 hrs at 383 K. In order to prepare MCM-41 more economic further decrease in the synthesis time is desirable. The influence on the formation of Si-MCM-41 was investigated at temperature in the range (383 K to 423 K). The synthesis of Si-MCM-41 was carried using fumed silica as a silica source with molar gel composition: SiO_2 : 0.18 CTMABr : 0.25 TMAOH : 25 H_2O. The gel obtained was divided into three equal portions, transferred into three autoclaves and was heated at different temperatures viz. 383 K, 408 K and 423 K. Time dependant study was carried out similar to as mentioned in section 3.1.1.1 for each temperature. From each set of systematic runs, the as-synthesized sample that has shown highest a_o value was selected for comparison purpose and were designated as MCM-41_{AS}-XXX where XXX indicates the temperature used for the synthesis. MCM-41_{AS}-383, MCM-41_{AS}-408 and MCM-41_{AS}-428 were obtained at 48, 36 and 24 hrs respectively. The calcined samples were designated by removing the suffix $_{AS}$, for eg. Calcined form of MCM-41_{AS}-383 was labeled as MCM-41-383. The quality of the MCM-41 materials formed were compared from the relative intensity and sharpness of the XRD peaks. The XRD profiles of as-synthesized and calcined samples prepared at 383 K, 408 K and 423 K are shown in Fig. 3.1.1.2.1 (A) and Fig. 3.1.1.2.1 (B), respectively. Calcined materials have shown considerable increase in the intensity of low angle reflection. As-synthesized and calcined forms of samples prepared at

383 K and 408 K exhibit a typical four-peak pattern with a very strong (100) diffraction peak and three (110), (200) and (210) diffraction peaks. Although MCM-41_{AS}-423 shows strong (100) diffraction peak and two (110), (200) diffraction peaks, upon calcination the higher angle peaks are not resolved by broadening due to loss of some orderness. A possible cause for this may be due to thinner pore walls formed by faster rate of dissolution/depolymerization of the silica source and accelerated build up of the mesophase at higher temperature.

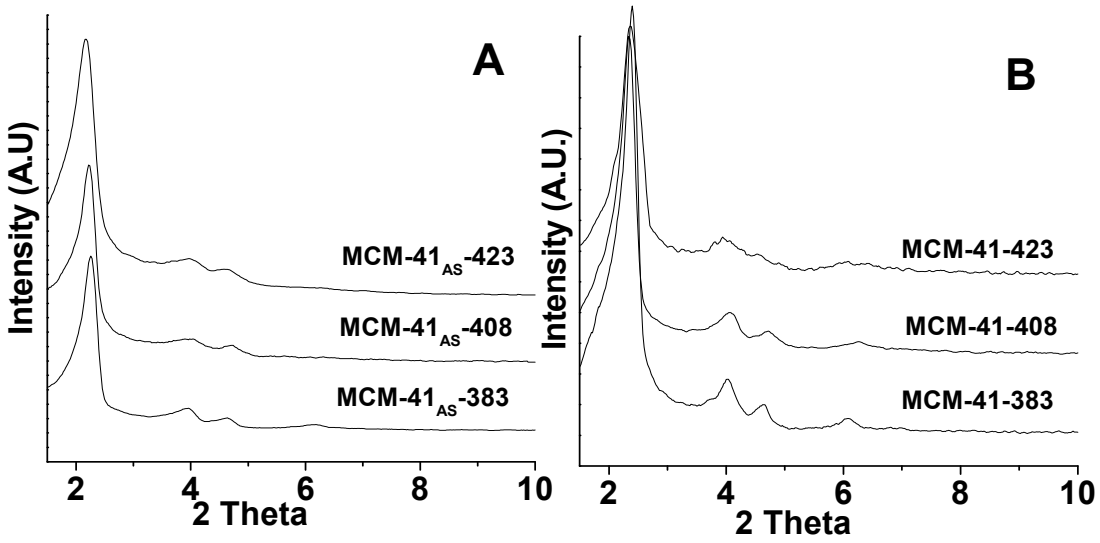

Fig. 3.1.1.2.1: Powder XRD patterns of (A) as-synthesized and (B) calcined Si-MCM-41 prepared at 383 K, 408 K and 423 K.

Even though MCM-41 was obtained at 408 K and 423 K but the relative intensity of XRD patterns of the calcined form of these samples was less as compared to calcined MCM-41-383 which may be due to less concentration of the surfactant present in the final gel [16]. Hence further optimization of gel parameters such as surfactant concentration, water content etc are required to obtain good quality MCM-41 at 408 K and 423 K. Therefore further studies were conducted at 383 K for 48 hrs at which good quality of MCM-41 is produced.

3.1.1.3. Effect of Gel Parameters

The gel composition comprises of various components such as surfactant source and concentration, silica source, organic and/or inorganic OH^- source and concentration and water. Each component contributes to a specific aspect on the formation of reaction mixture. There is substantial interplay between these components during the course of synthesis.

3.1.1.3.1. Effect of pH

pH of the final gel is important as it can decide the type and quality of a particular mesophase formed [16 - 19]. The effect of gel pH within a range of 8.2 to 12.2 value on the formation of MCM-41 was studied by hydrothermal synthesis. The gel obtained with molar gel composition SiO_2 : 0.18 CTMABr : 0.25 TMAOH : 25 H_2O using fumed silica as a silica source had a pH value of 12.2, which was divided into three equal portions, the first portion was autoclaved without adjusting the pH, while the pH value of the gel of other 2 portions were adjusted to 10.2 and 8.2 value by addition of appropriate amount of dilute hydrochloric acid and autoclaved at 383 K for 48hrs. Three samples that were thus obtained are designated as MCM-41-12.2, MCM-41-10.2 and MCM-41-8.2 by varying gel pH to 12.2, 10.2 and 8.2 value respectively. The quality of the MCM-41 materials formed were evaluated from the relative intensity and sharpness of the XRD peaks. Fig 3.1.1.3.1.1 shows XRD pattern of as-synthesized Si-MCM-41 samples prepared at various pH keeping all other synthesis parameters constant. MCM-41-12.2 exhibited well defined XRD pattern which matches well with the characteristics of hexagonal mesoporous MCM-41 phase, while MCM-41-8.2 shows only strong (100) diffraction peak and the higher angle peaks merge with each other forming a broad peak indicating poor quality of the material formed.

MCM-41-10.2 also shows well defined XRD pattern of hexagonal mesoporous MCM-41 but the relative intensity of higher angle peaks is less as compared to MCM-41-12.2.

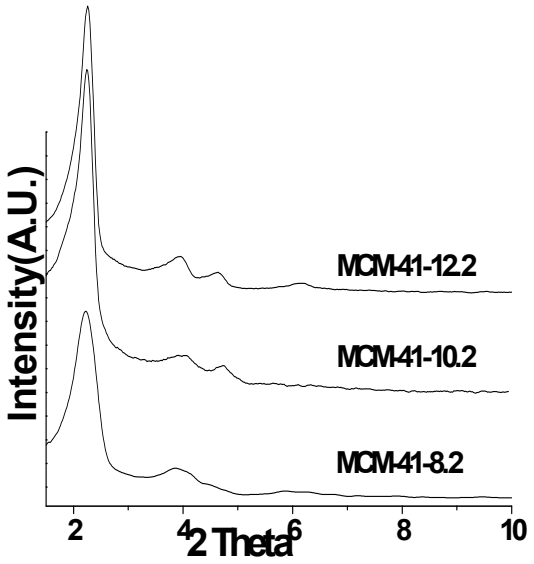

Fig 3.1.1.3.1.1: Powder XRD patterns of as-synthesized Si-MCM-41 prepared at 8.2, 10.2 and 12.2 pH values.

Thus from above studies it can concluded that good quality MCM-41 is formed with molar gel composition SiO_2 : 0.18 CTMABr : 0.25 TMAOH : 25 H_2O having a pH value of 12.2, while at lower pH values formation of hexagonal MCM-41 are not easily reversed due to which the synthesis becomes very sensitive to timing and temperature for the pH adjustment during silicate polymerization.

3.1.1.3.2. Influence of Nature and Concentration of the Surfactant

Nature and concentration of the surfactant plays an important role in the pathway of the formation of mesophases. Since surfactant chemistry is the key to the formation of mesostructured silica, the silicate species and the surfactant molecules in solution play an important role in organizing and governing the extent of the electrostatic interactions between them. Generally four chemical raw materials are required for the formation of Si-

MCM-41 such as a surfactant source, an OH^- source, silica source and water. In most of the synthesis reports the source of OH^- are selected from TMAOH, NaOH and NH_4OH or mixtures of them, whereas the surfactant source are selected from N-cetyl-N, N, N trimethyl ammonium cationic surfactants. The role of hydroxide ion in the reaction mixture is to digest the silica. The hydroxide content of the system strongly influences formation of the mesophases. By varying hydroxide ion concentration, different mesophases also can be obtained. While cationic surfactant molecules which consists of a polar hydrophilic head group and a non-polar hydrophobic tail are used as structure directing agents in water-surfactant system. The synthesis procedure will become very facile if hydroxide ions and surfactant molecules are obtained from a single reagent. Therefore if CTMAOH is used in the preparation of gel for synthesis of Si-MCM-41, it serves as a simultaneous source of surfactant and OH^- species. Thus silica source and aqueous CTMAOH solution are only required to prepare the starting synthesis gel. Even though synthesis of MCM-41 type mesoporous materials has been reported earlier [20] with CTMAOH at temperature 408 K and 423 K but no details were given for 383 K. Although, synthesis of these materials with CTMAOH in the presence of CTMABr is known [20] no systematic study was reported with regard to influence of various synthesis parameters and its physicochemical properties. Prompted by this we have conducted in depth studies for the synthesis of Si-MCM-41 using CTMAOH and with CTMAOH in the presence of CTMABr at 383 K. Initially, synthesis was conducted using fumed silica as silica source with molar gel composition SiO_2 : 0.18 CTMABr : 0.25 TMAOH : 25 H_2O at 383 K for 48 hrs, as this molar gel composition, temperature and time have yielded good quality MCM-41. Further synthesis runs were carried out by replacing CTMABr and TMAOH with CTMAOH

keeping molar ratios of $CTMA^+/SiO_2$ and OH^-/SiO_2 fixed. This was done in view to investigate the effect of source of $CTMA^+$ and OH^- of different surfactants on the formation of the MCM-41 materials and their properties. Si-MCM-41 was prepared with molar gel compositions SiO_2 : x CTMABr : y CTMAOH : z TMAOH : w H_2O , where x = 0-0.18, y = 0-0.32, z = 0-0.25, w = 25-33. Each system was subjected to identical set of synthesis conditions including down-stream processing to investigate influence of different parameters on the quality of the phase formed. The degree of ordering of the Si-MCM-41 samples prepared were monitored by varying the gel composition. The details of systems, their molar compositions and products obtained there from are given in Table 3.1.1.3.2.1.

Table 3.1.1.3.2.1: Details of systems and their molar composition, and product obtained

System Designation	Molar Composition					Product
	SiO_2	**CTMABr**	**CTMAOH**	**TMAOH**	**H_2O**	
RH-1	1	0.180	0.000	0.250	25	MCM-41
RH-2	1	0.135	0.045	0.205	25	MCM-41
RH-3	1	0.090	0.090	0.160	25	MCM-41
RH-4	1	0.045	0.135	0.115	25	Disordered MCM-41
RH-5	1	0.000	0.180	0.070	25	Disordered MCM-41
RH-6	1	0.000	0.180	0.120	25	Disordered MCM-41
RH-7	1	0.000	0.180	0.170	25	Disordered MCM-41 +Lamellar
RH-8	1	0.000	0.180	0.220	25	Lamellar
RH-9	1	0.000	0.180	0.000	25	Disordered MCM-41
RH-10	1	0.000	0.250	0.000	25	Disordered MCM-41
RH-11	1	0.000	0.320	0.000	33	Disordered MCM-41

Comparing the gel compositions of systems RH-1 to RH-5, it can be concluded that the formation of good quality Si-MCM-41 occurs when molar gel ratio of $CTMABr/SiO_2$ is high as compared to $CTMAOH/SiO_2$. Fig. 3.1.1.3.2.1 shows the XRD patterns of phases

obtained from systems RH-1 to RH-5. Si-MCM-41 obtained from a system RH-1 exhibited well defined XRD pattern which matches well with the characteristics of hexagonal mesoporous MCM-41 phase. The XRD patterns of as-synthesized samples obtained from systems RH-2 and RH-3 exhibit strong d_{100} peak and two d_{110} and d_{200} peaks indicating good quality MCM-41, while samples obtained from systems RH-4 and RH-5 form poor quality MCM-41. The decrease in the quality of RH-4 and RH-5 was evidenced by the reduced intensity and broadening of low angle reflection, also the higher angle peaks d_{110} and d_{200} merge indicating loss of orderness. Even after increasing the synthesis time to 72 hrs for systems RH-4 and RH-5 there was no considerable increase in the sharpness of the d_{100} peak and orderness of the material.

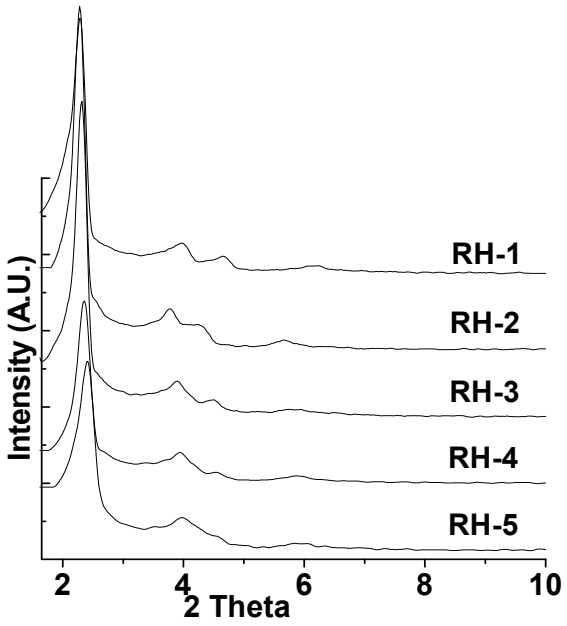

Fig. 3.1.1.3.2.1**:** Powder XRD patterns of as-synthesized phases prepared from systems RH-1 to RH-5.

It is evident from Table 3.1.1.3.2.1 and Fig. 3.1.1.3.2.1 that disordered MCM-41 is obtained from systems wherein OH^- ions in the gel are obtained from CTMAOH with fixed OH^-/SiO_2. A possible cause of this may be due to ineffective supply of OH^-

concentration needed for digestion of silica. The system with lower concentration of TMAOH was found to lead to the formation of more disordered MCM-41 structure, with fixed OH^-/SiO_2 to 0.25. In view of above results further synthesis runs were taken with $CTMAOH/SiO_2$ molar ratio 0.18 fixed and varied $TMAOH/SiO_2$ in the range (from 0.12 to 0.22). More OH^- concentration from TMAOH in the gel will produce larger de-polymerization of silica source and hence could yield better quality, but when TMAOH concentration was increased in the gel from 0.07 to 0.12 value only minor improvement in the quality was observed in terms of sharpness of the characteristic d_{100} and d_{110} peaks of MCM-41. Additional increase in the $TMAOH/SiO_2$ molar ratio to 0.17 gave mixed phase consisting of disordered MCM-41 and lamellar phase. Lamellar phase was obtained after further increase in the TMAOH concentration. The XRD patterns with fixed $CTMAOH/SiO_2$ molar ratio to 0.18 and varying $TMAOH/SiO_2$ molar ratio are given in Fig 3.1.1.3.2.2 (A) and its detail molar composition with products obtained are given in Table 3.1.1.3.2.1. Totally amorphous phase was obtained after calcination at 813 K for 6 hrs from systems RH-6, RH-7 and RH-8 probably on account of the thinner pore walls of the materials formed. On the basis of the results obtained from systems RH-1 to RH-7 the role of source of $CTMA^+$ and OH^- in the synthesis of Si-MCM-41 can be very well seen. It is interesting to note that, there was slight decrease in the unit cell parameter and the characteristic peak d_{100} was found to shift towards higher 2θ value when $CTMABr/SiO_2$ is decreased with simultaneous increase in the $CTMAOH/SiO_2$ molar ratio maintaining $CTMA^+/SiO_2$ and OH^-/SiO_2 ratios constant. In order to verify the variation in the degree of ordering, the unit cell parameter 'a_o' was calculated using X-ray diffraction data and is summarized in Table 3.1.1.3.2.2.

Table 3.1.1.3.2.2: Variation in unit cell parameter, lattice contraction of as-synthesized materials obtained by varying different template concentration.

Sample Designation	Synthesis time (hrs)	d_{100} Spacing and unit cell parameters (nm)				Δa_0 (nm)	% Lattice contraction
		As synthesized		Calcined			
		d_{100}	a_o (nm)	d_{100}	a_o (nm)		
RH-1	48	3.89	4.50	3.61	4.24	0.26	5.90
RH-2	48	3.86	4.45	3.57	4.12	0.33	7.41
RH-3	48	3.78	4.36	3.34	3.85	0.51	11.69
RH-4	48	3.74	4.31	3.29	3.79	0.52	12.06
RH-5	48	3.71	4.28	3.26	3.76	0.52	12.14

Upon calcination, sample obtained from systems RH-1 to RH-5 have shown considerable increase in the intensity of low angle reflection and shifting of 2θ to higher values as compared to their as-synthesized forms. A shift in low angle reflection was found comparatively more pronounced for samples with higher CTMAOH/SiO_2 molar ratio which may be probably related to a greater contraction of the lattice after calcination. Contraction of the lattice occurs during the surfactant removal process on account of condensation of the silanol groups on the wall. An extent of such lattice contraction was estimated by calculating the difference in unit cell parameters, before and after calcination (denoted as 'Δa_0 ') and provided in Table 3.1.1.3.2.2. Samples RH-3, RH-4 and RH-5 has shown more or less same amount of lattice contraction. In present studies, the % lattice contraction was observed in the range of 5.90 to 12.14. All the samples listed in Table 3.1.1.3.2.2 were subjected to textural/structural characteristics after calcination. These calcined samples were designated by adding a suffix 'C' to the labels of as-synthesized samples. For e.g. calcined sample of RH-1 was designated as RH-1C. The specific pore

volume, BET surface area and average BJH pore diameter deduced from the nitrogen sorption isotherms are summarized in Table 3.1.1.3.2.3.

Table 3.1.1.3.2.3: Textural/structural characteristics of various calcined MCM-41 phases.

Sample designation	Total pore Volume, cc/gm	BET surface area, m^2g^{-1}	BJH Pore diameter, (nm)	Wall thickness (nm)
RH-1C	0.63	1070	2.36	1.88
RH-2C	0.66	935	2.55	1.57
RH-3C	0.64	1015	2.57	1.28
RH-4C	0.70	1049	2.69	1.10
RH-5C	0.86	1101	3.13	0.63

The wall thickness of MCM-41 materials was calculated by the difference between the unit cell parameter a_o and the pore diameter. High pore volume in case of RH-5C indicates presence of few secondary mesopores, which may have formed either during calcination process. RH-1C sample has yielded well ordered MCM-41 with highest wall thickness, while as the molar gel ratio of $CTMAOH/SiO_2$ increases the wall thickness decreases. The alteration in the trend may be associated with the variation in the type of source of $CTMA^+$ and OH^- in the synthesis and the reactivity of silica source materials in terms of ease of providing Q^3 i.e. $Si(OSi)_3(OH)$ and Q^4 i.e. $Si(OSi)_4$ structural units in the different synthesis conditions. From these results it can be seen that there is an additional factor controlling the formation of good quality MCM-41, the counter ion (anion) attached to the cationic surfactants. The degree of dissociation for $C_{16}TMA$-X surfactants increase in the order X: $Br^- < Cl^- < F^- < OH^-$ [16]. The greater degree of dissociation, less stable the micelles are. The stability of a micelle array and the sphere-to-rod transformation are also closely related to the degree of dissociation of the anion from the surfactant in the micelle array. Therefore CTMAOH, which has a relatively high degree of dissociation as

compared to CTMABr, has high electric field at short distances and binds hard to their hydrated water. The rod like geometry is even less stable for CTMAOH than for CTMABr. Thus gels with higher CTMAOH/SiO_2 molar ratios as compared to CTMABr/SiO_2 molar ratio have produced disordered MCM-41 with fixed $CTMA^+/SiO_2$ and OH^-/SiO_2 ratios.

Further investigation on the dependence of the phase quality was carried out by varying molar ratio of CTMAOH/SiO_2 in the range of 0.18 to 0.32 in the absence of CTMABr and TMAOH keeping other synthesis conditions constant, whose powder XRD patterns are shown in Fig. 3.1.1.3.2.2 (B).

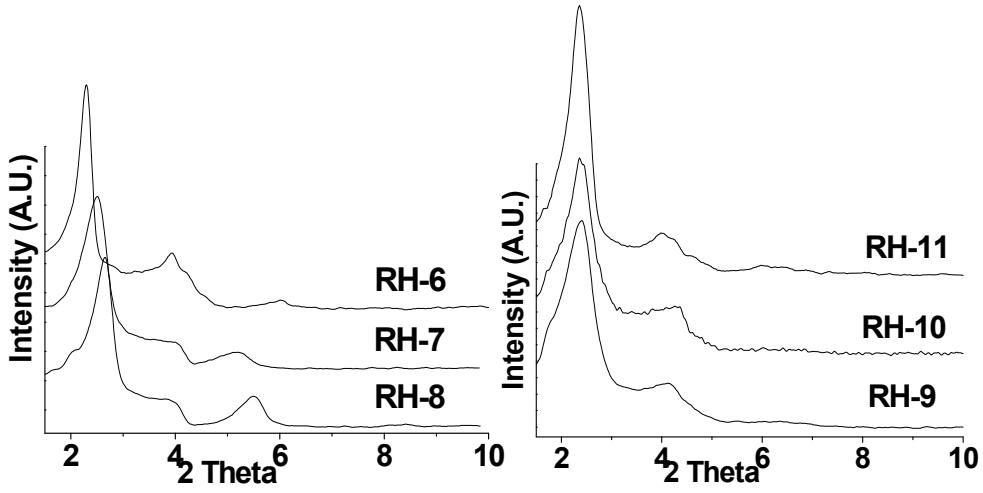

Fig 3.1.1.3.2.2: Powder XRD patterns of as-synthesized samples (A) with varying TMAOH at fixed CTMAOH/SiO_2 and (B) with varying CTMAOH/SiO_2.

The details of systems, their molar compositions and products obtained there from are given in Table 3.1.1.3.2.1. From previous studies it is clear that the reduction in CTMAOH concentration will only degrade the quality, the CTMAOH/SiO_2 molar ratio was increased to 0.25. No improvement in the quality was observed. Further increasing the CTMAOH/SiO_2 molar ratio to 0.32 only marginal increase in the intensity of d_{100} peak was observed with no improvement in the orderness. The minimum water concentration that comes from 14% CTMAOH was used as a source of water for the hydrothermal synthesis

when CTMAOH/SiO_2 molar ratio was 0.32. Further increase in the concentration on CTMAOH produced comparatively poor quality of MCM-41 compared with sample prepared with system RH-11.

Fig. 3.1.1.3.2.3 shows representative SEM images of as-synthesized samples prepared from systems RH-1 to RH-6 and RH-9 to RH-11.

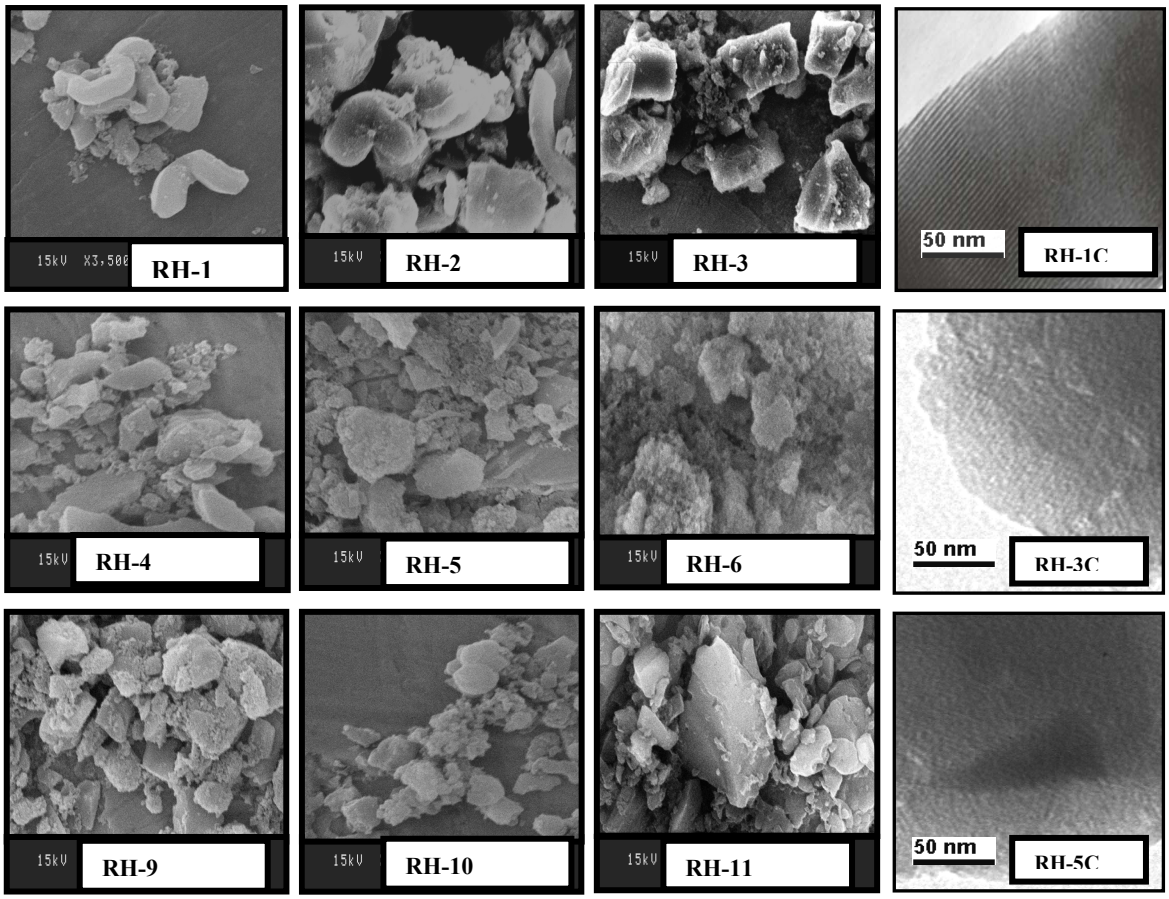

Fig. 3.1.1.3.2.3**:** SEM images of as-synthesized samples prepared from systems RH-1 to RH-6, RH-9 to RH-11 and TEM images of samples RH-1C, RH-3C and RH-5C.

The variation in the morphology of MCM-41 materials was found to depend on the nature and concentration of the surfactant used in the hydrothermal synthesis. When CTMAOH/SiO_2 molar ratio is higher in the gel as compared to CTMABr/SiO_2 molar ratio

there is no considerable change in the morphology. Sample RH-1 has shown worm/rope like morphology, while sample RH-2 has show a mixture of ropes and irregular shaped particles. Presence of rectangular and triangle shaped particles in sample RH-3 have been observed for the first time in case of MCM-41 phase. Samples RH-4 to RH-11 has shown no change in morphology except some marginal variation in agglomerate size. TEM images of samples RH-1C, RH-3C and RH-5C with different orderness are also included in this figure. Well ordered structure of sample RH-1C is depicted in its TEM image while loss of orderness can be seen in TEM images of samples RH-3C and RH-5C. This observation also supports the earlier findings

From thermo-gravimetric analyses of the as-synthesized samples it is possible to analyze the decomposition behaviour of the various surfactants in the mesoporous materials and design a suitable calcination program for surfactant removal. Three samples RH-1, RH-3 and RH-5 were selected for TG/DTG studies as sample RH-1 is prepared in absence of CTMAOH while sample RH-5 is prepared in absence of CTMABr. Sample RH-3 was selected as it contains equal moles of both CTMABr as well as CTMAOH. The TG/DTG measurements performed on these samples have shown that there is approximately 48 wt% loss in as-synthesized MCM-41 samples. This weight loss can be categorized into four stages. 1) 4 wt% loss amid 323 - 423 K due to physically adsorbed water 2) 33 wt% loss between 473 K - 573 K corresponding to decomposition of surfactant 3) 7 wt% loss at 653 K due to breaking of hydrocarbon chains of the surfactant 4) 4 wt% loss between 773 K – 973 K due to combustion of surfactant and water loss associated with condensation of silanol groups. Fig 3.1.1.3.2.4 depicts TG/DTG patterns of samples

RH-1, RH-3 and RH-5, which indicates that the decomposition of the organic surfactants with different counter ions takes place at different temperatures.

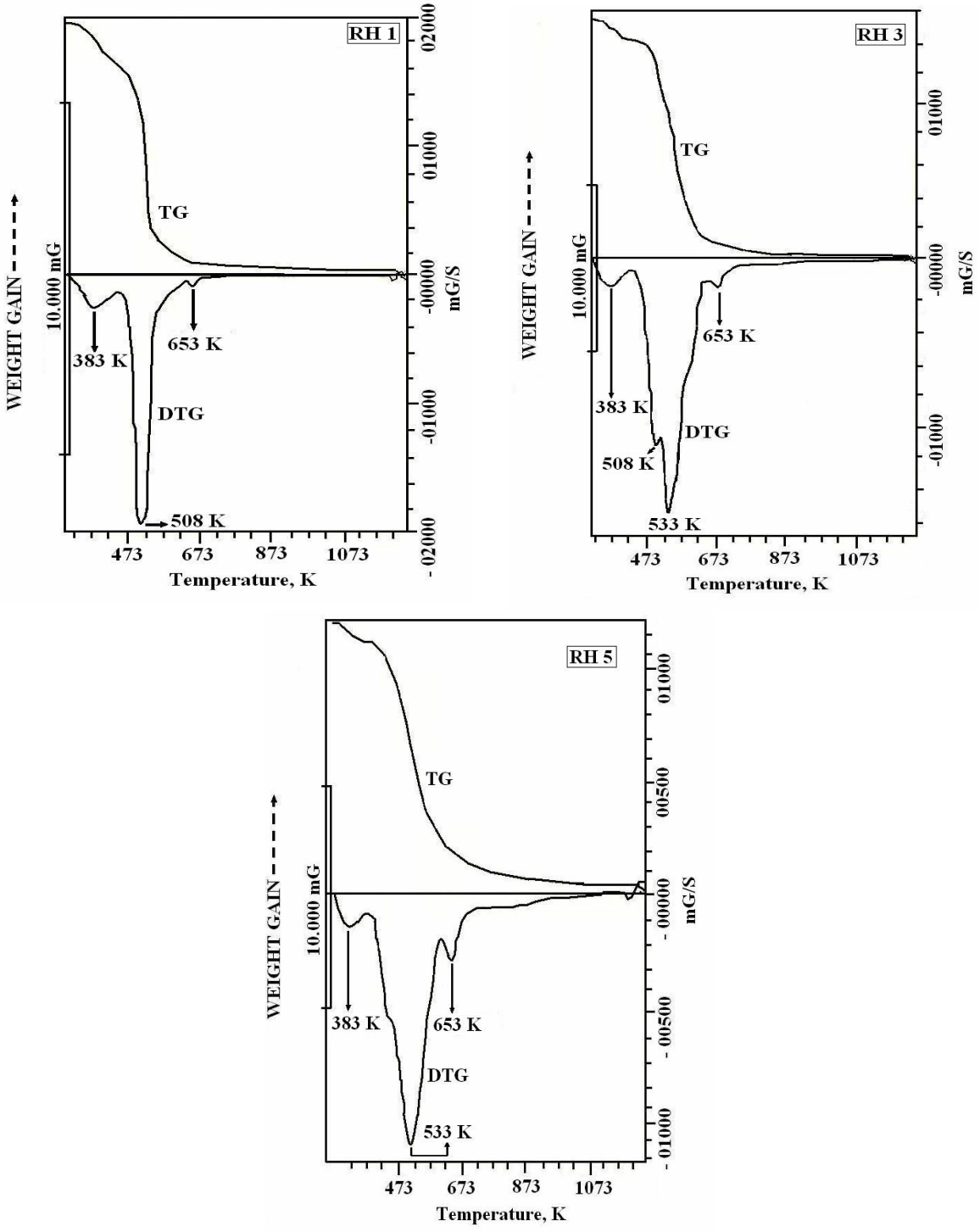

Fig 3.1.1.3.2.4: TG/DTG curves of as-synthesized samples obtained from systems RH-1, RH-3 and RH-5

In all cases the peaks in DTG curves indicate 4 temperature zones in a process of removal of the water, surfactant and residual species. The first peak at 383 K step which involves loss of physically adsorbed water is common for all the three samples, but the peak indicating decomposition of cationic surfactant has occurred in different temperature range. For sample RH-1 the peak signifying decomposition of cationic surfactant had at a peak top value of 508 K while sample RH-5 had a peak top value of 533 K. It is interesting to note that the sample RH-3 has a peak top value of 533 K with a shoulder at 508 K, indicating that amount of occluded CTMAOH surfactant in the as-synthesized materials is more as compared to CTMABr. The interaction between the counter ions and concentration of the surfactant with the silica source seems to play a crucial role in directing the process involved in the removal of the surfactant. The peak at 653 K which is common in all the samples is due breaking of hydrocarbon chains of the surfactant. This shows that after decomposition of the surfactants with same chain length having different counter ions the breaking of chains takes place at common temperature. Additional broad peak between 773 K - 973 K is due to some water loss associated with condensation of silanol groups and conversion of residual species to CO_2.

3.1.1.3.3. Effect of various Silica Sources

The nature of the silica source not only affects the pathway of formation of mesophases but also the characteristics of the particular phase formed. In addition to this, it is also important to design the methodology to develop cost effective process via formation of product in high yield from the low volume of the initial starting reaction mixture. Therefore, in present work we have used different silica sources and investigated the variations in the textural/structural, stability and morphological properties of MCM-41

materials. For this, fumed silica, spray dried precipitated silica, flash dried precipitated silica, ethyl silicate and silica sol were considered as a suitable silica sources in present studies. Even though sodium silicate is also a cheap silica source we have not done any studies on this silica source as the presence of Na^+ in mesoporous silica is often undesirable with respect to stability and in some cases unfavorable to the incorporation of hetero atoms. Time dependant study was carried for all silica sources mentioned above. From each set of systematic runs, the sample that has shown highest a_o value was selected and compared.

The motivation behind selecting spray dried precipitated silica and flash dried precipitated silica was to seek the possibility of using them for designing simple, cost-effective, eco friendly and successful scalable synthetic strategies for a process to prepare MCM-41 with high throughput. Ethyl silicate used in the present studies is a mixture of linear, branched and cyclic ethoxysiloxanes and gives 40 wt % SiO_2 after hydrolysis compared to TEOS which gives only 28 wt % SiO_2 after hydrolysis. The ease of availability of ethyl silicate and high silica content has also triggered our interest in using inexpensive ethyl silicate in place of TEOS in the hydrothermal synthesis of Si-MCM-41. It may be pertinent to mention that this is the first report on the use of ethyl silicate as a silica source in the preparation of MCM-41.

Hydrothermal syntheses of Si-MCM-41 have been performed with an initial gel molar composition of SiO_2 : 0.18 CTMABr : 0.25 TMAOH : 25 H_2O by following the procedure similar to described in Chapter 2 section at 383 K using all the silica sources mentioned above. When ethyl silicate, fumed silica and silica sol were used as silica sources, good quality Si-MCM-41 was obtained as compared to Si-MCM-41 obtained

using spray dried precipitated silica and flash dried precipitated silica. Since the gel composition employed was not suitable to get the Si-MCM-41 with comparable qualities using all the silica sources, further optimization of the gel was done. For this purpose, first the molar ratio of $TMAOH/SiO_2$ in the gel was varied from 0.20 to 0.30 keeping all other synthesis variables constant. At molar ratio $TMAOH/SiO_2$ = 0.20 disordered materials were obtained. This may be attributed partly to lack of sufficient quantity of OH^- concentration needed for digestion of silica. On the other hand mixed phase of disordered MCM-41 and lamellar was obtained, when $TMAOH/SiO_2$ was increased to 0.30. Thus the dependence of the phase quality on the concentration of CTMABr was further investigated by increasing molar $CTMABr/SiO_2$ ratio to 0.24 keeping fixed $TMAOH/SiO_2$ = 0.25. H_2O/SiO_2 was slightly increased to a value of 26 in order to dissolve higher quantity of the CTMABr. Quality of the samples was obtained improved when spray dried precipitated silica and flash dried precipitated silica was prepared with molar gel composition SiO_2 : 0.24 CTMABr : 0.25 TMAOH : 26 H_2O, but same composition has yielded the disordered materials when ethyl silicate and silica sol were used.

In view of above results obtained the samples prepared with five different silica sources were compared in two different sections. In the first section samples were prepared with molar gel composition SiO_2 : 0.18 CTMABr : 0.25 TMAOH : 25 H_2O using fumed silica (FS_1), ethyl silicate (ES) and silica sol (SS) were compared and in other section samples prepared with SiO_2 : 0.24 CTMABr : 0.25 TMAOH : 26 H_2O using fumed silica (Labeled as FS_2 in this section), spray dried precipitated silica(PS_1) and flash dried precipitated silica(PS_2) were compared. Fumed silica was chosen as a common source for

comparison in both sections as it was only source which formed good quality MCM-41 with the two different molar gel compositions.

In the first section syntheses of Si-MCM-41 have been performed with an initial gel molar composition of SiO_2 : 0.18 CTMABr : 0.25 TMAOH : 25 H_2O using fumed silica, ethyl silicate and silica sol as silica sources. From the time dependant study carried out before using fumed silica, silica sol and ethyl silicate the as-synthesized sample that has shown highest a_o value was selected and labeled as MCM-41_{AS}-XX where XX indicates silica source used [FS_1 - fumed silica, SS - silica sol and ES - ethyl silicate]. The synthesis time required to obtain MCM-41 phases with highest a_o values using different silica sources are provided in Table 3.1.1.3.3.1.

Table 3.1.1.3.3.1: X-ray data, unit cell parameters and degree of lattice contraction MCM-41 materials.

Sample designation	d_{100} (nm)	FWHM $2\theta^0$	Unit cell parameter a_0 (nm)	Hydrothermal Synthesis time (hrs)	Δa_0 (nm)	% Contraction
MCM-41-FS_1	3.61	0.18	4.24	48	0.26	5.9
MCM-41-SS	3.42	0.23	3.96	66	0.31	7.3
MCM-41-ES	3.09	0.27	3.57	24	0.43	10.8

On the basis of time required to obtain highly ordered MCM-41, the silica source reactivity trend observed in the present studies was: ethyl silicate > fumed silica > silica sol. A rapid hydrolysis process of ethyl silicate assisted by efficient condensation may be responsible for achieving high ordering degree within the shorter synthesis period as compared to silica sol and fumed silica source materials. Furthermore, fumed silica has shown higher efficiency in achieving structural regularity in shorter period as compared to silica sol. This can be partly attributed to the higher rate of depolymerization process in fumed silica as compared to silica sol. Upon calcination, MCM-41_{AS}-FS_1, MCM-41_{AS}-ES

and MCM-41$_{AS}$-SS resulted in the formation of surfactant-free MCM-41 materials, which were designated as MCM-41-FS$_1$, MCM-41-ES and MCM-41-SS respectively. Freshly calcined materials have shown considerable increase in the intensity of low angle reflection and shifting of 2θ to higher values as compared to their as-synthesized forms. Contraction of the lattice occurs during the surfactant removal process on account of condensation of the silanol groups on the wall. The influence of type of silica source used on the extent of contraction was investigated by calculating the difference in unit cell parameter 'Δa_0' before and after calcination. It is clearly evident from Table 3.1.1.3.3.1 that, the extent of contraction strongly depends upon the type of silica source. In case of MCM-41-FS$_1$, the % contraction was 5.9 while higher % contraction was observed for MCM-41-ES (10.8) and MCM-41-SS (7.3). Fumed silica has shown the least lattice contraction in MCM-41 materials. This can be attributed partly to the lower degree of condensation of the silanol groups on the walls. All the calcined samples listed in Table 3.1.1.3.3.1 were subjected for their textural/structural characteristics. The data concerning their specific pore volume, specific surface area, average pore diameter and the wall thickness are summarized in Table 3.1.1.3.3.2.

Table 3.1.1.3.3.2: Textural/structural characteristics of mesophases obtained from various silica sources

Sample designation	Specific pore Volume cc/gm	Specific surface area m^2g^{-1}	Average Pore diameter (nm)	Wall thickness (nm)
MCM-41-FS$_1$	0.63	1070	2.36	1.88
MCM-41-SS	0.84	1498	2.24	1.33
MCM-41-ES	0.73	1170	2.49	1.47

The mutual inverse proportion was observed between the BET specific surface area and wall thickness. This can be justified on the basis of definition of the specific surface area.

Since it takes into account the weight of the sample, the material with higher wall thickness will certainly have lower specific surface area. Moreover, the specific surface areas and specific pore volumes were found in direct proportion in these samples. The wall thickness of MCM-41 materials was calculated by the difference between the unit cell parameter a_o and the pore diameter. It is evident from Table 3.1.1.3.3.2 that, the magnitude of the wall thickness follows the trend as: MCM-41-FS_1 > MCM-41-SS > MCM-41-ES. Structural stability tests were performed on all the calcined samples that are listed in Table 3.1.1.3.3.2. The structural stability was inspected by comparing the XRD patterns of the samples, which were rehydrated followed by calcinations with those of freshly calcined ones. The difference between the intensity of the characteristics d_{100} XRD peak, before and after the test was taken as a measure for evaluating the structural stability. Typical XRD powder patterns of Si-MCM-41 of freshly calcined ones and after subjecting to rehydration followed by calcination test have shown in Fig. 3.1.1.3.3.1.

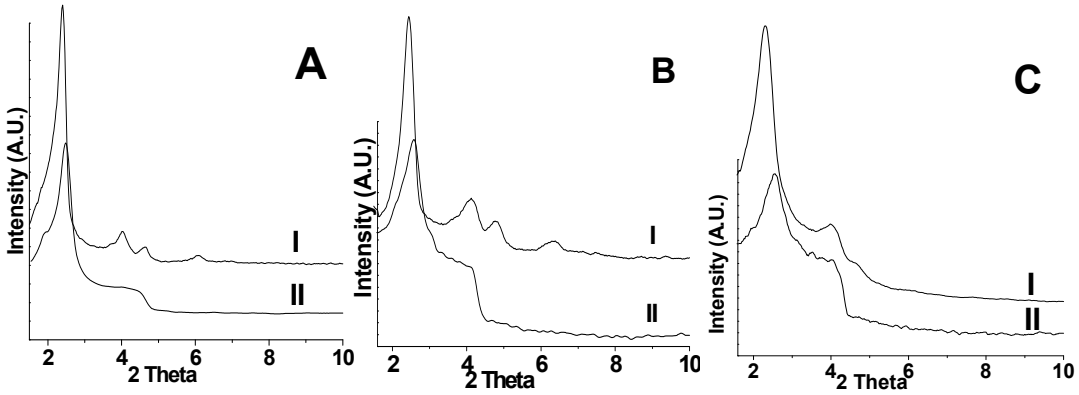

Fig. 3.1.1.3.3.1. XRD powder patterns of silica mesophases obtained from different silica sources after subjecting to rehydration followed by calcinations (A) MCM-41- FS_1, (B) MCM-41-SS and (C) MCM-41-ES samples (I- before and II- after thermal test)

The intensity for the (100) diffraction peak of each freshly calcined MCM-41 sample was taken as a reference. The extent of drop in the ordering degree was evaluated

by comparing the drop in intensity of these peaks with respect to the reference one. An investigation on rehydration followed by calcinations of MCM-41-FS_1 has shown that it has retained 85 % of degree of orderness as compared to the parent one. Whereas, under similar conditions, MCM-41-ES and MCM-41-SS were found to retain only 50 and <5 % of the degree of ordering respectively. The results obtained by performing thermal and hydrothermal stability tests were also match well with that of obtained from rehydration followed by calcination test. These results show that, structural stability increases with the increase in the wall thickness. Thus, on the basis structural stability of ordered MCM-41, the trend observed in the preferred silica source was fumed silica > silica sol > ethyl silicate. MCM-41 sample prepared using fumed silica has shown high structural stability. The above results showed that the variation in the silica source material used in the initial reaction mixture affect textural/structural properties of silica based mesostructures to a considerable extent. SEM and corresponding TEM images are shown in Fig. 3.1.1.3.3.2.

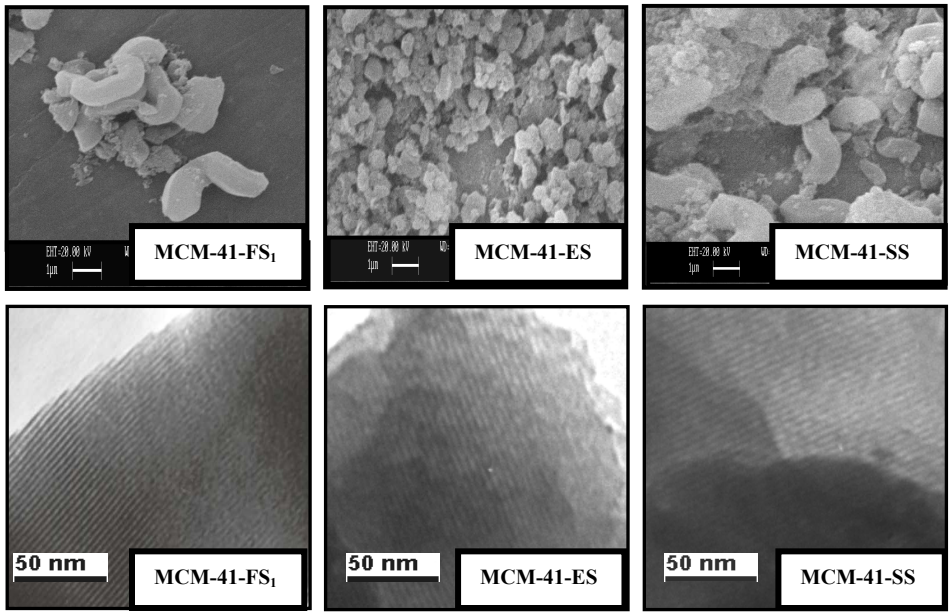

Fig. **3.1.1.3.3.2**. SEM and TEM micrographs of MCM-41 samples prepared with different silica sources.

As illustrated in Fig. 3.1.1.3.3.2, the morphology of the particles was found to be influenced by the silica source used. The MCM-41-FS_1 and MCM-41-SS have shown worm like morphology whereas MCM-41-ES has shown the presence of fused particles. This may be due to the fast hydrolysis of ethyl silicate. It is clearly evident from TEM images of MCM-41 samples prepared with different silica sources that well ordered MCM-41 materials can synthesized using the fumed silica, ethyl silicate and silica sol.

In the second section syntheses of Si-MCM-41 have been performed with an initial gel molar composition of SiO_2 : 0.24 CTMABr : 0.25 TMAOH : 26 H_2O using fumed silica (Labeled as FS_2), spray dried precipitated silica (PS_1), flash dried precipitated silica (PS_2). A systematic and comparative studies on time dependant structural development of MCM-41 materials prepared using differently manufactured amorphous silica sources such as fumed silica (FS_2), spray dried precipitated silica (PS_1) and flash dried precipitated silica (PS_2) on the course of development and structural properties of hydrothermally prepared siliceous MCM-41 are performed and depicted in Fig. 3.1.1.3.3.3.

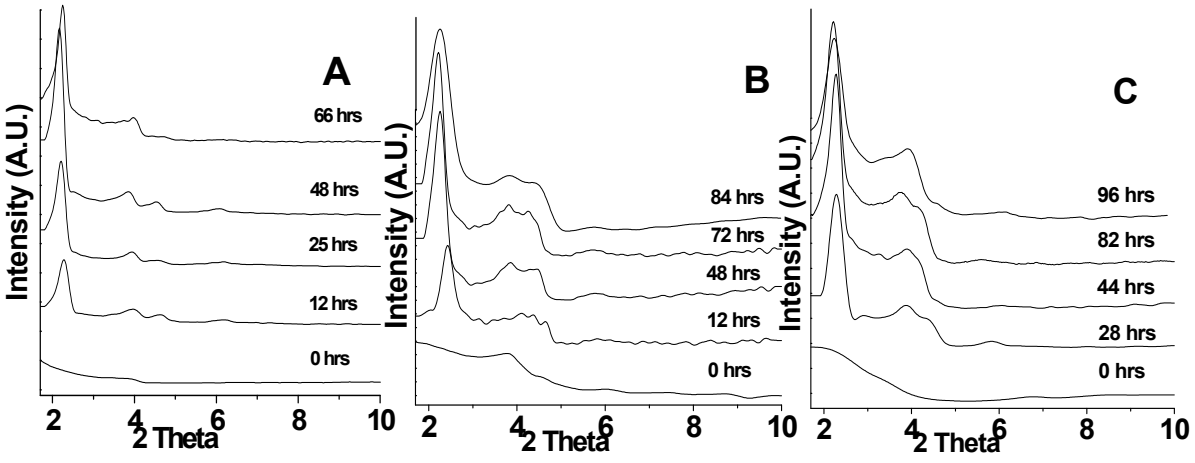

Fig. 3.1.1.3.3.3.: XRD patterns of as-synthesized samples showing progressive development of MCM-41 using (A) FS_2, (B) PS_1 and (C) PS_2

It is interesting to note that in all the cases, the intensity of characteristic peaks of MCM-41 phase was found to increase with synthesis time, reaches to maximum and then decreases on further heating. However, (100) peak was found to shift towards lower 2θ till its intensity reaches to maximum and then shifts to higher 2θ value. The a_o values calculated using X-ray diffraction data of the profiles shown in Fig. 3.1.1.3.3.3 are summarized in Table 3.1.1.3.3.3. In all the three systems, the unit cell parameter was found to increase with synthesis time, reaches to maximum and then decreases on further heating.

Table 3.1.1.3.3.3: Variation in unit cell parameter of as-synthesized materials obtained at different synthesis times using FS_2, PS_1 and PS_2 as a silica source.

MCM-41_{AS}-FS_2			MCM-41_{AS}-PS_1			MCM-41_{AS}-PS_2		
Synthesis time (hrs)	d_{100}	Unit cell parameter a_o (nm)	Synthesis time (hrs)	d_{100}	Unit cell parameter a_o (nm)	Synthesis time (hrs)	d_{100}	Unit cell parameter a_o (nm)
0	-	-	0	-	-	0	-	-
12	3.89	4.49	12	3.62	4.18	28	3.87	4.46
25	3.99	4.60	48	3.97	4.58	44	3.92	4.52
48	4.05	4.67	72	4.03	4.65	82	3.99	4.60
66	3.98	4.59	84	3.94	4.55	96	3.91	4.51

From each set of systematic runs, the as-synthesized sample that has shown highest a_o value was selected and labeled as MCM-41_{AS}-XX where XX indicates silica source used [FS_2 - fumed silica, PS_1 - spray dried precipitated silica and PS_2 - flash dried precipitated silica]. On the basis of time needed to obtain MCM-41_{AS}-XX sample, the reactivity of the source material has shown the trend as: $FS_2 > PS_1 > PS_2$. The quality of the final material was also found to commensurate with the source reactivity. Also MCM-41_{AS}- FS_2 was found to be highly ordered while MCM-41_{AS}-PS_1 and MCM-41_{AS}-PS_2 lack sharp higher diffraction angle peaks, which indicate poor orderness and presence of some contribution due to amorphous matter. Since the quality of the product depends on the fraction of Q^4

[Si $(OSi)_4$] units in the gel [21], among these three sources, the gel prepared using fumed silica may contain lower proportion of Q^4 units. Thus, lower degree of silica polymerization in the gel seems to be responsible for synthesizing high quality MCM-41. Therefore, it can be concluded that, higher the degree of silica polymerization in the gel lower the quality of product formed. This can be well correlated with the source reactivity trend observed in the present studies. Thus, under the identical set of synthesis conditions the degree of polymerization seems to depend on the way by which amorphous sources are manufactured. In other words, manufacturing process of amorphous silica source controls the formation of a special distribution of silicate polyanions and micellar cations and hence quality of MCM-41 materials. Upon calcination, MCM-41_{AS}- FS_2, MCM-41_{AS}-PS_1 and MCM-41_{AS}-PS_2 resulted in the formation of surfactant-free MCM-41 materials, which were designated as MCM-41- FS_2, MCM-41-PS_1 and MCM-41-PS_2 respectively. These materials have shown considerable increase in the intensity of low angle reflection and shifting of 2θ to higher values as compared to their as-synthesized forms. An extent of lattice contraction as a function of type of silica source used was estimated and (denoted as 'Δa_0'). All the details including Δa_0 values are summarized in Table 3.1.1.3.3.4.

Table 3.1.1.3.3.4: X- ray data, unit cell parameters and degree of lattice contraction of calcined MCM-41 materials.

Sample designation	d_{100} (nm)	FWHM $2\theta^0$	Unit cell parameter a_0 (nm)	Hydrothermal Synthesis time (hrs)	Δa_0 (nm)	% Contraction
MCM-41-FS_2	3.79	0.19	4.37	48	0.30	6.42
MCM-41-PS_1	3.84	0.28	4.43	72	0.22	4.73
MCM-41-PS_2	3.90	0.42	4.50	82	0.10	2.17

Higher degree of lattice contraction was occurred when fumed silica was used. This indicates that, the population of ≡Si-OH units in the channel wall increases in the order:

MCM-41- FS_2 > MCM-41-PS_1 > MCM-41-PS_2. The influence of the source material on the development of grains were also reflected in the variation the FWHM (Full Width at Half Maximum) of the (100) peak of these samples. The FWHM of the (100) peak of MCM-41-FS_2 was found to be much smaller than MCM-41-PS_1 and MCM-41-PS_2 indicating the presence of well-developed grains. All the calcined samples listed in Table 3.1.1.3.3.4 were subjected for their textural/structural characteristics. Nitrogen adsorption and desorption isotherms are given in Fig. 3.1.1.3.3.4. Inset in Fig. 3.1.1.3.3.4 depicts the pore size distribution curves obtained from desorption branch and BJH method.

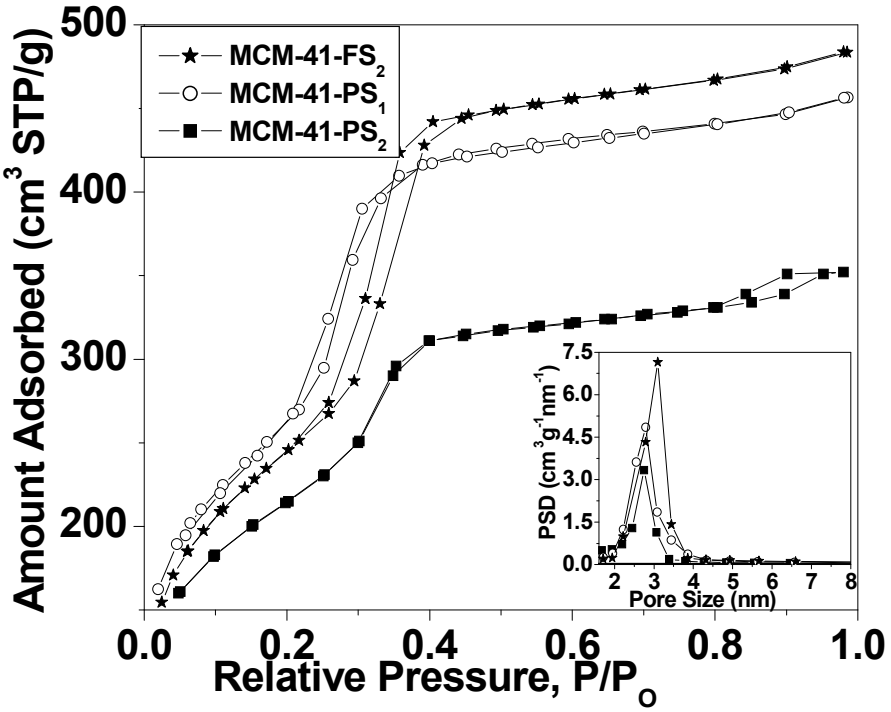

Fig. 3.1.1.3.3.4: Low temperature nitrogen adsorption/desorption isotherms and pore size distribution curves (inset) for calcined MCM-41- FS_2, MCM-41-PS_1 and MCM-41-PS_2.

All samples exhibit pronounced steep condensation step for relative pressures 0.2 to 0.4 arising from condensation of nitrogen inside the primary mesopores which is typical type IV adsorption-desorption isotherm. The condensation step on the isotherms is steep particularly for MCM-41- FS_2 and MCM-41-PS_1 as compared to MCM-41-PS_2. Gradual

development of hysteresis loops was observed for samples MCM-41- FS_2 and MCM-41-PS_1. The change in the shape of hysteresis loop was found to be consistent with increase in the primary mesopore size. The quality of the product was found to affect the width of hysteresis loops and steepness of the condensation. In addition to this, the appearance of hysteresis loops below relative pressure of 0.40 may be partly attributed to the instability of liquid nitrogen meniscus for nitrogen adsorption studies performed at 77K [22]. The data concerning their specific pore volume, specific surface area, average pore diameter and the wall thickness are summarized in Table 3.1.1.3.3.5. The mutual inverse proportion was observed between the BET specific surface area and wall thickness. Fumed silica has yielded well ordered MCM-41 with thinner wall. Considering the magnitude of wall thickness and unit cell contraction upon calcination for each sample, it can be concluded that more contraction in unit cell results in the formation of thinner walled MCM-41.

Table 3.1.1.3.3.5: Textural/structural characteristics of various calcined MCM-41 Phases.

Sample designation	Total pore Volume, cc/gm	BET surface area, m^2g^{-1}	BJH Pore diameter, (nm)	Wall thickness (nm)
MCM-41- FS_2	0.75	869	3.10	1.27
MCM-41-PS_1	0.71	856	2.79	1.64
MCM-41-PS_2	0.89	774	2.75	1.75

High pore volume in case of MCM-41-PS_2 indicates presence of few secondary mesopores due to which minor hysteresis loop at high relative pressure can been seen in Fig 3.1.1.3.3.4 for MCM-41-PS_2 sample. MCM-41- FS_2, MCM-41-PS_1 and MCM-41-PS_2 samples were subjected for the thermal stability test. The difference between the intensity of the characteristic d_{100} XRD peak before and after the thermal test was taken as a measure for evaluating the thermal stability. Fig. 3.1.1.3.3.5 illustrates the powder XRD

patterns of these samples, before and after thermal treatment. After subjecting to thermal test, MCM-41- FS_2 has exhibited 16.04 % structure collapse while 13.74 % and 12.20 % structure collapse was observed in case of MCM-41-PS_1 and MCM-41-PS_2 respectively. Though % collapse for MCM-41 prepared with FS was highest, even after thermal treatment it showed high diffraction angle peaks which were absent in case of MCM-41 prepared using precipitated silica's. The lower degree of structure collapse might be associated with the poor orderness and the higher wall thickness of the MCM-41-PS_1 and MCM-41-PS_2 materials.

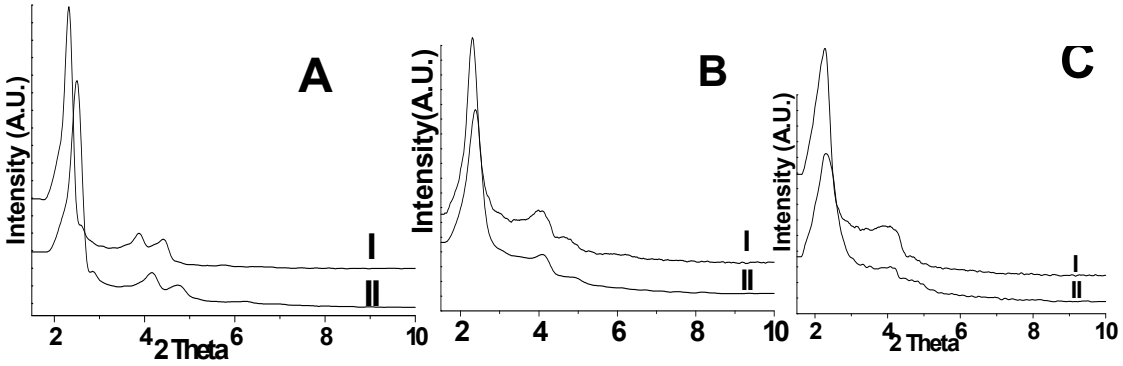

Fig 3.1.1.3.3.5: Powder XRD patterns of (A) MCM-41- FS_2, (B) MCM-41-PS_1 and (C) MCM-41-PS_2 samples (I- before and II- after thermal test)

Structural stability tests were performed as mentioned in chapter 2 section 2.2.8. By performing these tests, it was observed that the trend in structural stability obtained by performing the thermal stability tests are identical with that of observed by performing rehydration followed by calcination and hydrothermal tests.

SEM and TEM micrographs of various MCM-41 samples are illustrated in Fig. 3.1.1.3.3.6. The morphology of MCM-41 materials was found to depend on the type of the silica source used in their preparation. When fumed silica was used as a silica source worm/rope like morphology was observed. However, half doughnut and doughnut like

morphology was observed when PS_1 and PS_2 were used as a silica source In case of MCM-41-PS_2, some contribution due to amorphous matter was also seen. The TEM image of MCM-41- FS_2 sample shows formation of well ordered MCM-41, while TEM images of samples MCM-41-PS_1 and MCM-41-PS_2 illustrate disordered material.

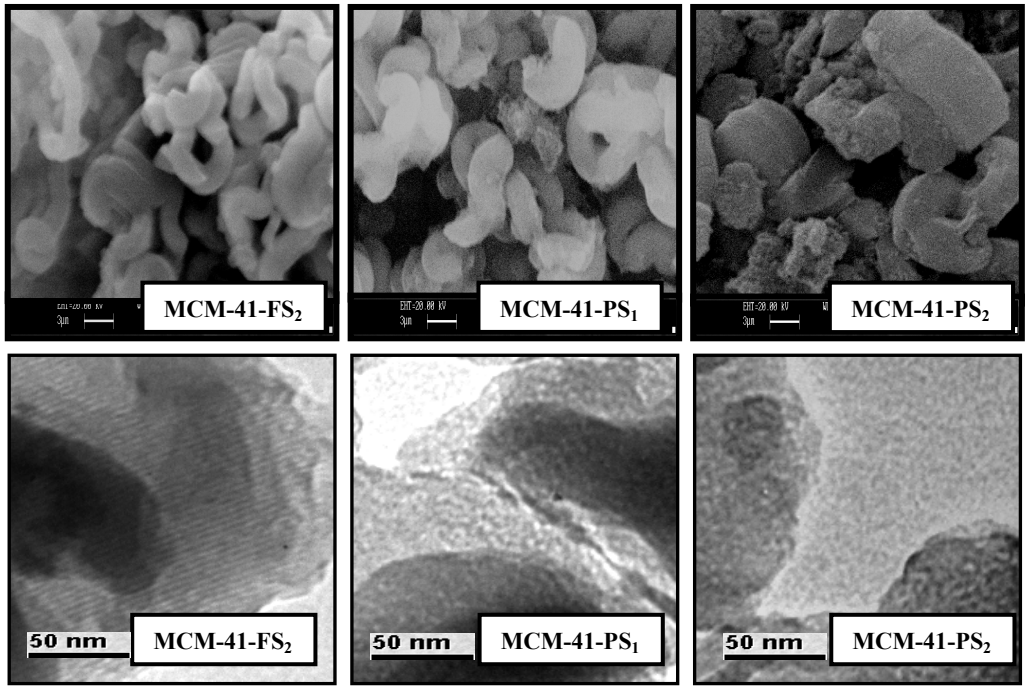

Fig. 3.1.1.3.3.6: SEM and TEM micrographs of various MCM-41 materials

3.1.2. Room Temperature Synthesis of Si-MCM-41

Two commonly followed routes for the synthesis of MCM-41 type materials is either by hydrothermal method or room temperature method. Some of the most cost bearing factors in the preparation of Si-MCM-41 are the source of silica, quantity of surfactant, length of time required and the synthesis temperature. In this regard, the room temperature synthesis route has several advantages over hydrothermal method for the synthesis of MCM-41 such as 1) short reaction times, 2) cost and power savings, 3) excellent reproducibility and 4) no need to use expensive autoclaves. In spite of these benefits, the room-temperature synthesis route has been imposing the challenges associated with the selection of convenient but less expensive silica source materials. In view of making the preparation of MCM-41 in more cost effective way, feasibility of using ethyl silicate in room temperature synthesis of Si-MCM-41 has been attempted. Thus, the present study was aimed at exploring the cause and effect relationship of several synthesis variables on the properties of Si-MCM-41 materials. As seen in section 3.1.1.1 synthesis time is a critical variable in the formation of M41S materials, hence similar time dependent studies from 0 hrs to 12 hrs were conducted at room temperature using TEOS as a silica source with molar gel composition SiO_2 : 0.12 CTMABr : 2.5 NH_4OH : 25 H_2O. The degree of ordering of the pore structures (structural regularity) of Si-MCM-41 samples was monitored by varying the syntheses time. From time dependent studies it was observed that good quality MCM-41 was obtained only after 4 hrs of synthesis time. The structure of the MCM-41 sample obtained at 2 hrs collapsed upon calcination, while the relative orderness and stability of the sample obtained after 4 hrs till 12 hrs remained almost same. Hence all the further synthesis runs were taken at 4hrs.

3.1.2.1. Optimization of gel parameters

Initially, trial runs were conducted using conventional TEOS as silica source for optimizing the gel composition. The results obtained from these runs indicated that, MCM-41 could be synthesized in high yield and in cost-effective manner from the reaction mixture with molar composition SiO_2 : 0.12 CTMABr : 2.5 NH_4OH : 25 H_2O. In order to investigate the influence of various synthesis parameters on the formation of the MCM-41 materials, numerous synthesis trials were conducted at room temperature using ethyl silicate as a source of silica by varying one parameter at a time. Therefore, it was thought to undertake further synthesis trials using this pre-optimized composition by replacing ethyl silicate in place of TEOS in equimolar quantity. Since, the same composition failed to yield MCM-41 when ethyl silicate was used; further optimization was aimed at screening various compositional variables in the initial gel such as molar ratios of NH_4OH/SiO_2, H_2O/ NH_4OH and $CTMABr/SiO_2$. Table 3.1.2.1.1 gives details regarding various systems that were subjected for the room temperature synthesis trials to prepare MCM-41 using ethyl silicate as a source of silica.

Table 3.1.2.1.1**:** Details of systems, their molar composition, and product obtained at room temperature using ethyl silicate as a silica source.

System Designation	Molar Composition				Product
	SiO_2	CTMABr	NH_4OH	H_2O	
$I_{2.5}$-25	1	0.12	2.50	**25**	Amorphous
$I_{2.5}$-50	1	0.12	2.50	**50**	Disordered MCM-41
$I_{2.5}$-100	1	0.12	2.50	**100**	Disordered MCM-41
$I_{2.5}$-150	1	0.12	2.50	**150**	**MCM-41**
$I_{2.5}$-185	1	0.12	**2.50**	**185**	Disordered MCM-41
$I_{12.5}$-185	1	0.12	**12.5**	185	**MCM-41**
$I_{22.5}$-185	1	0.12	**22.5**	185	Disordered MCM-41
$I_{32.5}$-185	1	0.12	**32.5**	185	Amorphous

The system and sample obtained there from was designated as Ix-Z where x = molar NH_4OH/SiO_2 ratio and Z = molar H_2O/SiO_2 ratio in the initial reaction mixture. Therefore, at initial stage of optimization, synthesis runs were conducted by increasing H_2O/NH_4OH molar ratio from 10 to 74 keeping NH_4OH/SiO_2 and $CTMABr/SiO_2$ molar ratios (2.5 and 0.12 respectively) fixed in the initial reaction mixture. The powder XRD patterns of the samples obtained by varying water content are illustrated in Fig. 3.1.2.1.1.

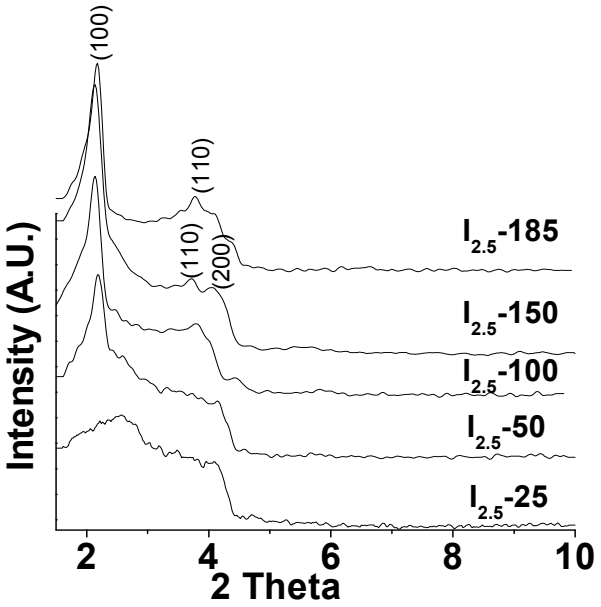

Fig. 3.1.2.1.1: Powder XRD patterns of as-synthesized products prepared with different H_2O/NH_4OH molar ratios keeping NH_4OH/ SiO_2 and $CTMABr/SiO_2$ molar ratios as 2.5 and 0.12 respectively.

It can be clearly seen from Fig. 3.1.2.1.1 that, though formation of MCM-41 phase occurred when the H_2O/NH_4OH ratio was 150, but samples prepared with 100 and 185 ratios lacked (110) and (200) reflection peaks. Although, sample prepared with 50 ratio was found to contain major contribution of amorphous matter, totally amorphous phase was obtained after calcination at 813 K for 6 hrs. Thus, it can be concluded that the extent of gel dilution also contributes to a significant extent in governing the type and quality of the phase. However, even if $I_{2.5}$-185 system yielded poorer quality of MCM-41 as

compared to $I_{2.5}$-150, it is the only composition where NH_4OH/SiO_2 molar ratio can suitably be varied (i.e. from 2.5 to 32.5) keeping all other parameters constant. Therefore, further synthesis runs were conducted by increasing NH_4OH/SiO_2 molar ratio from 2.5 to 32.5 keeping fixed H_2O/SiO_2 and $CTMABr/SiO_2$ molar ratios (185 and 0.12 respectively) for investigating the influence of molar NH_4OH/SiO_2 ratio on the type of the phase formed. The powder XRD patterns of the samples obtained by varying NH_4OH/SiO_2 ratios are depicted in Fig. 3.1.2.1.2.

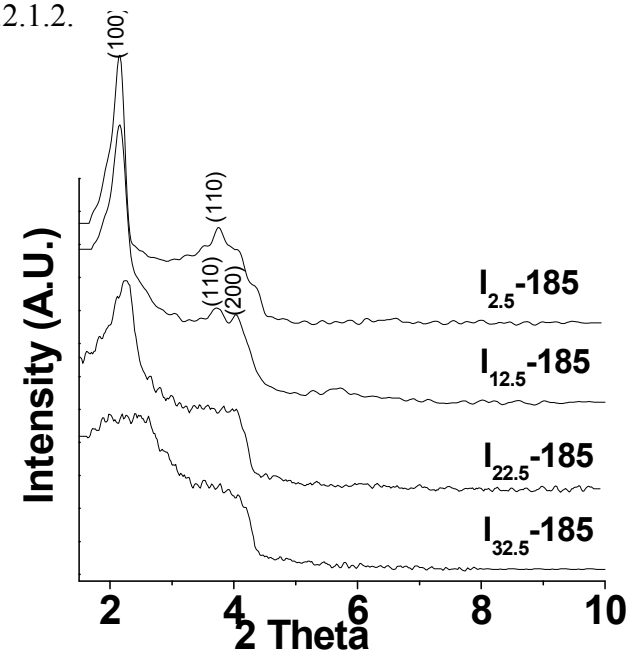

Fig. 3.1.2.1.2: Powder XRD patterns of as-synthesized Si-MCM-41 prepared with different NH_4OH/SiO_2 ratios in the gels

It can be distinctly observed that formation of MCM-41 phase is largely depends on NH_4OH/SiO_2 molar ratio in the initial reaction mixture. At given H_2O/SiO_2 and $CTMABr/SiO_2$ molar ratios, when NH_4OH/SiO_2 ratio was increased from 2.5 to 32.5, the intensity of d_{100} peak was found maximum at NH_4OH/SiO_2 molar ratio = 12.5. This suggests that there is an optimum NH_4OH/SiO_2 molar ratio for the formation of MCM-41 for given H_2O/SiO_2 and $CTMABr/SiO_2$ molar ratios. The subsequent investigations will be

focused in the specific influence of molar H_2O/NH_4OH ratios on the quality of phase formed by varying the NH_4OH/SiO_2 molar ratio in the initial reaction mixture.

Since there is an optimum NH_4OH/SiO_2 molar ratio for the formation of MCM-41 at given H_2O/SiO_2 and $CTMABr/SiO_2$ molar ratios, further synthesis trials were aimed at optimization of yet another gel compositional parameter i.e. molar H_2O/NH_4OH ratio using ethyl silicate as a source of silica. For this purpose, different gels comprising wide range of molar H_2O/NH_4OH ratios were prepared and the quality and formation of MCM-41 at room-temperature were assessed. The results obtained by increasing H_2O/NH_4OH molar ratio from 10 to 74 keeping fixed NH_4OH/SiO_2 and $CTMABr/SiO_2$ molar ratios (2.5 and 0.12 respectively) has already been described in earlier section. On the similar lines, synthesis trials were conducted with each NH_4OH/SiO_2 ratio. Table 3.1.2.1.2 summarizes the different phases obtained from different gels wherein water content is varied at different NH_4OH/SiO_2 ratios keeping $CTMABr/SiO_2$ molar ratio (0.12) fixed. From Table 3.1.2.1.2, it can be concluded that, the H_2O/ NH_4OH molar ratio in the gel affect the quality and type of the phase formed over entire range of NH_4OH/ SiO_2 ratio. These observations could be related to 1) the variation in the effective concentration of cationic species of surfactant $CTMA^+$ as the water content changes and 2) production of different extent of depolymerization of the silica species. Moreover, these results also indicated that, even though ethyl silicate has proved to be suitable source for the preparation of MCM-41 at room temperature, there exists an optimum value of H_2O/NH_4OH for different NH_4OH/SiO_2 molar ratios in the gel. In present studies, optimum values of H_2O/NH_4OH for NH_4OH/ SiO_2 molar ratios 2.5, 12.5, 22.5 and 32.5 were found to be 150, 185, 300 and 450 respectively.

Table 3.1.2.1.2: Details of systems and their molar composition, and product obtained using ethyl silicate as a silica source at room temperature.

System Designation	Molar Composition				Product
	SiO_2	CTMABr	NH_4OH	H_2O	
$I_{2.5}$-25	1	0.12	**2.50**	**25**	Amorphous
$I_{2.5}$-50	1	0.12	2.50	**50**	Disordered MCM-41
$I_{2.5}$-100	1	0.12	2.50	**100**	Disordered MCM-41
$I_{2.5}$-150	1	0.12	2.50	**150**	**MCM-41**
$I_{2.5}$-185	1	0.12	2.50	**185**	Disordered MCM-41
$I_{2.5}$-300	1	0.12	2.50	**300**	Disordered MCM-41
$I_{12.5}$-75	1	0.12	**12.5**	**75**	Amorphous
$I_{12.5}$-100	1	0.12	12.5	**100**	Disordered MCM-41
$I_{12.5}$-150	1	0.12	12.5	**150**	Disordered MCM-41
$I_{12.5}$-185	1	0.12	12.5	**185**	**MCM-41**
$I_{12.5}$-300	1	0.12	12.5	**300**	Disordered MCM-41
$I_{12.5}$-600	1	0.12	12.5	**600**	Amorphous
$I_{22.5}$-150	1	0.12	**22.5**	**150**	Amorphous
$I_{22.5}$-185	1	0.12	22.5	**185**	Disordered MCM-41
$I_{22.5}$-300	1	0.12	22.5	**300**	**Disordered MCM-41**
$I_{22.5}$-600	1	0.12	22.5	**600**	Disordered MCM-41
$I_{22.5}$-800	1	0.12	22.5	**800**	Amorphous
$I_{32.5}$-185	1	0.12	**32.5**	**185**	Amorphous
$I_{32.5}$-300	1	0.12	32.5	**300**	Disordered MCM-41
$I_{32.5}$-450	1	0.12	32.5	**450**	**Disordered MCM-41**
$I_{32.5}$-600	1	0.12	32.5	**600**	Disordered MCM-41
$I_{32.5}$-800	1	0.12	32.5	**800**	Amorphous

The powder XRD patterns of these as-synthesized Si-MCM-41 are shown in Fig. 3.1.2.1.3. Even though the resolution of peaks for most of the as-synthesized samples is poor, upon calcination, these samples have shown presence of three clear reflections [(100), (110) and (200)] indicative of well ordered MCM-41. It is interesting to note that,

the characteristic peak (100) was found to shift towards lower 2θ value when the NH_4OH/SiO_2 ratio in the starting gel was decreased. The shifting of the peak to lower 2θ values might be associated with well grown unit cell and larger mesopore size or thinner pore wall.

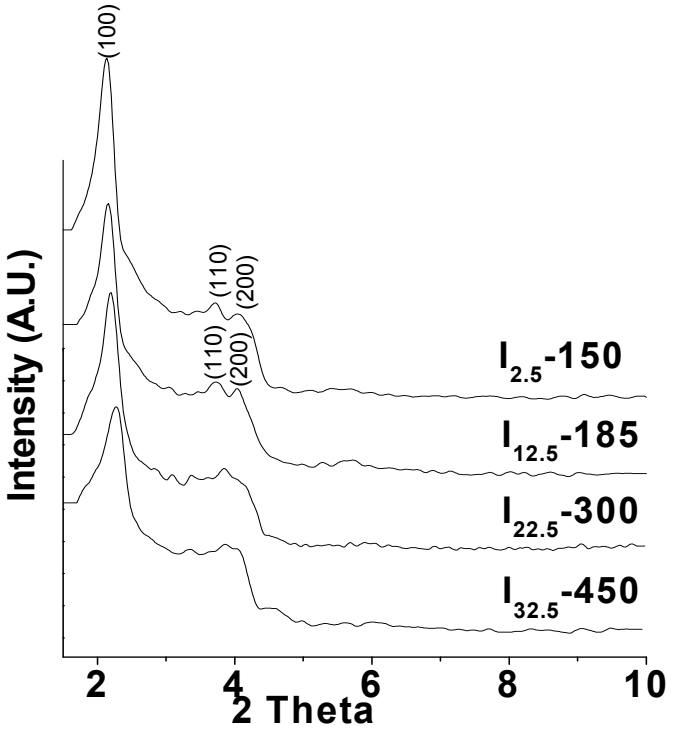

Fig. 3.1.2.1.3: Powder XRD patterns of as-synthesized Si-MCM-41 prepared with optimum H_2O/NH_4OH ratio at different NH_4OH/ SiO_2 molar ratio in the gel.

In order to verify such variation in the degree of ordering, the unit cell parameter 'a_o' using X-ray diffraction data are summarized in Table 3.1.2.1.3. Upon calcination, $I_{2.5}$-150, $I_{12.5}$-185 and $I_{22.5}$-300 materials have shown considerable increase in the intensity of low angle reflection and shifting of 2θ to higher values as compared to their as-synthesized forms. While structure of sample $I_{32.5}$-450 collapsed after calcination. A shift in low angle reflection was found comparatively more pronounced for sample $I_{12.5}$-185 and which may be probably related to a greater contraction of the lattice after calcination. An extent of lattice contraction (denoted as 'Δa_0 ') and provided in Table 3.1.2.1.3.

Table 3.1.2.1.3: The unit cell parameters and extent of contraction upon calcination of different MCM-41 synthesized using ethyl silicate at room temperature.

Sample designation	d_{100} (nm)		Unit cell parameter a_o (nm)		Δa_0 (nm)	% Contraction
	As synthesized	Calcined	As synthesized	Calcined		
$I_{2.5}$-150	4.12	3.59	4.75	4.14	0.61	12.8
$I_{12.5}$-185	4.07	3.54	4.70	4.08	0.62	13.2
$I_{22.5}$-300	4.01	3.53	4.63	4.07	0.56	12.1
$I_{32.5}$-450	3.90	--	4.50	--	--	--

Sample $I_{12.5}$-185 has shown maximum degree of lattice contraction. This indicates that, the population of ≡Si-OH units in the channel wall increases in the order: $I_{12.5}$-185 > $I_{2.5}$-150 > $I_{22.5}$-300. The % lattice contraction was observed in the range of 12.1 to 13.2 when ethyl silicate was used as a silica source. Low temperature nitrogen adsorption/desorption isotherms and pore size distribution of these samples are depicted in Fig. 3.1.2.1.4. Inset in Fig. 3.1.2.1.4 illustrates the pore size distribution curves obtained from desorption branch and BJH method. Except $I_{32.5}$-450, all other samples have shown nitrogen adsorption-desorption isotherms typically of type IV. Samples $I_{2.5}$-185 and $I_{12.5}$-150 exhibited pronounced steep condensation step for relative pressures 0.2 to 0.4 arising from condensation of nitrogen inside the primary mesopores. The condensation step is not steep particularly for $I_{22.5}$-300 indicating poor quality of MCM-41 formed as compared to $I_{12.5}$-185 and $I_{2.5}$-150. However, the isotherm obtained for $I_{32.5}$-450 can be considered as type I, since it presents very small inflection characteristics of capillary condensation process. Appearance of hysteresis loop at high relative pressure might be due to the presence of secondary mesopores arising from interparticle capillary condensation from the structure

collapse of portions of the mesopores during calcination. $I_{32.5}$-450 has exhibited quite broader pore size distribution as compared to other samples.

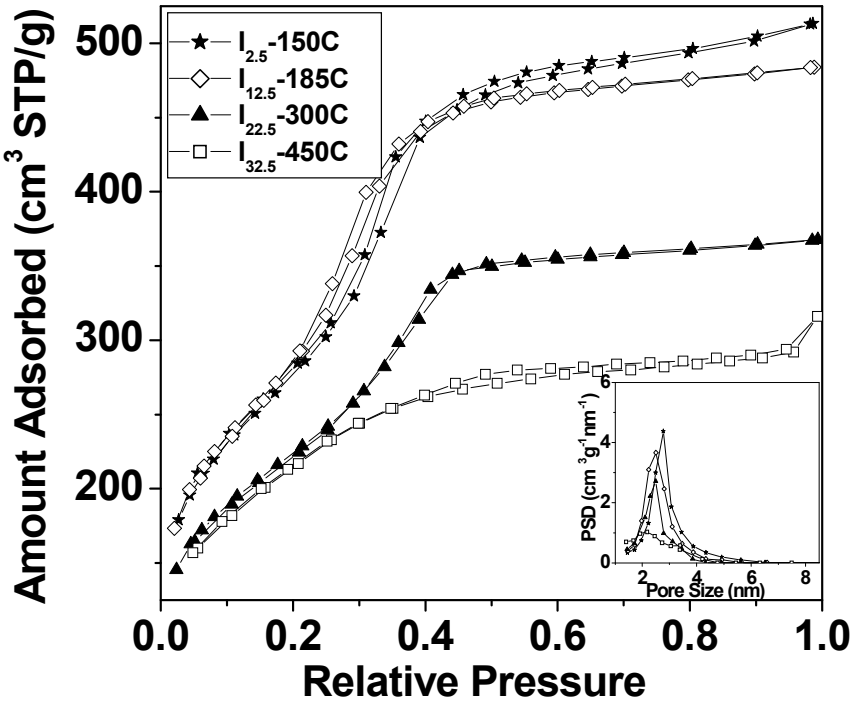

Fig. 3.1.2.1.4: Low temperature nitrogen adsorption/desorption isotherms [Inset: pore size distribution curves] for calcined samples prepared with optimum H_2O/NH_4OH ratio at different NH_4OH/ SiO_2 molar ratio in the gel.

The specific pore volume, BET surface area and average BJH pore diameter deduced from the nitrogen sorption isotherms for all these four samples are summarized in Table 3.1.2.1.4.

Table 3.1.2.1.4: Textural/structural characteristics of calcined samples obtained from gels having different NH_4OH/ SiO_2 with optimum H_2O/NH_4OH molar ratios.

Sample designation	Total pore Volume, cc/gm	BET surface area, m^2g^{-1}	BJH Pore diameter, (nm)	Wall thickness (nm)
$I_{2.5}$-150C	0.79	1012	2.71	1.43
$I_{12.5}$-185C	0.74	986	2.50	1.61
$I_{22.5}$-300C	0.56	811	2.41	1.67
$I_{32.5}$-450C	0.48	779	--	--

It also includes the magnitude of their wall thickness, which is calculated by taking the difference between the unit cell parameter a_o and the average pore diameter. The mutual inverse proportion was observed between the BET specific surface area and the wall thickness. The reduction in the surface area was accompanied by the decrease in pore volume. At optimum molar H_2O/NH_4OH ratio, an increase in NH_4OH/SiO_2 in the gel resulted in the drop in total pore volume. The observed change in the pore volume can be attributed to both the reduction in the pore diameter due to increased wall thickness and the structural irregularity. As described earlier the system and sample were designated as Ix-Z where x = molar NH_4OH/SiO_2 ratio and Z = molar H_2O/SiO_2 ratio in the initial reaction mixture. Upon calcination, this product was labeled as I_X-ZC. $I_{32.5}$-450C has exhibited quite broader pore size distribution as compared to other samples. $I_{2.5}$-150C presented narrower pore size distribution as compared to $I_{12.5}$-185C and $I_{22.5}$-300C. This may be attributed partly to the lower NH_4OH/SiO_2 molar ratio employed which is responsible for retarding the hydrolysis and condensation reaction rates.

The dependence of the phase quality on the concentration of CTMABr was also investigated using ethyl silicate as a source of silica. The molar $CTMABr/SiO_2$ ratio in the gel was varied in the range of 0.06 – 0.24 keeping fixed molar ratios of NH_4OH/SiO_2 and H_2O/SiO_2 as 2.50 and 150 respectively. The system and the product obtained there-from are designated as IIs-x where x is the molar $CTMABr/SiO_2$ ratio in the gel. The powder XRD patterns of as-synthesized phases obtained by varying molar $CTMABr/SiO_2$ ratios in the range of 0.06 – 0.24 in the gel are shown in Fig. 3.1.2.1.5. On account of insufficient surfactant, MCM-41 mesophase was not formed using system IIs-0.06. High quality MCM-41 was obtained from system IIs-0.12.

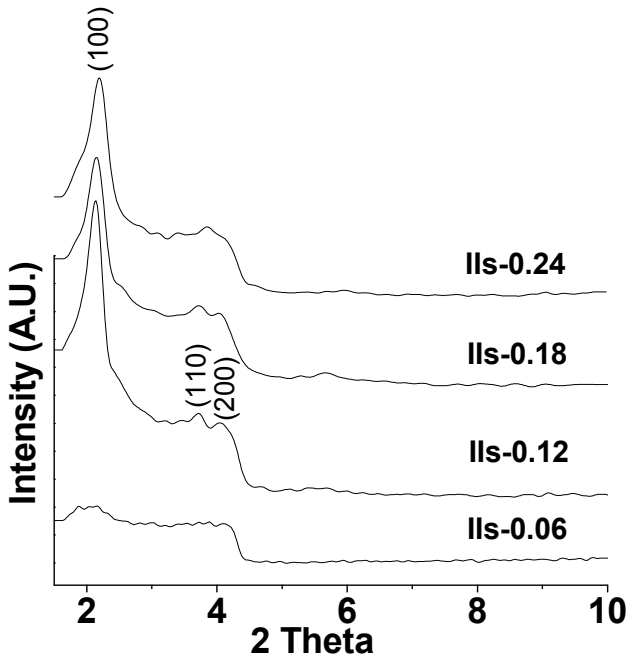

Fig. 3.1.2.1.5: Powder XRD patterns of as-synthesized Si-MCM-41 prepared with different molar CTMABr/SiO_2 ratios in the gel.

With further increase in CTMABr/SiO_2 molar ratio in the gel, the relative quality of the product was found to decrease. Furthermore, an increase in the surfactant concentration resulted in the broadening of the characteristic peak and shifting though marginally to the higher 2θ value. Such behavior may be attributed to prohibition from unit cell growth and decreased polymerization of silica by an excess of surfactant. Fig. 3.1.2.1.6 shows representative SEM images of as-synthesized samples prepared in different H_2O/NH_4OH and NH_4OH/SiO_2 molar ratio regions using ethyl silicate as source of silica.

The SEM images of the samples whose XRD patterns are shown in Fig. 3.1.2.1.1 are included in this figure to demonstrate the morphological changes occurred with the change in H_2O/NH_4OH molar ratio in the gel. It is clearly visible that, the sample $I_{2.5}$-150 exhibits well developed particles and most of them are almost perfectly hexagonal although some round shaped particles are visible. As the H_2O/NH_4OH molar ratio in the gel is reduced from 150 to 25, the extent of fusion of hexagonal and round shaped particles

increases giving rise to sheet like particles. However, these sheets or plates are not regular in size. On the contrary, on further dilution (H_2O/NH_4OH molar ratio = 185), there is not much difference in morphology but the hexagonal and round shaped particles become irregular and smaller in size. Similar changes in the morphology were observed when NH_4OH/SiO_2 molar ratio in the gel was changed. The SEM images of the samples whose XRD patterns are depicted in Fig. 3.1.2.1.2 are also included in Fig. 3.1.2.1.6.

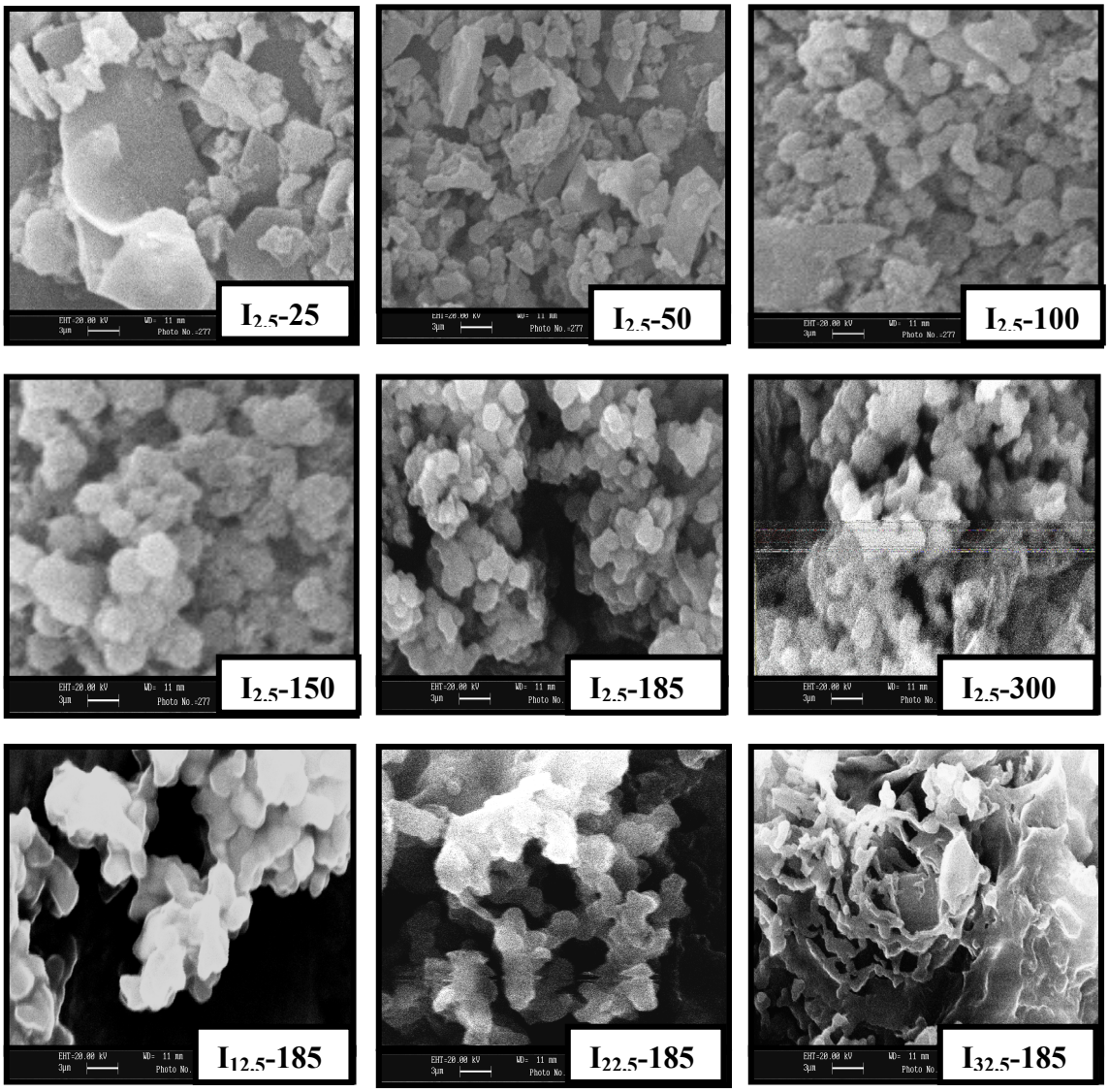

Fig. 3.1.2.1.6: Scanning electron micrographs of the samples designated as I_a –XX where 'a' and 'XX' are molar ratios of NH_4OH/SiO_2 and H_2O/NH_4OH in the gel.

From Fig. 3.1.2.1.6 it can be concluded that, each variable, molar ratios of H_2O/NH_4OH and NH_4OH/SiO_2, controls the morphology during the room-temperature synthesis of MCM-41 using ethyl silicate as a source of silica.

To gain further insight into the advantages and drawbacks of using ethyl silicate, we have assessed the crucial parameters such as the textural properties and the thermal stability of MCM-41 prepared at room temperature and compared with that of obtained using conventional TEOS. The molar composition of gel SiO_2 : 0.12 CTMABr : 2.50 NH_4OH : 150 H_2O was selected for carrying out the room temperature synthesis of Si-MCM-41 using conventional tetra-ethyl-ortho-silicate (TEOS) as a source of silica. The system in which equivalent quantity of TEOS was used in place of ethyl silicate and the as-synthesized product obtained there from is designated as $T_{2.5}$-150. Upon calcination, this product was labeled as $T_{2.5}$-150C. Sample$T_{2.5}$-150 has shown increased intensity of low angle reflection and shifting of 2θ to lower value as compared to sample $I_{2.5}$-150. The d_{100} values, unit cell parameters and an extent of lattice contraction on calcination as a function of type of silica source used are tabulated in Table 3.1.2.1.5.

Table 3.1.2.1.5: Comparison between the unit cell parameters and extent of contraction upon calcination of MCM-41 synthesized at room temperature using ethyl silicate and TEOS.

Sample designation	d_{100} (nm)		Unit cell parameter a_o (nm)		Δa_0 (nm)	% Contraction
	As synthesized	Calcined	As synthesized	Calcined		
$I_{2.5}$-150	4.12	3.59	4.75	4.14	0.61	12.8
$T_{2.5}$-150	4.09	3.54	4.72	4.08	0.64	13.5

The unit cell parameters of $I_{2.5}$-150 and $I_{2.5}$-150C are higher as compared to $T_{2.5}$-150 and $T_{2.5}$-150C respectively. However, higher lattice contraction was observed when TEOS was used. It is, however, noteworthy here, that the system $I_{2.5}$-150 yielded MCM-41

irrespective of the silica source used but MCM-41 could only form the system $I_{2.5}$-25 when TEOS was used. The low temperature nitrogen adsorption/desorption isotherms and pore size distribution of these samples are depicted in Fig. 3.1.2.1.7. Inset depicts the pore size distribution curves obtained from desorption branch and BJH method.

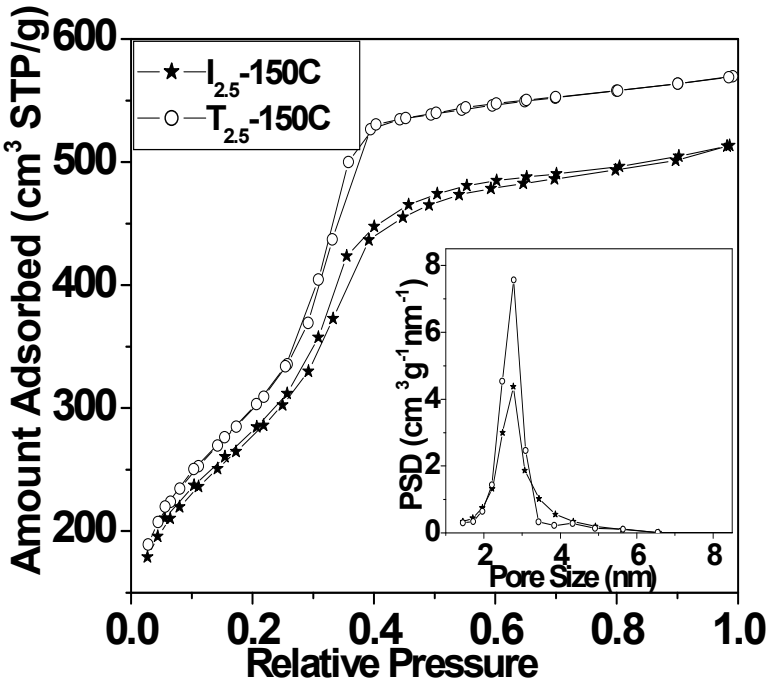

Fig. 3.1.2.1.7: Low temperature nitrogen adsorption/desorption isotherms for calcined MCM-41 materials synthesized with ethyl silicate and TEOS at room temperature [inset :their pore size distribution curves].

Both the samples $I_{2.5}$-150C and $T_{2.5}$-150C exhibit a reversible type IV isotherm which is a typical presentation of mesoporous materials. A sharp inflection noticed at relative pressures 0.2 to 0.4 corresponds to condensation of nitrogen inside the primary mesopores. The condensation step on the isotherms is steep particularly for $T_{2.5}$-150C as compared to $I_{2.5}$-150C. Thus, the quality of the product was found to affect the steepness of the condensation step. Gradual development of small hysteresis loops below relative pressure of 0.40 was observed for both the samples which may be partly attributed to the instability of liquid nitrogen meniscus for nitrogen adsorption studies performed at 77K

[22]. Sample $T_{2.5}$-150C has narrow pore size distribution as compared to $I_{2.5}$-150C. The presence of silica in a limited range of polymerization in ethyl silicate may be responsible for governing the rates of hydrolysis and condensation and in turn size and packing geometry of surfactant-silica primary particles. The data concerning specific pore volume, specific surface area, average pore diameter and the wall thickness of samples $I_{2.5}$-150C and $T_{2.5}$-150C are summarized in Table 3.1.2.1.6. It can be seen from Table 3.1.2.1.6 that, if not better but comparable and acceptable quality of MCM-41 can be obtained using ethyl silicate. The observed differences may be associated with the differences in the amount of silica monomers and hence their hydrolysis and condensation rates. Moreover, higher wall thickness of $I_{2.5}$-150C indicates that, MCM-41 with improved structural stability may be obtained just by replacing TEOS by ethyl silicate under identical set of synthesis conditions.

Table 3.1.2.1.6.: Comparison of textural/structural characteristics of calcined MCM-41 obtained at room temperature using ethyl silicate and TEOS.

Sample designation	Total pore Volume, cc/gm	BET surface area, m^2g^{-1}	BJH Pore diameter, (nm)	Wall thickness (nm)
$I_{2.5}$-150C	0.79	1012	2.71	1.43
$T_{2.5}$-150C	0.88	1064	2.79	1.29

To assess the thermal stability, $I_{2.5}$-150C and $T_{2.5}$-150C were further heated at different temperatures viz. 923 K, 1023 K and 1123 K. The heating rate was kept 1 K/min and sample was kept at end temperature for 6 hrs. The temperature at which sample is subjected for heat treatment was subscripted while labeling. As an illustration, when $I_{2.5}$-150C sample was heat treated at 923 K for 6 hrs, the treated sample is designated as $I_{2.5}$-$150C_{923}$. The difference between the intensity of the characteristic d_{100} XRD peak before and after the thermal test was taken as a measure for evaluating the thermal stability.

Fig. 3.1.2.1.8 illustrates the powder XRD patterns of these samples, before and after thermal treatment. It can be seen from Fig. 3.1.2.1.8 that, in both the cases, not only an intensity of d_{100} peak gradually decreases but also shifts to higher 2θ value as the heating temperature increases. The peaks of (200) and (210) reflections disappeared at higher temperatures. Powder XRD patterns were found featureless when samples were heated to 1123 K. It is interesting to note that, the % pore structure collapse was found relatively higher in case of MCM-41 prepared using TEOS.

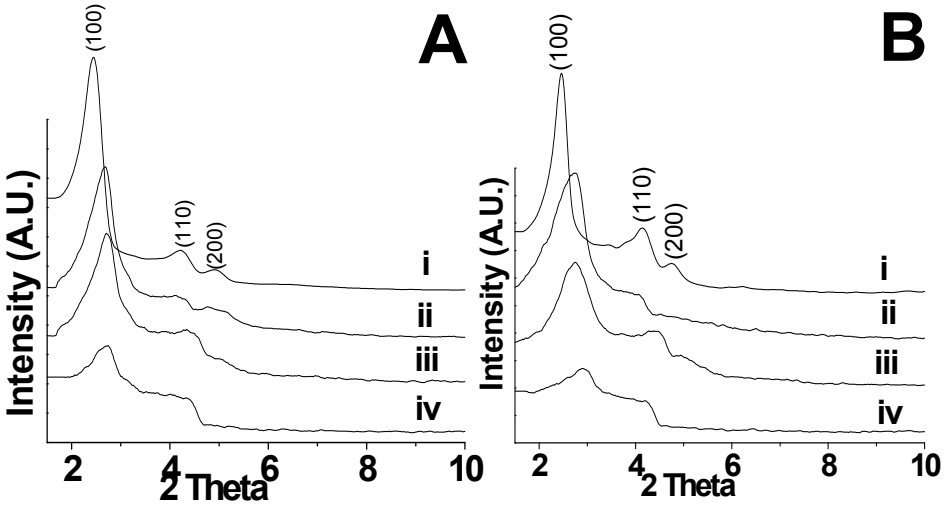

Fig. 3.1.2.1.8: Powder XRD patterns of Si-MCM-41 prepared using (A) ethyl silicate and (B) TEOS after subjecting to thermal treatments (i-freshly calcined, ii-heated at 923 K, iii- heated at 1023 K, iv- heated at 1123 K).

In other words, $I_{2.5}$-150C is more thermally stable or heat resistant as compared to $T_{2.5}$-150C sample. The higher thermal stability of $I_{2.5}$-150C may be partly due to its slightly thicker pore walls as compared to $T_{2.5}$-150C. To gain more insight in the influence of temperature on the status of unit cell parameter, Table 3.1.2.1.7 illustrates the values of d-spacings and unit cell parameters of heat treated samples. A close inspection of unit cell parameter data clearly indicates that $I_{2.5}$-150C and $T_{2.5}$-150C show similar thermal behaviours. When subjected to calcination temperature of 1123 K, $I_{2.5}$-150C suffers about

8.9 % decrease in the unit cell parameter, whereas, in case of $T_{2.5}$-150C unit cell parameter decreases about 9.3 % of the initial value.

Table 3.1.2.1.7: Influence of silica source materials on d-spacings and unit cell parameters of various MCM-41 samples obtained after thermal treatment.

Ethyl silicate			TEOS		
Sample designation	d_{100}-Spacing (nm)	Unit Cell Parameter a_o (nm)	Sample designation	d_{100}-Spacing (nm)	Unit Cell Parameter a_o (nm)
$I_{2.5}$-150C	3.59	4.14	$T_{2.5}$-150C	3.54	4.08
$I_{2.5}$-150C_{923}	3.29	3.79	$T_{2.5}$-150C_{923}	3.23	3.73
$I_{2.5}$-150C_{1023}	3.27	3.77	$T_{2.5}$-150C_{1023}	3.21	3.70
$I_{2.5}$-150C_{1123}	-	-	$T_{2.5}$-150C_{1123}	-	-

Thus, acceptable thermal stability of MCM-41 prepared at room temperature using ethyl silicate indicates that ethyl silicate is a suitable silica source for MCM-41 preparation at room temperature. To demonstrate the morphological changes occurred with the change in silica source with same molar gel composition the SEM and TEM images of the samples whose properties are given in Table 3.1.2.1.6 are included in the Fig. 3.1.2.1.9

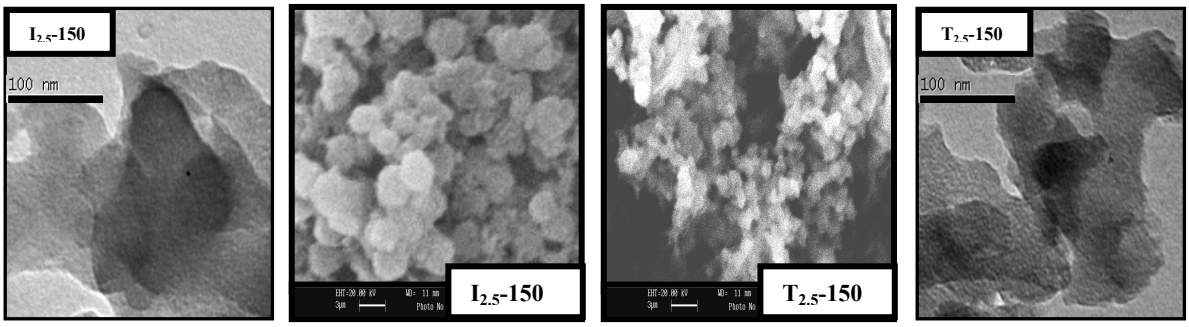

Fig. 3.1.2.1.9: SEM and TEM micrographs of MCM-41 materials prepared at room temperature with ethyl silicate and TEOS as a silica source with similar molar gel composition.

It is clearly visible that, the sample $I_{2.5}$-150 exhibits well developed particles and most of them are almost perfectly hexagonal although some round shaped particles are visible. The particle size and shape of $T_{2.5}$-150 is small as compared to $I_{2.5}$-150.

3.2. SYNTHESIS AND CHARACTERIZATION OF Sn-MCM-41 TYPE MESOPOROUS MATERIALS

Owing to the exceptional adsorption capacities and molecular sieving properties, MCM-41 type materials are very attractive for the design of new selective heterogeneous catalysts for various hydrocarbon conversion reactions. Catalytic functions can be generated by the incorporation of heteroelements preferably in their appropriate valence state as tetrahedral framework species. Mesoporous tin containing analogs of MCM-41 has been shown to catalyze the selective oxidation/epoxidation of organic compounds under mild conditions [23]. However, there is no report on systematic studies on the optimization of synthesis parameters for the preparation of Sn-MCM-41 and its use as a heterogeneous catalyst in Mukaiyama-type aldol reaction. Prompted by this, the optimization of various gel parameters and catalytic performance of Sn-MCM-41 in the said reaction was undertaken.

3.2.1. Hydrothermal Synthesis of Sn-MCM-41

Based on earlier findings, various synthesis trials were conducted for the hydrothermal synthesis of Sn-MCM-41. In initial probing runs, a system SiO_2 : 0.18 CTMABr: 0.25 TMAOH : 25 H_2O which has been proved to yield good quality of Si-MCM-41 was selected. When tin tetrachloride ($SiO_2/SnO_2 = 250$) was added to the same gel, disordered Sn-MCM-41 was obtained after 66 hrs at 383 K. No phase transformation or improvement in quality of MCM-41 was observed even if the synthesis period was prolonged up to 82 hrs. Therefore, further work was planned and carried out aiming at optimization of the gel parameters such as molar ratios of $TMAOH/SiO_2$, $CTMABr/SiO_2$, H_2O/SiO_2 in gel and sources for silica and tin.

3.2.1.1. Optimization of Synthesis Parameters

Keeping fumed silica and tin tetrachloride as source of silica and tin fixed, different gels with compositions SiO_2 : w SnO_2 : x CTMABr : y TMAOH : z H_2O where w, x, y and z were varied in the range of $0.004 < w < 0.01$, $0.18 < x < 0.32$, $0.25 < y < 0.35$, $25 < z < 45$ were prepared and subjected to hydrothermal treatment at 383 K. The details of systems, their molar composition and product obtained there from are tabulated in Table 3.2.1.1.1. The systems were formulated so as to deal with the influence of concentration of the various reactants on the formation of type and quality of the phase formed. The concentration of one reagent was varied at a time to optimize the suitable gel composition and synthesis time to yield well ordered Sn-MCM-41.

Table 3.2.1.1.1: Details of systems, their molar composition and product obtained there from using fumed silica and tin tetrachloride as sources of silicon and tin respectively.

System Designation	Molar Composition					Product by Powder XRD
	SiO_2	CTMABr	TMAOH	H_2O	SnO_2	
I	1	0.18	**0.25**	25	0.004	Disordered MCM-41
II	1	0.18	**0.30**	25	0.004	Disordered MCM-41
III	1	0.18	**0.35**	25	0.004	Lamellar
IV	1	**0.24**	0.35	25	0.004	Lamellar
V	1	0.24	**0.30**	25	0.004	**MCM-41**
VI	1	0.24	**0.25**	25	0.004	Disordered MCM-41
VII	1	**0.32**	0.30	25	0.004	Disordered MCM-41
VIII	1	0.24	0.30	**35**	0.004	Disordered MCM-41
IX	1	0.24	0.30	**45**	0.004	Disordered MCM-41

The influence of molar TMAOH/SiO_2 ratio on the quality of phase formed was investigated from systems I to III wherein molar TMAOH/SiO_2 ratio was varied from 0.25 to 0.35. The powder XRD patterns of the phases obtained from these systems are depicted

in Fig. 3.2.1.1.1. Though none of these products are of good quality Sn-MCM-41, among these three systems slightly improved quality of Sn-MCM-41 was obtained from system II as compared to the systems I and III. In view of improving the quality of Sn-MCM-41 still further, the effect of molar TMAOH/SiO_2 ratio was also investigated at higher concentration of surfactant (CTMABr/SiO_2 molar ratio 0.24).

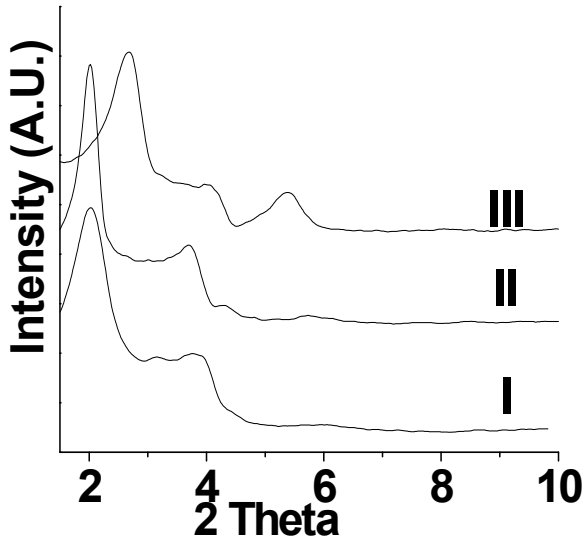

Fig. 3.2.1.1.1: Powder XRD patterns of as-synthesized phases prepared from systems with molar ratios of TMAOH/SiO_2 (I) 0.25 , (II) 0.30 and (III) 0.35 in the gels.

It is interesting to note that, the good quality of Sn-MCM-41 was obtained from System V, much better than that of obtained from system II. Thus, in present studies, the good quality of Sn-MCM-41 was obtained at an optimum TMAOH/SiO_2 ratio of 0.30, below and above which the product quality gets deteriorated. Probably, on account of lack of sufficient quantity of OH^- concentration needed for digestion of silica, the system with lower concentration of TMAOH was found to lead the formation of more disordered MCM-41 structure, while a system with higher TMAOH concentration tends to yield a lamellar phase. In the present studies, the products obtained from systems III and IV became

featureless after calcination. Moreover, comparing the gel composition of Si-MCM-41, it can be concluded that the formation of Sn-MCM-41 occurs when concentration of TMAOH is higher than that of Si-MCM-41. As described above, the quality of Sn-MCM-41 was found to improve on increasing the surfactant concentration keeping molar TMAOH/SiO_2 ratio = 0.30 fixed. The dependence of the phase quality on the concentration of CTMABr was further investigated by increasing molar CTMABr/SiO_2 ratio to a value of 0.32. Thus, system VII wherein the gel with molar compositions SiO_2 : 0.004 SnO_2 : 0.32 CTMABr : 0.30 TMAOH : 25 H_2O was prepared and subjected to hydrothermal treatment. Therefore, the role of concentration of CTMABr in the synthesis of Sn-MCM-41 can be very well seen from the product quality obtained from systems II, V and VII. The powder XRD patterns of as-synthesized Sn-MCM-41 samples obtained from these systems have shown in Fig. 3.2.1.1.2.

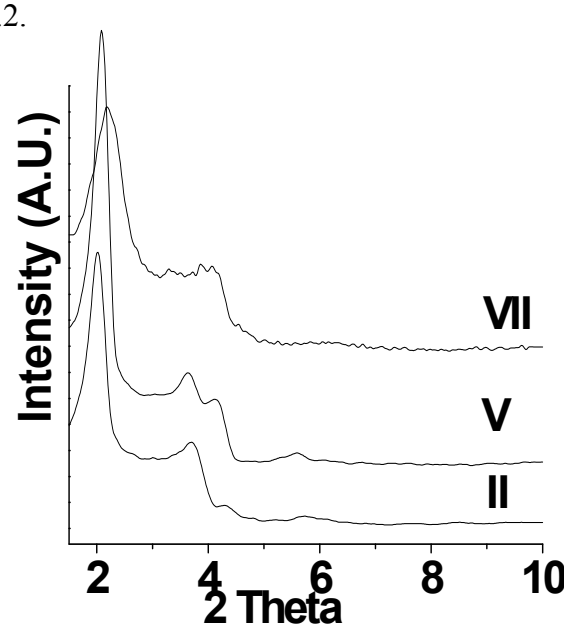

Fig. 3.2.1.1.2: Powder XRD patterns of as-synthesized Sn-MCM-41 prepared from systems with molar ratios of CTMABr /SiO_2, (II) 0.18, (IV) 0.24 and (V) 0.32 in the gels

It is evident from the figure that, with increase in the molar ratio of CTMABr/SiO_2, the quality of Sn-MCM-41 improves, reaches to maximum and then decreases. The decrease in the quality of Sn-MCM-41 was evidenced by the reduced intensity and broadening of low angle reflection. Such drop in the quality may be partly attributed to the prohibition from growing of MCM-41 crystallite and decreased polymerization of silica by excess of surfactant. Further optimization was concentrated on the molar H_2O/SiO_2 ratio in the gel. As can be seen from the compositions of systems V, VIII and IX, the molar ratio of H_2O/SiO_2 was varied systematically from 25 to 45 keeping other parameters constant. Powder XRD patterns of the products obtained from these systems are shown in Fig. 3.2.1.1.3.

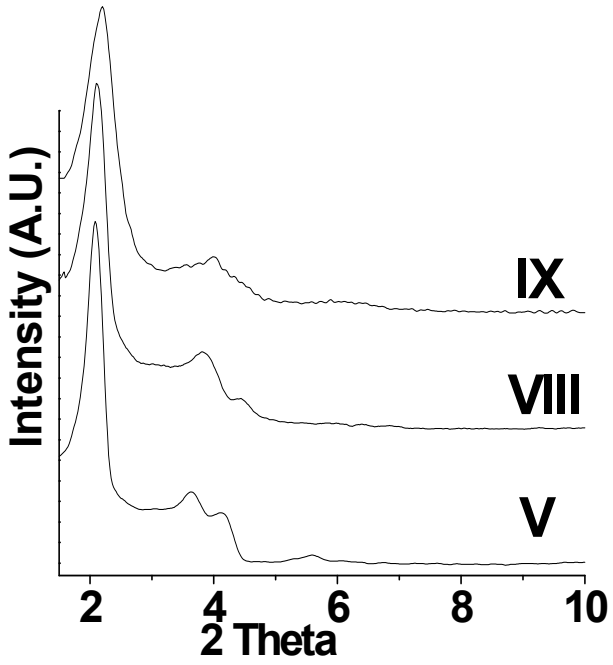

Fig. 3.2.1.1.3: Powder XRD patterns of as-synthesized Sn-MCM-41 prepared from systems with molar ratios of H_2O/ SiO_2 (V) 25 , (VIII) 35 and (IX) 45 in the gels.

With increase in the gel dilution, the quality of Sn-MCM-41 drops down as evidenced by the reduced intensity and broadening of low angle reflection. Such detrimental effect may

be partly attributed to the decrease in the effective concentrations of the reacting species with increase in the water content. Probably, at higher degree of dilution, prohibition from growing of MCM-41 crystallite and decreased polymerization of silica might be operative in the formation of poorer quality of Sn-MCM-41. On the basis of the results obtained from above optimization work, one can conclude that, although each synthesis variable contributes to a specific aspect of synthesis of Sn-MCM-41, there is a substantial interplay between them. Thus, keeping fixed molar ratio of SiO_2/SnO_2 = 250, the optimum values for other crucial compositional variables in the initial gel such as molar ratios of $TMAOH/SiO_2$, $CTMABr/SiO_2$, H_2O/SiO_2 were found to be 0.30, 0.24 and 25.0 respectively. On summarizing the results on optimization studies for molar ratios of $TMAOH/SiO_2$, $CTMABr/SiO_2$ and H_2O/SiO_2, it can be concluded that, a system having gel composition SiO_2 : 0.004 SnO_2 : 0.24 CTMABr : 0.30 TMAOH : 25 H_2O is the better choice for hydrothermal synthesis of good quality of Sn-MCM-41. The well-ordered Sn-MCM-41 was obtained from this gel after undergoing the hydrothermal treatment at 383 K for 66 hrs.

As described earlier, well ordered Sn-MCM-41 (SiO_2/SnO_2=250) was successfully synthesized from a gel with an optimum molar composition SiO_2 : 0.004 SnO_2 : 0.24 CTMABr : 0.30 TMAOH : 25 H_2O using fumed silica and tin tetrachloride as silicon and tin sources respectively. In order to investigate the influence of silica and/or tin source materials on the quality of Sn-MCM-41, gels with different combinations of silica and tin sources were prepared and subjected to hydrothermal treatment. Three silica and three tin sources were used in this study for the preparation Sn-MCM-41 under the identical set of synthesis conditions. Except desired silica and/or tin source, other synthesis parameters

such as gel composition (same as stated above), addition sequence, synthesis temperature, ratio of charged reaction mass to autoclave volume and downstream process conditions were kept constant. Varying the syntheses times for each system also monitored the degree of ordering of the pore structure of Sn-MCM-41. From such time dependant studies, the optimum synthesis period required to obtain a sample with highest peak intensities and unit cell parameter 'a_0' from this each system was identified. The details regarding sample designation, the synthesis time required to obtain most ordered Sn-MCM-41 from each system, type of source combinations used, chemical analyses in terms of molar SiO_2/SnO_2 ratio in product and XRD data for each Sn-MCM-41 are summarized in Table 3.2.1.1.2.

Table 3.2.1.1.2: Sample designation, silica and tin source combination used in gel, hydrothermal synthesis period required, composition and XRD data of various Sn-MCM-41 materials.

Sample Code	Sources		Molar SiO_2/SnO_2 ratio		Synthesis time (hrs)	XRD data	
	Silica	Tin	Gel	Product		d_{100} (nm)	Unit cell parameter a_0 (nm)
A	Fumed Silica	Tin tetrachloride	250	247	66	4.24	4.89
B	Fumed Silica	Tin tert-butoxide	250	248	66	4.30	4.96
C	Fumed Silica	Sodium stannate	250	243	72	3.84	4.43
D	Silica sol	Tin tetrachloride	250	247	72	4.12	4.75
E	Ethyl Silicate	Tin tetrachloride	250	246	36	4.01	4.63
F	Fumed Silica	Tin tetrachloride	100	98	72	4.37	5.04

Powder XRD patterns of as-synthesized Sn-MCM-41 prepared from various combinations of silica and tin sources are depicted in Fig. 3.2.1.1.4. Samples A, B and C

form one set where silica source viz. fumed silica was kept constant and tin sources were varied in such a way that molar SiO_2/SnO_2 ratio in gel should remain 250.

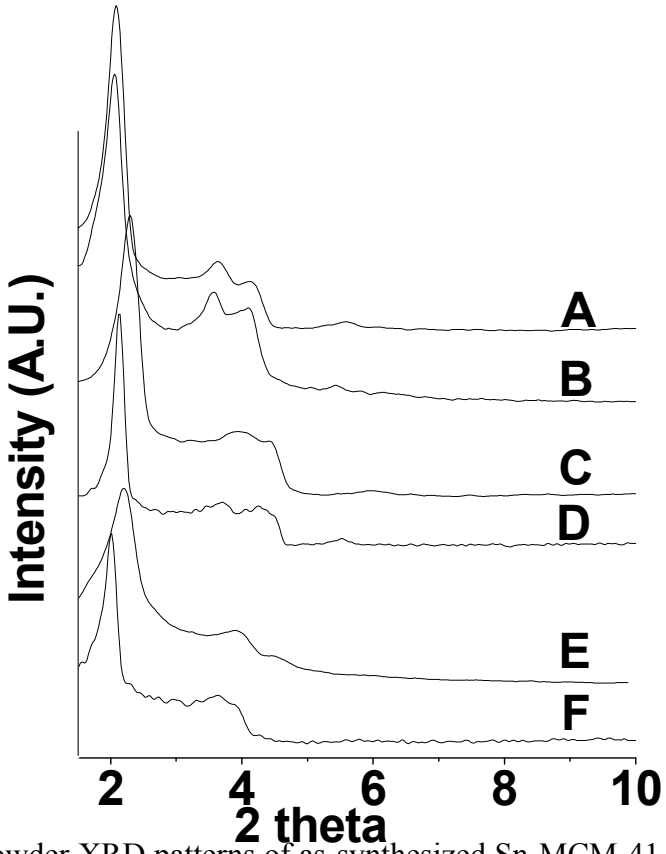

Fig. 3.2.1.1.4: Powder XRD patterns of as-synthesized Sn-MCM-41 prepared from various combinations of silica and tin sources

If relative intensity and sharpness of the XRD peak (d_{100}) were taken as a measure of relative orderness and quality of Sn-MCM-41, it is evident from Fig. 3.2.1.1.4 that, samples A and B both were found to be more ordered and of high quality as compared to samples C. Similarly, samples A, D and E form another set where tin source viz. tin tetrachloride was kept constant and silica sources were varied without disturbing molar SiO_2/SnO_2 ratio in the gel. From XRD examinations, samples A and D both were found to be more ordered and of high quality as compared to samples E. Thus, among silica sources, fumed silica and silica sol were proved to better sources when they were used in combination with tin tetrachloride. Moreover, a well ordered Sn-MCM-41 was also

obtained using combination of fumed silica and tin tert-butoxide. It is noteworthy here that, a combination of ethyl silicate and sodium stannate sources has failed to the form a well ordered Sn-MCM-41 even if the hydrothermal synthesis was allowed to last for 92 hrs. Unit cell parameter 'a_0' for each product are included in Table 3.2.1.1.2. It is interesting to note that, using the same source materials, synthesis period was found to increase with the increase in the tin content in the gel. It is noteworthy here that, despite the identical molar SiO_2/SnO_2 ratio in the gel, the nature of silicon and tin sources seems to be operative in controlling the progressive development of Sn-MCM-41 phase and hence their structural characteristics. On account of larger size of Sn^{4+} (radius, 0.055 nm) compared with Si^{4+} (radius, 0.026 nm) as well as to the longer bond length of Sn-O than that of Si-O [24], the Sn-MCM-41 samples containing nearly same molar SiO_2/SnO_2 ratio, should have shown identical values of unit cell parameters. But, in present studies, the nature of silicon and tin sources seems to be operative in controlling the growth of unit cell parameters. The variations in the XRD data caused by the change in the source materials may be associated with differences in the packing of the surfactant, the electrical double layer in the surfactant aggregate and the long-order structure [25]. Thus, at this juncture, it can be assumed that, even though, the molar SiO_2/SnO_2 ratio in Sn-MCM-41 is nearly identical, the population of tetravalent tin responsible for expansion in hexagonal unit cell need not be necessarily same. However, with decreased molar SiO_2/SnO_2 ratio in Sn-MCM-41, an increase in the a_0 value suggest the increase in the population of tetravalent tin that incorporated in the silicate framework of MCM-41. It is evident from Table 3.2.1.1.2 that, the population of tetravalent tin incorporated in the silicate framework of MCM-41 which can be assumed to be responsible for the expansion of unit cell follows the trend as: F > B

> A > D > E > C. Sn-MCM-41 samples obtained from each system have shown lower molar SiO_2/SnO_2 ratio in comparison with their molar SiO_2/SnO_2 ratio in the synthesis gel. All the calcined samples have shown considerable increase in the intensity of low angle reflection and shifting of 2θ to higher values as compared to their as-synthesized forms. Surface and textural properties of these calcined samples were examined by low temperature nitrogen sorption. Nitrogen sorption isotherm of each sample exhibited a sharp and well-developed step in the relative pressure range of 0.2 to 0.4, characteristic of capillary condensation of nitrogen within uniform mesopores. The textural characteristics such as specific pore volume, BET surface area and average BJH pore diameter deduced from the nitrogen sorption isotherms for all these samples are summarized in Table 3.2.1.1.3. It also includes the magnitude of their wall thickness. It can be very well seen from this table that, the textural properties changes with change tin concentration and type of source materials.

Table 3.2.1.1.3: Textural/structural characteristics of Si- and various Sn-MCM-41

Sample designation	Total pore Volume, cc/gm	BET surface area, m^2g^{-1}	BJH Pore diameter, (nm)	Wall thickness (nm)
A	0.86	1150	2.49	1.58
B	0.84	1168	2.48	1.63
C	0.71	959	2.45	1.72
D	0.79	972	2.56	1.75
E	0.90	875	3.10	2.16
F	0.83	904	3.11	1.26
Si-MCM-41	0.63	1070	2.36	1.88

Diffuse reflectance UV-vis spectroscopy is a very sensitive probe for the detection of type and coordination state of Sn species. It also relates to the verification of the incorporation of tin in MCM-41 structure. Fig. 3.2.1.1.5 shows the typical UV-Vis diffuse

reflectance spectra of calcined Sn-MCM-41 samples with varying tin content and prepared by using different combination of source materials. For comparison, the spectra of pure SnO_2, tin-free Si-MCM-41 and Sn-impregnated MCM-41 are also included.

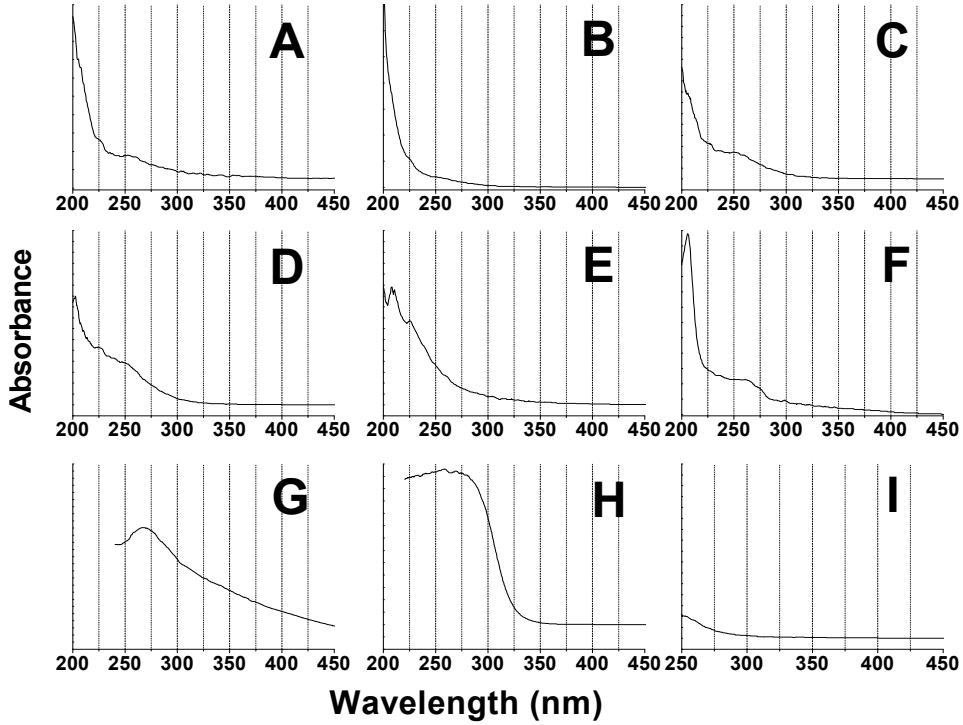

Fig. 3.2.1.1.5: Diffuse reflectance UV-vis spectra of calcined Sn-MCM-41 samples as labeled in table 2 from A to F. G = Sn-impregnated, H = Pure SnO_2, I = Si-MCM-41.

It is evident from the above figure that, pure SnO_2 and Sn-impregnated MCM-41 exhibit a broad absorption at ~ 280 nm which may be assigned to hexacoordinated polymeric Sn-O-Sn type species [24]. It is not surprising that, no absorption band relevant to detection of type and coordination state of Sn species was observed in tin-free MCM-41. Although, spectra of all the calcined Sn-MCM-41 samples reveal absorption at ~ 208 nm suggesting the presence of Sn^{4+} in tetrahedral coordination in the silica framework, it is manifested by the broader character. Moreover, the intensity of a band at ~ 208 was found to increase with the increase in the tin content. We believe

that site-isolated Sn in a distorted tetrahedral environment and/or in penta- or octahedral coordination sphere may be associated with such broadening character of Sn-MCM-41 spectra. Probably, the amorphous nature of the pore wall having wide range of Sn-O-Si bond angles might cause the distortion in tetrahedral environment of Sn species. For comparison, the spectra of pure SnO_2, tin-free Si-MCM-41 and Sn-impregnated Moreover, it is also likely that, on account of less crystallographic order in the pore walls, higher surface area and the larger pore dimensions, hydration of some of the Sn sites might result in the formation of Sn sites with coordination number higher than four [38]. This implies that, any differences in the catalytic behavior of these materials can be attributed to the differences in Sn siting. The presence of small absorption band at 280 $\pm$ 5nm in sample F indicates presence of hexacoordinated polymeric Sn-O-Sn type species [24]. It is evident from Fig. 3.2.1.1.5 that, samples C, D, E and F have exhibited different spectral features than samples A and B. Though with minor differences, the spectral features of A and B are matching with each other with regard to non-appearance of a broad absorption at ~ 280 nm and presence of absorption at ~ 208 nm with more or less same intensity and broadening. Thus, when fumed silica is used in the combination of either tin tetrachloride or tin tert-butoxide, it was found to favor the incorporation of Sn^{4+} in tetrahedral coordination in the silica framework of Sn-MCM-41 as compared to other source combinations. In conclusion, at this juncture, the spectral features of most of the samples under investigations suggest that, the nature and concentration of tin source and/or silica source used in the present studies have influenced the not only the synthesis times but also configuration of incorporated tin species.

SEM micrographs of Sn-MCM-41 samples are illustrated in Fig. 3.2.1.1.6. The structure of the Sn-MCM-41 samples were also characterized by TEM. Fig. 3.2.1.1.6 shows typical TEM images of sample 'B' taken during the electronic beam perpendicular and parallel to the pore direction with selected area electron diffraction pattern (SAED).

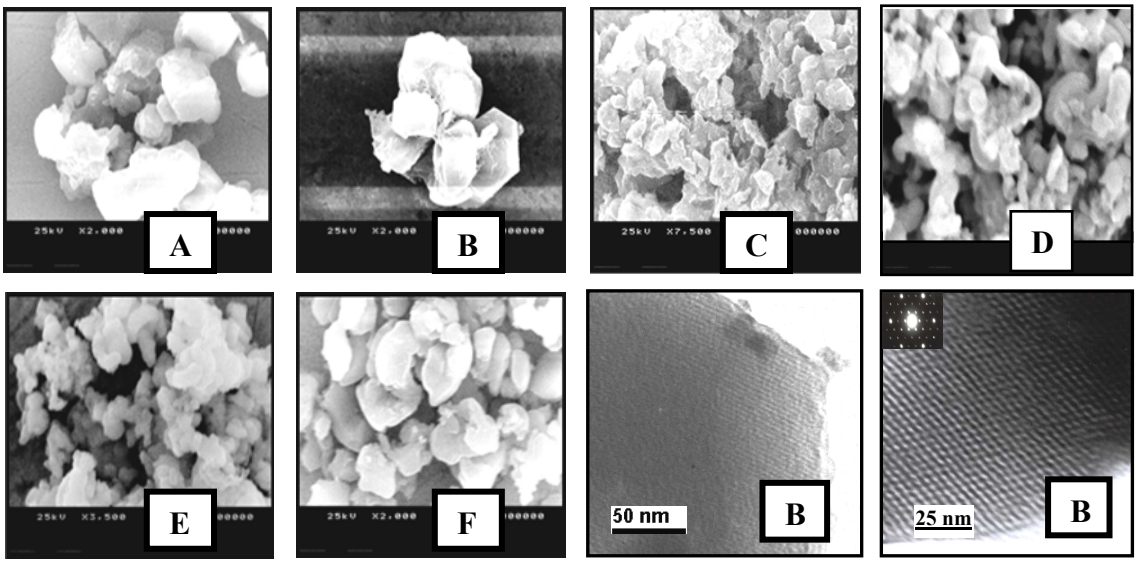

Fig. 3.2.1.1.6: SEM micrographs of Sn-MCM-41 prepared from various silica and tin sources.

The morphology of Sn-MCM-41 materials was found to depend largely on the type of the silica source rather than type of tin source used in their preparation. Keeping tin tetrachloride source fixed when fumed silica was used as a silica source, irregular and indefinite shaped large agglomerates were obtained. Whereas, worm/rope like and fused particles were observed with use of silica sol and ethyl silicate respectively. Keeping fumed silica source fixed, tin tetrachloride, tin tert-butoxide and sodium stannate showed some variation in their sizes with no definite shaped agglomerates. The possible cause for change in morphology with change in silica source may be the variation in the formation rate of surfactant micelles and micelle–silicate composites; hence variation in subsequent rate of silicate condensation might be responsible for giving rise to different morphology and sizes of the Sn-MCM-41 agglomerates.

3.3. CATALYTIC EVALUATION OF Sn-MCM-41 FOR MUKAIYAMA ALDOL CONDENSATION REACTION

In spite of having higher structural stability and Lewis acid type properties which are potentially useful for catalytic purposes, a fewer number of studies deal with catalytic application of Si-MCM-41 with partially substituted Sn. Prompted by this, we have investigated for the first time, an efficiency of Sn-MCM-41 for carbon-carbon bond formation in heterogeneously catalyzed Mukaiyama aldol condensation reaction. Catalytic liquid-phase Mukaiyama-aldol condensation reaction of methyltrimethyl silyl ketene acetal and benzaldehyde was performed at 373 K to produce β-hydroxy ester under solvent free system. On the basis of some similarities and differences in the characteristics of Sn-MCM-41 samples, four samples viz. samples A, B, E and F were selected from Table 3.2.1.1.3 for evaluating their efficiency in Mukaiyama-aldol condensation was examined using methyl trimethylsilyl dimethylketene acetal and benzaldehyde to produce the corresponding β-hydroxy ester. In present heterogeneous system, prior to conducting the Mukaiyama type aldol reaction, all the catalysts were activated in vacuum overnight at 523 K. In this reaction, to get the aldol (final) product, the reaction was quenched by the 1N HCl solution as shown in the Scheme 1.

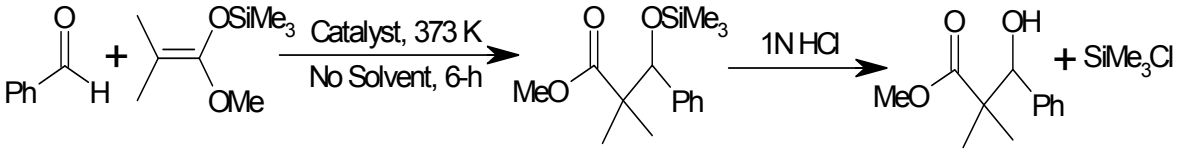

Scheme 1

The progress of the reaction was monitored by analyzing the aldol products removed at different time intervals (upto 24 hrs). All the samples have shown the maximum conversion after 6 hrs. continuing the reaction upto 24 hrs, only marginal increase in

conversion was observed [e.g. 87% at 6 hrs and 88.9% at 24 hrs for sample A]. Therefore, for comparison purpose, the catalytic data after 3 hrs and 6 hrs was considered. Invariably, the β-hydroxy ester selectivity was found to be 100 % irrespective of the conversion levels. The activity data are therefore presented in terms of yield for desired product in Table 3.3.1.

Table 3.3.1: Catalytic activity of Si-MCM-41 and various Sn-MCM-41 catalysts in solvent free Mukaiyama-aldol reaction [a]

Sample designation	Reaction time (h)	Yield [b](%)	TON [c]	TOF [d]
A	3	81	341.77	113.92
	6	87	367.08	61.08
B	3	85	357.14	119.04
	6	91	382.35	63.72
E	3	17	72.64	24.21
	6	35	149.57	24.92
F	3	55	94.82	31.60
	6	95	146.55	24.42
Si-MCM-41	6	-	-	-

[a] Reaction conditions :10 mmol of methyl trimethylsilyl dimethylketene acetal , 10 mmol of benzaldehyde , 0.35 g pre-activated catalyst, 3- 6 hrs of reaction at 373 K under nitrogen atmosphere

[b] The yield was estimated by isolation of β-hydroxy ester.

[c] Turnover number (number of molecules converted per mole of Sn).

[d] Turnover frequency (turnover number per hour).

The inactivity of Mukaiyama-aldol condensation reaction on Si-MCM-41 suggests that Sn ions are necessary for the activity. Interestingly, considering the activity data as a function of molar SnO_2 /SiO_2 ratio in the catalyst, the yield was found to increase with the increase in the tin content. This effect was found much pronounced when compared the activities of sample E and F. On the contrary, with nearly same difference in the tin content, sample F has shown marginal increase in the conversion when compared

with conversions shown by samples A and B. Moreover, the TON (turnover number – number of molecules converted per Sn atom) decrease with increasing Sn content (sample A and F). If all the Sn ions were equally active and mono-atomically dispersed in the samples then the TON would have been same, which is not true for all the samples in present case. If all of the tin atoms were in the form of isolated tetrahedrally coordinated accessible sites, then the activity should commensurate with the Sn content. Thus, it seems that, when Sn concentration was increased from about molar SiO_2/SnO_2 ratio of 247 to about 98, not all Sn atoms are in the form of active sites for the reaction in the present studies. Sample F has shown the presence of hexacoordinated polymeric Sn-O-Sn type species alongwith tetrahedrally coordinated Sn species. This suggests that, with the increase in tin content, either proportionate concentration of active sites decreases due to some buried sites, which are within the walls making them inaccessible to the reactants [27] and/or there is an increase in the proportion of less active Sn species among the accessible active sites [24]. However, less active/inactive/inaccessible tin species do not affect the selectivity of the catalyst. Moreover, when we compare the TOF (turnover frequency) values, the similar performance of samples E and F can also be justified.

Considering the product yields for samples A and B it can be concluded that, at such a low tin content level (0.8 wt. % Sn), an efficiency of the Sn-MCM-41 was found to be excellent. Sample B has shown 91 % product yield. Solvent free Mukaiyama aldol-type reaction between PhCHO and silyl ketene acetal over Ti-MCM-41 containing 5.0 wt % TiO_2 showed 82 mol % PhCHO conversion with 100 % selectivity under the given reaction conditions [27]. Although, samples A, B and E are having more or less identical tin content, the catalytic performance of sample E was found to be very poor as compared

to samples A and B. Sample B has shown the superior activity among these three catalysts. As evident from UV-vis studies, the differences in the catalytic behavior may partly be attributed to differences in Sn siting. Another important aspect that can be considered for explaining the differences in their catalytic efficiency is the differences in the pore regularity in these materials. An amorphous mesoporous catalyst with tetra-coordination sites shows lower activity as compared with well ordered structure, thus showing benefit of regular pore dimensions of MCM-41[27]. Thus, the lower activity of sample E may also be due to its lower orderness, less expanded unit cell and lower surface area as evident from Fig. 3.2.1.1.4 and Tables 3.2.1.1.2 and 3.2.1.1.3. Hence, well-ordered Sn-MCM-41 with Sn species in tetrahedral coordination in the walls of its regular pores can prove as an efficient catalyst for this reaction. Moreover, when we compare the TOF (turnover frequency) values, the similar performance of samples A and B can also be justified. Since there were no samples having the only differences in the morphologies**,** no meaningful conclusions can be drawn with regard to the effect of morphology on the catalytic performance of Sn-MCM-41 in the present studies. However, all these results suggest that, with further tuning of synthesis variables and reaction conditions, Sn-MCM-41 may prove a potential catalyst for the preparation of 2, 2-dimethyl–3-phenyl-3-hydroxy propanoic acid methyl ester with yield as high as 100 %. Sn-MCM-41 was found to be excellent heterogeneous catalyst for solvent free Mukaiyama-aldol reaction in present studies. The product yield 95 % has been achieved over Sn-MCM-41 catalyst containing SiO_2/SnO_2 molar ratio of 98.

3.4 REFERENCES

[1] N. Igarashi, K. Koyano, Y. Tanaka, S. Nakata, K. Hashimoto, T. Tatsumi, Micropor. Mesopor. Mater. 59 (2003) 43.

[2] K. Kassiers, T. Linssen, M. Mathieu, M. Benjelloun, K.Schrijnemakers, P.Van Der Voort, P. Cool, E.F. Vansant, Chem. Mater. 14 (2002) 2317.

[3] D.H. Park, C.F. Cheng, J. Klinowski , Bull. Korean Chem. Soc. 18 (1997) 379.

[4] M. Luechinger, L. frunz, G.D. Pirngruber, R. Prins, Micropor. Mesopor. Mater. 64 (2003) 203.

[5] T.R. Gaydhankar, U.S. Taralkar, R.K. Jha, P.N. Joshi,R. Kumar, Catalysis Commun. 6 (2005) 361.

[6] C.N. Wu, T.S. Tsai, C.N. Liao, K.J. Chao, Micropor. Mater. 7 (1996) 173.

[7] Z. Luan, H. He, W. Zhou, C.F. Cheng, J. Klinowski, J. Chem. Soc. Faraday Trans. 91 (1995) 2955.

[8] M. Kruk, M. Jaroniec, A. Sayari, J. Phys. Chem. B 101 (1997) 583.

[9] R.Ryoo, C.H.Ko, I.S.Park, , J.Chem.Soc., Chem.Commun. (1999) 1413.

[10] J. Yan, J.L. Shi, L.Z. Wnag, M.L. Ruan, D.S. Yan, Mater. Letters 48 (2001) 112.

[11] A.C. Voegtlin, A. Matijasic, J. Patarin, C. Sauerland, Y. Grillet, L. Huve, Micropor. Mater. 10 (1997) 137.

[12] F. Kleitz, W. Schmidt, F. Schüth, Micropor. Mesopor. Mater. 65 (2003)1.

[13] M. Broyer, S. Valange, J.P. Bellat, O. Bertrand, G. Weber ,Z. Gabelica , Langmuir 18 (2002) 5083.

[14] C.T. Kresge, M.E. Leonowicz, W.J. Roth, J.C. Vartuli, J.S. Beck, Nature 359 (1992) 710.

[15] J.S. Beck, J.C. Vartuli, W.J. Roth, M.E. Leonowicz, C.T. Kresge, K.D. Schmitt, C.T.W. Chu, D.H. Olson, E.W. Shepp- ard, S.B. McCullen, J.B. Higgins, J.L. Schlenker, J. Am. Chem. Soc. 114 (1992) 10834.

[16] S. Biz, M.L. Occelli, Cata.Rev. 40 (1998) 329.

[17] A. Corma, Chem. Rev. 97 (1997) 2373.

[18] P. Selvam, S.K. Bhatia, C.G. Sonwane, Ind. Eng. Chem. Res. 40 (2001) 3237

[19] A. Corma, Q.B. Kan and F. Rey, Chem. Commun., (1998) 579

[20] M.L. Pena, Q. Kan, A. Corma, F. Rey, Micropor. Mesopor. Mater. 44 (2001) 9

[21] C.F. Cheng, D.H. Park, J. Klinowski , J.Chem.Soc., Faraday Trans. 93 (1997) 193.

[22] A. Sayari, M. Kruk, M. Jaroniec, Chem. Mater. 11 (1999) 492-500

[24] K. Chaudhari, T.K. Das, P.R. Rajmohanan, K. Lazar, S. Sivasanker, A.J. Chandwadkar, J.Catal. 183 (1999) 281.

[25] Y. Luo, G.L. Lu, Y.L.Guo, Y.S. Wang, Catalysis Commun. 3 (2002) 129.

[26] W. Zhang, M. Fröba, J. Wang, P. T. Tanev, J. Wong and T. J. Pinnavaia, J. Am. Chem. Soc., 118 (1996) 9164

[27] R. Garro, M. T. Navarro, J. Primo, A. Corma, J. Catal. 233 (2005) 342.

CHAPTER – 4

SUMMARY AND CONCLUSIONS

4.1 A Brief Description on Summary and Conclusions

Porous materials have been intensively studied with regard to technical applications as catalysts and catalyst supports. Among the family of microporous materials, the best known members are zeolites which have a narrow and uniform micro pore size distribution due to their crystallographically defined pore system. However, zeolites present severe limitations when large reactant molecules are involved, due to the fact that mass transfer limitations are very severe for microporous solids. The discovery of the M41S family of mesoporous molecular sieves brought about the beginning of a new age in the porous materials chemistry by opening a new way for expanding the range of uniform pore sizes from microporous (< 1.3 nm, as found in zeolites) into mesopore range (> 2 nm). Among M41S family of ordered materials, MCM-41 is known to present a hexagonal arrangement of unidimensional mesopores with uniform and controllable diameter in the range of 2 - 10 nm. By virtue of its high specific pore volumes, larger specific surface areas, high thermal stability and narrow adjustable pore size distribution, it has attracted considerable interest in material science, heterogeneous catalysis, molecular/supramolecular hosts, chemical separation of bulky molecules, biomedicine, membranes, adsorbents and advance composite materials and other relevant areas. Several synthesis routes have been developed for these materials with an objective to investigate the influence of different synthesis parameters such as time, pH, temperature, surfactant to silica ratio, type and concentration of surfactant, calcination etc. on the synthesis mechanism, stability, morphological and textural properties of these mesoporous structures. The challenges associated with synthesizing and developing new synthetic strategies for these known molecular sieves possessing unique pore size distribution

coupled with their thermal, structural and compositional peculiarities continue to attract the attention not only in scientific communities but also in industries. However, use of expensive reagents constitutes the main drawback in order to conceive large-scale processes for the production of MCM-41 materials. In this regard, by following the synthesis strategies such as the use of 1) low cost silica source, 2) minimum quantity of surfactant, 3) shorter time length and 4) low synthesis temperature may emerge a cost-effective and eco-friendly way for approaching this issue. The present work deals with optimization of synthesis parameters for the preparation of Si-MCM-41 and Sn-MCM-41 mesoporous materials which is cost-effective, facile, scalable, reproducible and environmentally friendly producing high yield. Samples were characterized by powder XRD, N_2 adsorption-desorption, TG/DTG, TEM, SEM, UV-Vis and Chemical Analyses.

Three variables have a major influence on the formation and properties of mesostructured phases: the gross composition of the reaction mixture, temperature and time. Even though each variable contributes to a specific aspect of the formation, there is substantial interplay between these elements during the course of synthesis.

As nature and concentration of the surfactant plays an important role in the pathway of the formation of ordered MCM-41 type mesoporous materials, hydrothermal synthesis was carried out using fumed silica as silica source with molar gel compositions SiO_2 : x CTMABr : y CTMAOH : z TMAOH : w H_2O, where x = 0-0.18, y = 0-0.32, z = 0-0.25, w = 25-33 at 383 K for 48 hrs. This was done in view to investigate the effect of source of $CTMA^+$ and OH^- on the formation of the MCM-41 type mesoporous materials and their properties. Gels with higher molar ratio of CTMAOH/SiO_2 have produced disordered MCM-41, while higher molar ratio of CTMABr/SiO_2 yielded well ordered MCM-41

keeping OH^-/SiO_2 fixed. Thus quality of MCM-41 depends not only on the nature and concentration of surfactant but also on the counter ion (anion) attached to the cationic surfactants.

From above studies of type and concentration of surfactant it was observed good quality MCM-41 could be obtained with molar gel composition SiO_2 : 0.18 CTMABr : 0.25 TMAOH : 25 H_2O therefore further optimization of synthesis was conducted with same molar composition in order to investigate various synthesis parameters such as time, temperature, molar ratios of $CTMABr/SiO_2$, $TMAOH/SiO_2$ and H_2O/SiO_2 in gel, pH of gel and silica sources influencing the formation and quality of Si-MCM-41. From temperature screening experiments, it was observed that MCM-41 can be obtained at 408 K and 423 K but the relative intensity of XRD patterns of the calcined form of these samples was less as compared to MCM-41 prepared at 383 K. Further optimization of gel parameters such as surfactant concentration, water content etc is required to obtain good quality MCM-41 at 408 K and 423 K. The pH value of the gel having molar gel composition SiO_2 : 0.18 CTMABr : 0.25 TMAOH : 25 H_2O was found to be 12.2 at which good quality MCM-41 was acquired after hydrothermal synthesis at 383 K. At lower pH values poor quality materials were obtained. Using the same molar gel composition the results obtained by varying synthesis time and have indicated that there is progressive increase in unit cell parameter with synthesis time, reaches to maximum and then decreases slightly on further heating. Such time dependant study was also carried out using ethyl silicate - ES, fumed silica - FS_1 and silica sol - SS as a source of silica. Well ordered MCM-41 materials were synthesized using fumed silica - FS_1, ethyl silicate - ES and silica sol - SS under the identical set of synthesis conditions. Depending upon the type of silica source used, upon

calcination MCM-41 materials exhibited 5.9 to 10.8 % contraction in unit cell parameter. The type of silica source was found to control the magnitude of the wall thickness and in turn the structural stability of highly ordered MCM-41. On the basis of the magnitude of the wall thickness and structural stability of MCM-41 phases, the suitability of these sources was found to follows the trend: fumed silica > silica sol > ethyl silicate. The well ordered MCM-41 prepared using fumed silica and silica sol have shown worm like morphology whereas fused particles were formed when ethyl silicate was used as a silica source.

Hydrothermal synthesis of Si-MCM-41 with the molar gel composition: SiO_2 : 0.24 CTMABr : 0.25 TMAOH : 26 H_2O using fumed silica - FS_2, spray dried precipitated silica - PS_1 and flash dried precipitated silica - PS_2 was carried out at 383 K. The motivation behind selecting these cheaper high silica precursors was to seek the possibility of use of these precursors for designing simple, cost-effective, eco-friendly and successful scalable synthetic strategies for a process to prepare MCM-41 with high throughput. After conducting a systematic and comparative time dependant studies on structural development of MCM-41 using FS_2, PS_1 and PS_2 similar results were obtained as seen in previous time dependant studies. On the basis of results obtained from time dependant study on the progressive development of MCM-41 mesophases, the reactivity trend of silica sources observed was as: FS > PS_1 > PS_2. The population of ≡Si-OH units in the channel wall was found to increases in the order: MCM-41-FS_2 > MCM-41-PS_1 > MCM-41-PS_2. MCM-41 synthesized using least expensive PS_2 having less surface area has exhibited thicker pore walls but poor orderness, while MCM-41 prepared from expensive fumed silica having high surface area has thinner pore walls and well ordered. Thermal

stability and morphology of MCM-41 materials were found to depend on the manufacturing process of silica sources used.

In spite of the benefits, the room-temperature synthesis route has been imposing the challenges associated with the selection of convenient but less expensive silica source materials. The information on prerequisites and economic considerations has triggered our interest in using inexpensive polymeric version of ethyl silicate in place of TEOS in the room temperature synthesis of Si-MCM-41. In view of making the preparation of MCM-41 in more cost effective way, feasibility of using ethyl silicate in room temperature synthesis of Si-MCM-41 has been attempted for the first time. We have presented in depth report of room-temperature synthesis of Si-MCM-41 using ethyl silicate, a cheaper, readily available and high silica containing source material which is a partially hydrolyzed or polymeric version of TEOS. The synthesis variables such as molar ratios of H_2O/NH_4OH, NH_4OH/SiO_2 and $CTMABr/SiO_2$ in the initial gel composition play a crucial role in governing the textural, stability and morphological properties of Si-MCM-41 phases. The optimum values of H_2O/NH_4OH for NH_4OH/SiO_2 molar ratios 2.5, 12.5, 22.5 and 32.5 were found to be 150, 185, 300 and 450 respectively when optimum $CTMABr/SiO_2$ molar ratio was 0.12 in the initial gel. Under identical set of synthesis conditions, if not better but comparable and acceptable quality of MCM-41 can be obtained using ethyl silicate in place of TEOS. The observed differences in textural characteristics may be associated with the differences in the amount of silica monomers and hence their hydrolysis and condensation rates. Moreover, higher wall thickness of MCM-41 obtained from ethyl silicate indicates that, MCM-41 with improved structural stability may be obtained just by replacing TEOS by ethyl silicate under identical set of synthesis conditions. With stepwise

reduction in H_2O/NH_4OH molar ratio in the gel, the extent of fusion of hexagonal and round shaped particles was found to increase, giving rise to sheet like particles.

Even though Sn-MCM-41 type mesoporous materials have higher structural stability and Lewis acid type properties which are potentially useful for catalytic purposes, a fewer number of studies deal with optimization of synthesis parameters and its catalytic application. Prompted by this we have investigated for the first time, optimization of various synthesis parameters and catalytic performance of Sn-MCM-41 type mesoporous materials for carbon-carbon bond formation in heterogeneously catalyzed Mukaiyama aldol condensation reaction. The suitable gel composition and the required synthesis time to obtain well ordered Sn-MCM-41 was established by optimizing the synthesis variables such as synthesis period and compositional gel components viz. molar ratios of $TMAOH/SiO_2$, $CTMABr/SiO_2$, H_2O/SiO_2, keeping SiO_2/SnO_2 molar ratio (250) and source materials fixed. Each synthesis variable was found to contribute to a specific aspect of synthesis of Sn-MCM-41. Well ordered Sn-MCM-41 with 0.8 wt. % Sn was obtained from the optimized gel of molar composition SiO_2 : 0.004 SnO_2: 0.24 CTMABr : 0.30 TMAOH : 25 H_2O using fumed silica and tin tetrachloride. Under this judiciously pre-optimized synthesis conditions, the different combinations of silicon sources and tin sources was found to influence the synthesis time, structural properties, tin configuration and morphology of Sn-MCM-41. Among silica sources, fumed silica and silica sol were proved to better sources when they were used in combination with tin tetrachloride. Moreover, a well ordered Sn-MCM-41 was also obtained using combination of fumed silica and tin tert-butoxide. A combination of ethyl silicate and sodium stannate sources has failed to the form a well ordered Sn-MCM-41 even if the hydrothermal synthesis was

allowed to last for 92 hrs. The population of tetravalent tin incorporated in the framework which can be assumed to be responsible for the expansion of unit cell follows the trend as: F > B > A > D > E > C. The textural properties changes with change in tin concentration and type of source materials used for the synthesis of Sn-MCM-41. Sn-MCM-41 prepared using fumed silica in the combination of either tin tetrachloride or tin tert-butoxide has shown maximum incorporation of Sn^{4+} in tetrahedral coordination in the silica framework of Sn-MCM-41 as compared to other source combinations. The noticeable change in morphology with change in silica source may be arising from the variation in the formation rate of surfactant micelles and micelle-silicate composites; hence variation in subsequent rate of silicate condensation. Well-ordered Sn-MCM-41 with Sn species in tetrahedral coordination in the walls of its regular pores was found to be excellent heterogeneous catalyst for solvent free Mukaiyama-aldol condensation between methyl trimethylsilyl dimethylketene acetal and benzaldehyde. Invariably, the β-hydroxy ester selectivity was found to be 100 % irrespective of the conversion levels. The product, 2, 2-dimethyl–3-phenyl-3-hydroxy propanoic acid methyl ester with 95 % yield has been achieved over Sn-MCM-41 catalyst containing SiO_2/SnO_2 molar ratio of 98. Sn-MCM-41 has shown remarkable activity (91 % product yield) even with tin content as low as 0.8 wt. % Sn. The differences in Sn siting, the changes in structural and textural properties are the crucial factors which were found to influence the catalytic performance of Sn-MCM-41 materials in solvent-free Mukaiyama-aldol condensation at stated conditions.

4.2 A List of Paper Publications Resulted from this Work

1. Textural/structural, stability and morphological properties of mesostructured silicas (MCM-41 and MCM-48) prepared using different silica sources.

   T.R. Gaydhankar, U.S. Taralkar, R.K. Jha, P.N. Joshi and R. Kumar.
   Catalysis Communications, 6 (2005) 361–366.

2. Hydrothermal synthesis of MCM-41 using differently manufactured amorphous dioxosilicon sources

   T.R. Gaydhankar, V. Samuel, P.N. Joshi
   Material Letters 60 (2006) 957-961.

3. Room temperature synthesis of Si-MCM-41 using polymeric version of ethyl silicate as a source of silica

   T.R. Gaydhankar, V. Samuel, R.K. Jha, P.N. Joshi and R. Kumar.
   Material Research Bulletin
   (Accepted, 3rd Nov 06, Manuscript No: MRB-06-736R1)

4. Optimal synthesis parameters and application of Sn-MCM-41 as an efficient heterogeneous catalyst in solvent-free Mukaiyama-type Aldol condensation

   T. R. Gaydhankar, P.N. Joshi, P.Kalita and R. Kumar
   Journal of Molecular Catalysis A: Chemical
   (Accepted, 18th Oct 06, Manuscript No: MOLCAA-D-06-00875)

5. Counter ions cooperation and competition in the synthesis of mesoporous materials

   T. R. Gaydhankar, M. W. Kasture and P.N. Joshi
   Chemistry of Materials (Under Review, Manuscript No: cm0627645)